EVALUATION OF CYCLIC PORE PRESSURE INDUCED MOISTURE DAMAGE IN ASPHALT PAVEMENT

By

TAIT K. KARLSON

A THESIS PRESENTED TO THE GRADUATE SCHOOL
OF THE UNIVERSITY OF FLORIDA IN PARTIAL FULFILLMENT
OF THE REQUIREMENTS FOR THE DEGREE OF
MASTER OF SCIENCE

UNIVERSITY OF FLORIDA

2005

This document is dedicated to James Ryan Howell, engineer and friend.

ACKNOWLEDGMENTS

I would like to thank my advisor, Dr. Bjorn Birgisson, for all of his guidance and supervision as well as the opportunity to continue my education. I would also like to thank my committee, Dr. Reynaldo Roque and Dr. Scott Washburn, for their time, knowledge, and ideas that they have so generously passed on to me. I would like to thank the Florida Department of Transportation for its support, the use of its equipment, and the help of its engineers and technicians.

A great deal of gratitude goes to Mr. George Lopp whose expertise kept the laboratory operational in spite of us graduate students. I would like to thank Eli Esquivel who drew my attention to this field of engineering. Special thanks go to Jeff Frank, Tipakorn Samarmrak, Jagannatha Katkuri, Minh Le, and Adam Jajliardo whose efforts and friendships made it possible for me to complete my research. I also wish to thank everyone both formerly and currently in the Materials Group at the University of Florida whose friendship and help made my experience there something I will always remember: Zhanwu Cui, Claude Villiers, Hong-Joong Kim, Sungho Kim, Jaeseung Kim, Erkan Ekingen, Boonchai Sangpetngam, Daniel D. Darku, Booil Kim, Chote Soranakom, Marc Novak, Sylvester Asiamah, Linh Viet Pham, Michael P. Wagoner, Oscar F. Garcia, and D.J. Swann.

I would like to thank my parents who have always given the support and parental nudge I needed. Finally, I would like to thank my beautiful wife, Cynthia, whose love, devotion, and runs to Wendy's kept me going through the long hours of research.

TABLE OF CONTENTS

LIST OF TABLES

LIST OF FIGURES

Abstract of Thesis Presented to the Graduate School
of the University of Florida in Partial Fulfillment of the
Requirements for the Degree of Master of Science

EVALUATION OF CYCLIC PORE PRESSURE INDUCED MOISTURE DAMAGE IN ASPHALT PAVEMENT

By

Tait K. Karlson

December 2005

Chair: Bjorn Birgisson
Cochair: Reynaldo Roque
Major Department: Civil and Coastal Engineering

Moisture damage, occurring in several forms, can cause deterioration of asphalt pavements leading to a shortened service life of the pavement. Some of these forms include stripping (a loss of adhesion of the asphalt binder from the aggregate), hydraulic scouring (where fines are transported through the voids in the pavement when a traffic load causes positive and negative pore pressures), and a loss of cohesion in the asphalt binder when repetitive positive and negative pore pressures break the connections between the aggregate.

Several attempts have been made to create a test procedure that will accurately determine the susceptibility of an asphalt pavement to moisture damage. None have gained wide acceptance due to lack of repeatability, complication of the process, the need for expensive equipment, or lack of quantitative results. A new cyclic loading and pore pressure conditioning system was used to evaluate four different cyclic pressure/temperature conditions. These conditions were 5-15 psi at 25ºC, 5-25 psi at

25ºC, 5-30 psi at 25ºC, and 5-15 psi at 40ºC. The SuperPave™ IDT test was used to obtain the tensile strength, resilient modulus, fracture energy limit (FE), dissipated creep strain energy limit (DCSE), and creep properties from the conditioned and unconditioned samples. These properties were used to determine a fracture mechanics-based performance specification criterion, termed the "Energy Ratio" (ER), which measures the fracture resistance of mixtures.

The results show that cyclic pore pressure conditioning at an elevated temperature of 40ºC results in moisture damage patterns that are consistent with expected behavior. Limestone mixtures with proven field performance track records showed little or no moisture damage. The Georgia granite mixtures, which are known to exhibit moisture damage without the presence of anti-stripping agents, showed a reduced ability to resist fractures after conditioning.

CHAPTER 1
INTRODUCTION

1.1 Problem Statement and Background

Moisture has been sighted as a cause of several forms of damage in hot-mix asphalt (HMA) pavements. These forms include rutting, raveling, and cracking and they severely affect the performance and service life of HMA pavements. Moisture damage in HMA mixtures occurs when water can penetrate the pavement system. This damage can then cause stripping (a loss of adhesion of the asphalt binder from the aggregate), hydraulic scouring (where fine aggregate particles are transported through the voids in the pavement when a traffic load causes positive and negative pore pressures), or by a loss of cohesion in the asphalt binder when the positive pore pressures push the aggregate apart.

Depending on materials, loading, and environment, it may be that one or all of the mechanisms of water damage are present and are contributory in a pavement in the field. However, for a proper evaluation of any given mixture and testing procedure, it is necessary to isolate and quantify the effects of each of the predominant mechanisms contributing to moisture damage. In fact, the lack of delineation between pore water effects and actual moisture damage may lead to erroneous conclusions. The damage caused by water in HMA pavements may be represented by two extreme conditions, 1) the rapid application of cyclic pore pressures under saturated conditions that correspond to critical field conditions, and 2) the long term continuous low level exposure to water without pore pressures. This project deals more with the first condition.

The problems of water damage in asphalt pavement have directed attention towards the phenomenon called stripping in recent years. Several techniques can be used to reduce the sensitivity of HMA mixtures to stripping. Liquid anti-strip chemicals are commonly used throughout the United States as an additive to asphalt cement. Florida summer days can be very harsh on HMA pavements. Many days will include extremely high pavement temperatures and then cool midday downpours followed by hot afternoons. These conditions could contribute to the stripping problems that Florida has faced. As a result Florida has specified the use of approved anti-stripping agents in all friction course and recycled mixtures.

There have been several projects developed through the years that have looked at the phenomenon of water damage. Most of these studies have used destructible strength tests on unconditioned and then on comparable conditioned samples to determine how much the samples were affected by the conditioning. These conditioning procedures have included cycling water in and out of the pores and cycling the pressures in the pores of the specimens.

1.2 Objectives and Scope

The primary objective of this study was to accurately determine the effects of cycling pore pressures in Superior Performing Asphalt Pavement (SuperPave^{TM}) samples. Other purposes of this research included evaluating the possible effects of aggregate mixture (course and fine-graded) and aggregate type (Georgia granite and oolitic limestone) on pore pressures and moisture damage susceptibility.

1.3 Research Approach

In this project, the permeability was found for six granite mixtures using the Florida Department of Transportation (FDOT) method. Three of these granite mixes and

two limestone mixes were used in a newly developed cell to condition them and test for changes in their dynamic and resilient moduli.

An introduction to different mechanisms of moisture damage and previous research are presented in Chapter 2. The materials and methodologies used are located in Chapter 3. Chapter 4 describes the equipment used during this project. Chapter 5 contains the permeability results as well as the hot-mix asphalt fracture mechanics discussion. In Chapter 6, the specimen conditioning procedure is discussed. Finally, Chapter 7 states the results of the project and recommendations for future research.

CHAPTER 2
LITERATURE REVIEW

A major objective with this research project is to either identify or develop new methods of evaluating the potential for moisture damage in mixtures. In order to determine optimal ways to condition and test mixtures, it is important to include the most likely mechanism(s) that cause moisture damage in the field and use that mechanism for conditioning in the laboratory. It is equally as important to develop a strong understanding of the key mixture properties that are affected by moisture damage, so that the evaluation and quantification of the effects of moisture damage can be robust and effective. In this chapter, the current state of knowledge about moisture damage in mixtures is reviewed. In particular, the focus is on 1) Review of key mechanisms of moisture damage, and 2) Methods and evaluation protocols that have been either proposed or used recently for conditioning of mixtures.

In the following, the chemistry of the asphalt-aggregate bond is discussed, with a focus on factors that may contribute to stripping. Then, the mechanisms of stripping are reviewed, followed by a discussion of existing test methods and evaluation protocols.

2.1 Adhesion and Stripping

The phenomenon of stripping is directly related to the sensitivity of the bond between aggregates and asphalt in an asphalt mixture. Therefore, to determine why this adhesive bond is broken, it is first necessary to understand the physics of how aggregates and asphalt combine and adhere to each other to form an asphalt mixture. Numerous theories have been proposed to explain the adhesion. Rice (1958) classified these

theories as mechanical interlocking, chemical reaction, and molecular orientation or surface energy. Chemical interactions are believed to be the best explanation of the adhesive bond (Curtis, Einsley, and Epps, 1993a). Furthermore, all theories assume that the bond is influenced by the composition and surface chemistry of the aggregates.

A discussion of the chemistry of the asphalt-aggregate bond, as well as the aggregate properties that promote adhesion follows. In addition, some others factors that contribute are commented upon.

2.1.1 Chemistry of the Asphalt-Aggregate Bond

The asphalt-aggregate bond arises due to the presence of acidic and basic components in an asphalt mixture that react forming water-insoluble compounds. The adhesion of asphalt to aggregate must occur and be maintained for a good pavement to exist. To investigate and control stripping problems, it is necessary to understand the chemistry of both the asphalt and aggregate at the asphalt-aggregate interface, and the effects of moisture on this bonding.

Asphalt is composed of a mixture of hydrocarbons that contain some polar functionality, as well as constituents that contain metals such as nickel, vanadium, and iron. The aggregate provides a surface that is heterogeneous and has a variety of sites of different composition and levels of activity. These active sites are frequently charged or contain partial charges that attract and orient the polar constituents of asphalt. Curtis, Einsley, and Epps (1993b), in an investigation of the chemical and physical processes that govern adhesion between aggregates and asphalt, stated that the polar functionalities present at the point of contact between the asphalt film and the aggregate surface adhere to the surface through electrostatic forces, hydrogen bonding, or Van der Waals interactions.

When hot asphalt coats the aggregates particles, it tends to enter any available pores. Short-range chemical interactions in asphalt molecules are feasible because of electrostatic interactions that occur between the charged surface and the molecules attracted to the surface. Adamson (1976) pointed out that polar molecules will position themselves along a surface according to the difference in charge. A charged aggregate surface attracts an oppositely charged or partially charged species or functional group contained in the species. The part of the attracted molecule that is available for interaction with other asphalt molecules would then be the charge of the aggregate and hence would have electrostatic interaction with other oppositely charged or partially charged asphalt molecules.

The intrusion of water or moisture may substantially affect the pH of the local environment. According to Scott (1978), changes in the pH of the microscopic water accumulations at the aggregate surface can alter the type of polar groups adsorbed, as well as their state of ionization/dissociation, leading to the build-up of opposing, negatively charged, electrical double layers on the aggregate and asphalt surfaces. The drive to reach equilibrium attracts more water and leads to physical separation of the asphalt from the aggregate.

In short, the bond that develops between asphalt and aggregate is primarily due to relatively weak dispersion forces that cause molecular orientation to occur. Water molecules, on the other hand, are highly polar and thus are attracted to aggregates by much stronger orientation forces.

Therefore, if a three-phase interface consisting of aggregate, asphalt, and water exists, water is better than asphalt for reducing the free surface energy of the system to a

thermodynamically stable condition of minimum surface energy (Figure 2-1). According to Fromm (1974), once the asphalt film is breached and water enters under the asphalt, surface tensions may force the water between the remaining asphalt-aggregate interface, causing stripping.

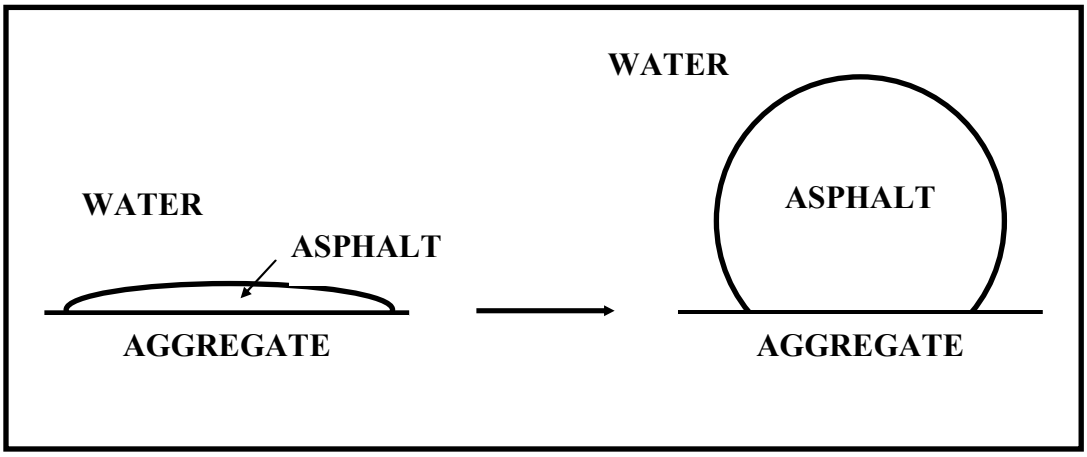

Figure 2-1. Illustration of the Surface Energy Theory of Adhesion.

According to Thelen (1958), the surface or interfacial tensions (χ) between these phases are approximately as follows:

χ_{ab} = interfacial tension between aggregate and asphalt = 17 ± 3 ergs/cm2

χ_{wb} = interfacial tension between water and asphalt = 30 ± 5 ergs/cm2

χ_{aw} = interfacial tension between aggregate and water = 0 ergs/cm2 (since under usual ambient temperature the aggregate surface is approximately a free water surface).

The energy potential to cause stripping is calculated as shown in the following equation:

$$\Delta F = \chi_{ab} + \chi_{wb} - \chi_{aw} = 47 ergs / cm^2$$

Thus, usual asphalt and normal organic materials will voluntarily spread over water films on aggregate, and will also tend to be stripped from these films by water. The rate

at which these processes occur no doubt depends somewhat on the magnitude of the free energy evolved (DF), but in practice probably is controlled chiefly by the viscosity of the asphalt.

2.1.2 Aggregate Properties

Failure of the bond can fail at the interface, within the asphalt as a cohesive failure, or within the aggregate as a structural failure. Curtis et al. (1993b) showed that the physicochemical surface properties of mineral aggregate are more important for moisture induced stripping compared to the properties of asphalt cement binder.

The surface charge of the aggregate determines, to some degree, the extent of attraction and adsorption of the asphalt. This surface charge can be quantified by measuring the streaming potential or Zeta potential of the aggregate. Consequently, the aggregate surface can be modified to effect favorable attraction between the asphalt and aggregate.

Electron transfer from the asphalt at the interface relies on the ability of aggregates to accept or donate these electrons. Scott (1978) observed that pH value varies depending on whether the aggregates are siliceous or calcareous. In addition, Curtis et al. (1993b) concluded, from studies of the electron donor and electron acceptor properties of four aggregates, ranging from quartz, to silicate, to calcite-based, that aggregates composed of quartz exhibit the strongest acceptor character, while silicate materials are less strong. The carbonate rocks show a range of donor-acceptor properties.

Some mineral aggregates are inherently very susceptible to stripping. Interlocking properties of the aggregate particles, which include individual crystal faces, porosity, angularity, absorption, and surface coating are also believed to improve the bond strength

in an asphalt mixture. Kiggundu and Roberts (1988) postulated that the absence of a sound interlocking network of these properties might induce stripping.

It is often observed that siliceous aggregates have slick, smooth areas, which may give rise to stripping, while roughness may help to promote bonding. Besides, some limestones and lime-treated aggregates tend to form stronger, more robust, and durable bonds with asphalt. The insensitivity of these bonds to the action of water is believed to cause this. The bonds formed in this case are strong, insoluble bonds. Curtis et al. (1993a) observed, from reactivity measurements with model carboxylic acids, that even within limestones, their ability to form insoluble salts varies substantially, depending on the availability of the surface calcium to enter into bond formation.

2.2 Other Causative Factors

Tunnicliff and Root (1984) performed a survey to summarize and analyze the use of anti-stripping additives in asphalt mixtures in the United States by submitting a questionnaire to members of the American Association of State Highway and Transportation Officials (AASHTO) Subcommittee on Materials, agencies, asphalt cement producers, trade associations, and anti-stripping additive producers. Responses from the questionnaire imply that other factors contribute to stripping, such as asphalt cement characteristics, and construction practice.

On the other hand, Taylor and Khosla (1983) concluded, from a comprehensive survey of the literature regarding moisture damage in asphalt pavements, that stripping is a complex problem related to a large number of variables, including also the type and use of mix, environment, and traffic.

Based on an evaluation of the factors responsible for inducing stripping, Kandhal (1994) listed and discussed external factors and/or in-place properties of asphalt pavements, dealing basically with the same factors stated before.

A proper knowledge of these factors is essential in identifying and solving the stripping problem. A discussion of the most frequently listed factors identified by Taylor and Khosla (1983) and Kandhal (1994) follows.

2.2.1 Type and Use of Mix

It has been found that the type and use of an asphalt mixture is related to the likelihood of the stripping of the mix. The majority of pavement failures caused by stripping occur in open-graded mixes, base courses, and surface treatments, all of which are relatively permeable to water when compared with dense-graded mixes. Surface treatments have been noted to be particularly vulnerable to stripping. Stripping in dense-graded, hot-mix paving mixtures is generally not considered a large problem unless the mixtures exhibit excessive air voids, insufficient bitumen, inadequate compaction, or aggregate with adsorbed coatings. The practice of adding anti-stripping agents to the mixture may be improving the field performance of these mixtures. The inherent resistance to stripping exhibited by dense-graded, hot-mix paving mixtures may be caused, in part, by the use of hot, dry aggregate in those mixtures. However, there is a need to evaluate all mixtures for their susceptibility to moisture damage. In particular, since the use of anti-stripping agents is common in mixtures, it is important to evaluate mixtures that contain anti-stripping agents in an accurate and robust manner.

The small percentage of normally present air voids and the common presence of anti-stripping agents in well-compacted, dense-graded hot mixes is probably largely responsible for their excellent moisture resistance because the virtual absence of voids

renders the mixes much less permeable. Full-depth (deep strength) asphalt pavements, as proposed by The Asphalt Institute, have been shown to provide excellent resistance to stripping. The dense-graded asphalt bases often used in full-depth pavements are observed to act as a vapor barrier so that little or no free moisture accumulates beneath the pavements.

2.2.2 Asphalt Characteristics

The relationship most often referenced between the characteristics of the asphalt in a paving mixture and the tendency of the mix to strip relates stripping resistance to the viscosity of the binder in service. Binders of high viscosity have been observed to resist displacement by water much better than those of low viscosity, although even 60-penetration bitumen has been observed to strip. Fromm (1974) observed that high viscosity asphalt resisted pulling along an air-water interface and that the pulling of the asphalt film increased as asphalt viscosity decreased.

Low viscosity, however, is desirable during mixing operations because a low viscosity fluid has more wetting power than one of high viscosity. Observations made by Schmidt and Graf indicate that most asphalts appear to behave similarly with respect to moisture, provided they are of the same viscosity; i.e., the effect of asphalt composition is negligible. In contrast, Fromm (1974) observed that the rate of emulsion formation in an asphalt submerged in water depends on the nature of the asphalt rather than its viscosity. Logically, an emulsified asphalt may be more prone to stripping by spontaneous emulsification if some concentration of emulsifier remains in the binder after mixing. The presence of paraffin in asphalt is believed to be detrimental to stripping resistance.

Moreover, high viscosity asphalt cements cannot be used in many instances because of other considerations such as low-temperature cracking in cold regions and

potential reduction in fatigue life of the surface courses. There is a need to understand the fundamentals of aggregate-asphalt adhesion so that the problem can minimized by other means rather than increasing the asphalt cement viscosity, which is not effective in all cases and which may result in other performance problems.

Asphalt is composed of such a variety of chemical species that it most likely will also have a continuum of electron donor and acceptor behavior, the exact range of which is dependent on its chemistry. The matching of the electron donation and accepting abilities of the aggregates and asphalts, respectively, may lead to improvements in road performance.

One factor affecting the wetting of the aggregate surface by asphalt depends on the interfacial tension, promoting wetting, and facilitating close contact between the asphalt and the aggregate surface. However, the effectiveness of an additive, particularly an anti-stripping agent, varies with the type of the additive, as well as with the asphalt and aggregate.

After the asphalt has wetted the aggregate surface, some of its organic chemical functionalities enter into bond formation with the aggregate constituents. Frequently, these functional groups, such as carboxylic and phenolic acid, combine with alkali metals present on the aggregate surface to form water-insoluble salts (e.g., sodium salts). Consequently, these asphalt-aggregate bonds are ionic bonds that weaken or solubilize over time with exposure to moisture. They become moisture susceptible because of their inability to withstand solubilization and disbonding over an extended amount of time. Thus, even though tensile strength ratio (TSR) measurements may exhibit high values,

these are reflective of only the physical strength of the bonds and do not measure their ability to withstand exposure or weathering.

2.2.3 Construction Practice

Inadequate surface and/or subsurface drainage provides water or moisture vapor, which is the necessary ingredient for inducing stripping. If excessive water or moisture is present in the pavement system the HMA pavement can strip prematurely. Kandhal, Lubold, and Roberts (1989) have reported case histories where the stripping was not a general phenomenon occurring on the entire project but rather a localized phenomenon in areas of the project saturated with water and/or water vapor due to inadequate subsurface drainage conditions.

Water can enter the HMA pavement layers in different ways. It can enter as run-off through the road surface, primarily through surface cracks. It can enter from the sides and bottom as seepage from ditches and high water table in the cut areas.

The most common water movement is upward by capillarity under a pavement. Above the capillary fringe, water moves as a vapor. Many subbases or subgrades in the existing highway system lack the desired permeability; therefore, are saturated with the capillary moisture. The construction of multilane highways (or widening) to greater widths, gentler slopes and milder curves in all kinds of terrain has compounded the subsurface drainage problem. Quite often, a four-lane highway is rehabilitated by paving the median and shoulders with HMA resulting in a fully paved width of 72-78 feet, which is equivalent to a six-lane highway without any increase in the subsurface drainage capability.

Air voids in the HMA pavement may become saturated with water even from vapor condensation due to water in the subgrade or subbase. A temperature rise after this

saturation can cause expansion of the water trapped in the mixture voids resulting in significant void pressure when the voids are saturated. The pore pressure from stresses induced by traffic can also cause the failure of the binder-aggregate bond. Initially, the traffic stresses may further compact the mixture and trap or greatly reduce the internal water drainage. Therefore, the internal pore water is in frequent motion (cyclic) and considerable pore pressure may be built up under the traffic action.

Kandhal (1994) described telltale signs of water damage to HMA overlays (over concrete pavements). He observed wet spots on the HMA overlay surface scattered throughout the project. Usually at these wet spots water oozed out during hot afternoons. Some of the wet spots contained fines suspended in the water, which were driven on and turned into fatty areas (resulting from asphalt stripping from the aggregate and migrating to the surface). This often preceded the formation of potholes.

Usually stripping in a four-lane highway facility occurs first in the slow traffic lane because it carries more and heavier traffic compared to the passing lane. Typically, but not always, stripping starts at the bottom of HMA layer, or a layer interface, and progresses upwards.

It is evident from the preceding discussion that inadequate subsurface drainage is one of the primary factors inducing premature stripping in HMA pavements.

Other construction factors that may cause or enhance stripping include:

- Inadequate Compaction,
- Excessive Dust Coating on Aggregate,
- Use of Open-Graded Asphalt Friction Course,
- Inadequate Drying of Aggregates,
- Use of Weak and Friable Aggregate,
- Placement of Overlays on Deteriorated Concrete Pavements,
- Use of Waterproof Membranes and Seal Coats.

2.3 Mechanisms of Stripping

Despite the fact that several factors have been associated with stripping, there is a consensus that this phenomenon is principally caused by water. For this to occur, however, water has to penetrate the asphalt film. This can occur under various conditions and by several mechanisms.

There may be as many as five different mechanisms by which stripping of asphalt cement from an aggregate surface may occur. Those five mechanisms include (e.g. Stuart, 1990; Kandhal, 1994; Kandhal and Rickards, 2001):

- Detachment,
- Displacement,
- Spontaneous emulsification,
- Pore pressure, and
- Hydraulic scouring.

It appears that these mechanisms may act individually or together to cause adhesion failure in bituminous mixtures. In addition to these mechanisms outlined, other less likely, but potential mechanisms for stripping have been suggested such as osmosis due to presence of salts or salt solution in the aggregate pores that creates an osmotic pressure gradient that sucks water through the asphalt film. A discussion of each of the five mechanisms follows.

2.3.1 Detachment

The most likely mechanism occurs when there is a discontinuity and, hence, a line of juncture where asphalt, free water and aggregate are all in contact. In other words, detachment is the separation of an asphalt film from an aggregate surface by a thin layer of water, with no obvious break in the asphalt film (Figure 2-2).

In this case, the aggregates are completely uncoated in the presence of moisture, indicating a complete loss of adhesion. The theory of interfacial energy provides the rationale for explaining the detachment mechanism.

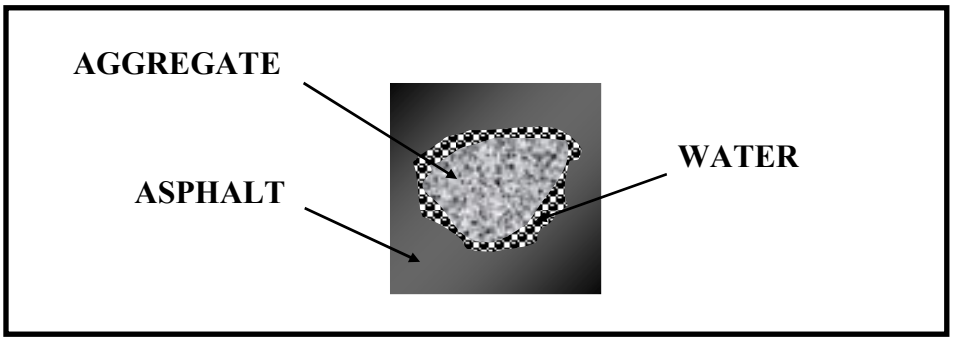

Figure 2-2. Illustration of Stripping by Detachment.

2.3.2 Displacement

Stripping by displacement results from the penetration of water to the aggregate surface through a break in the asphalt film. This break can be caused by incomplete coating of the aggregate initially or by film rupture. Because the asphalt film at these locations is generally thinner and under tension, rupture of the asphalt film is probable at the sharp edges and corners of angular aggregate pieces as a result of traffic loading. Stripping by displacement can result from pinholes in the asphalt film, which can form soon after coating of a dusty aggregate. Both the surface energy and the chemical reaction theory of adhesion can be used to explain stripping by displacement.

2.3.3 Spontaneous Emulsification

In spontaneous emulsification, water and asphalt combine to form an inverted emulsion, where asphalt represents the continuous phase and water represents the discontinuous phase. When such an emulsion is formed, the adhesive bond between the asphalt and the aggregate is broken. This can be further aggravated by the presence of

emulsifiers such as mineral clays and some asphalt additives. The chemical reaction theory of adhesion can be used to explain stripping by spontaneous emulsification.

Fromm (1974), investigating how water penetrates asphalt films, observed that spontaneous emulsification occurs whenever asphalt films were immersed in water. The rate of emulsification depended, however, on the nature of the asphalt and the presence of additives. The fact that stripping has been observed to be reversible lends support to the spontaneous emulsification mechanism because evaporation of the water from the emulsion returns the asphalt to its original condition.

2.3.4 Pore Pressure

The effects of pore pressure take place when the air voids in the HMA pavement are reduced due to loading and the water in the voids is compressed to create pressure against the asphalt film. Once the pore pressure increases to a high level, the asphalt film on the aggregate will rupture under the pressure and create a break in the film where water can infiltrate to the surface of the aggregate. Pore pressure usually affects newly placed HMA pavements because the pavement is placed at a higher than designed air void content with the assumption that traffic loadings will decrease the air void content over time. The voids are interconnected and allow the water to move through the pavement. Once the pavement starts to become dense, the interconnected voids close and traps water in the voids. Further densification causes the pores to collapse and increase the pressure on the water. Several reasons are attributed to the increase in pore pressure including traffic loadings, thermal expansion, freezing expansion, and thermal shock (Lottman, 1982b). Once the asphalt film ruptures, then the displacement mechanism removes the asphalt film.

The pore pressure can affect the pavement system even when the pavement is not fully saturated. The unsaturated voids can create a capillary tension within the pavement, causing the pore pressure to become negative. This can cause the effective stresses to increase beyond the effective stresses when the pavement is saturated. However, when a load is applied to the pavement, the total stress and the pore pressures will increase according to the load intensity. In turn, the effective stresses within the pavement will decrease. This will cause a cycling of compression and tension within the voids. This is illustrated in Figure 2-3.

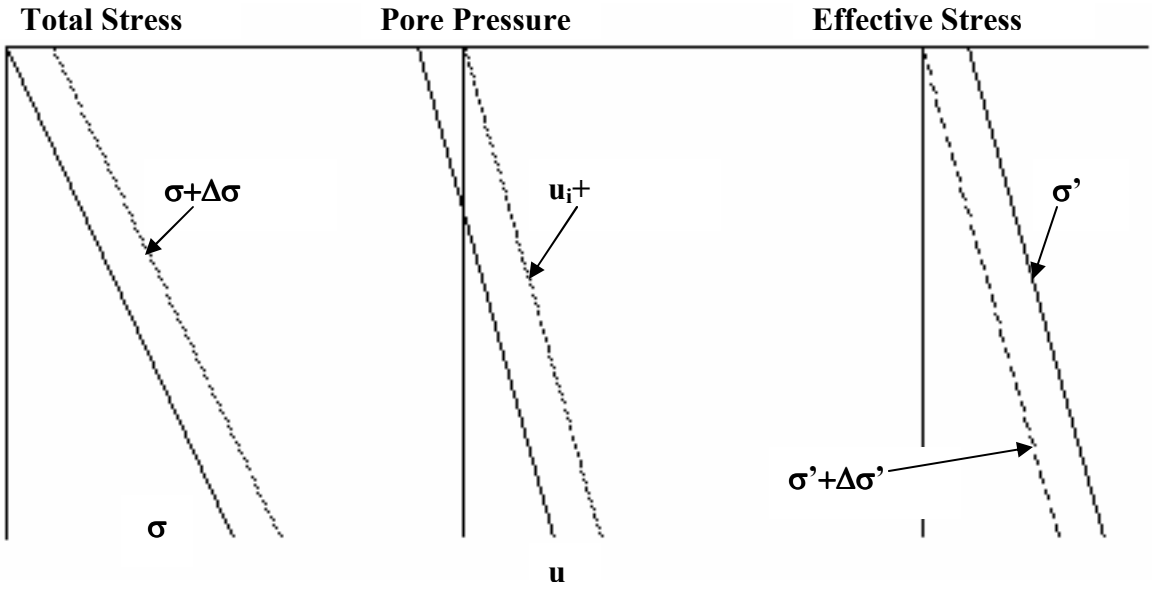

Figure 2-3. Illustration of the Effects of Pore Pressures on the Effective Stresses.

Inspection of field specimens of stripped pavements has revealed that stripping begins at the bottom of layer interfaces and works its way up, stripping mostly the coarse aggregate. This behavior can be explained by the pore pressure mechanism, because:

- The asphalt at the bottom of a pavement layer is in tension upon the application of load and is often subject to prolonged exposure to moisture from water trapped within a granular base course above the subgrade.
- The observed hourglass distribution of air voids in compacted field mixtures, where the top and the bottom of the layer have larger air voids and higher permeability,

but the middle of the layer has lower air voids and less permeability (Masad, Birgisson, Al-Omari, and Cooley, 2005). The higher permeability parts of the compacted layer are more likely to contain moisture, thus resulting in pore pressures due to vehicle loadings. For pavements with "wet feet", where there is a source of moisture underneath the pavement, stripping from the bottom more permeable part of the asphalt layer is therefore more likely.

2.3.5 Hydraulic Scouring

Hydraulic scouring is a mechanism of stripping that is applicable only to surface courses. Stripping due to hydraulic scouring results from the action of vehicle tires on a saturated pavement surface. This causes water to be pressed down into the pavement in front of the tire and immediately sucked away from the pavement behind the tire (Figure 2-4). This compression-tension cycle can move sediment in and out of the pavement, causing scouring. This is believed to contribute to the stripping of the asphalt film from the aggregate.

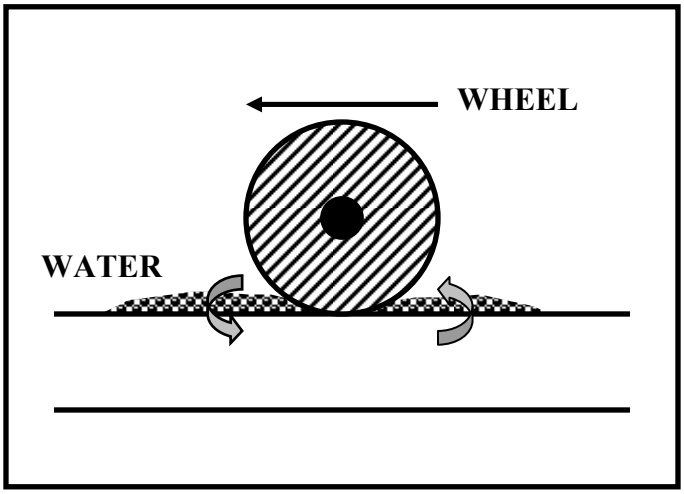

Figure 2-4. Illustration of Stripping by Hydraulic Scouring.

2.4 Anti-Stripping Additives

It is common practice to use anti-stripping (AS) additives to prevent stripping and improve the asphalt pavement performance. Tunnicliff and Root (1984) defined anti-stripping additives as substances that convert the aggregate surface to one that is more

easily wetted with asphalt than water. Both liquid and lime additives are used effectively to resist stripping.

2.4.1 Liquid Additives

Most of the liquid AS agents are surface-active agents, which, when mixed with asphalt cement, reduce surface tension and, therefore, promote increased adhesion to aggregate. The chemical composition of most commercially produced AS agents is proprietary. However, the majority of AS agents currently in use are chemical compounds that contain amines (Kandhal, 1992 and Tunnicliff and Root, 1982). These AS agents must be "heat stable." That is, they should not lose their effectiveness when the modified asphalt cement is stored at high temperatures for a prolonged period of time.

The simplest and most economical way is to mix the AS agent with the asphalt cement in a liquid state prior to mixing the asphalt cement with the aggregate. Although this method is most commonly used, it is inefficient because only a portion of the AS agent reaches the aggregate-asphalt cement interface. Direct application of the AS agent to the aggregate surface is undoubtedly the most efficient way to ensure high quality bonding between the asphalt and the aggregate. However, this is generally not practical because of cost considerations in ensuring full coating of all aggregates, including the dust component. Normally, only small amounts of AS agents (for example 0.5 percent by weight of asphalt cement) are used in the binder.

The amount of AS agent to be used is important. Too little may not be effective and too much may be detrimental to the HMA mix. The long-term effectiveness of liquid AS agents during the service life of the HMA pavements has not been fully established.

Some agencies maintain an approved list of AS agents and require the contractors to use an AS agent in all HMA mixes without conducting any moisture-susceptibility test (Kandhal, 1994).

2.4.2 Lime Additives

Unlike liquid AS agents, which are added to the asphalt cement, lime is added to the aggregate prior to mixing with asphalt cement. Many studies indicate that lime is a very effective anti-stripping agent (e.g. Hicks, 1991; Kandhal, 1994). However, its anti-stripping mechanism is not well understood. Various mechanisms have been postulated, (a) lime interacts with acids in the asphalt cement that are readily absorbed on the aggregate surface, (b) lime provides calcium ions which can replace hydrogen, sodium, potassium and other cations on the aggregate surface, and (c) lime reacts with most silicate aggregates to form a calcium silicate crust which has a strong bond to the aggregate and has sufficient porosity to allow penetration of the asphalt cement to form another strong bond.

Both hydrated lime $Ca(OH)_2$ and quick lime CaO (in slurry form) are effective, although the former is most commonly used. Dolomitic limes have also been used as anti-stripping additives. However, as a carbonate $CaCO_3$, lime is not as effective. Generally, 1 to 1 1/2 percent of lime by weight of dry aggregate is used. Finer aggregates may require higher percentages because of increased aggregate surface area.

Aggregates have been treated with lime by the following four methods (Hicks, 1991):

- Dry hydrated lime: The main problem in using dry lime is to maintain its coating on the aggregate surface until it is coated with asphalt cement. It is more critical in drum mixers, which tend to pick up some of the lime in the exhaust gas flow. However, Georgia DOT has successfully instituted the use of dry hydrated lime in drum mixers by injecting lime into the drum just ahead of the asphalt cement. The

pick up of lime by the gas stream is prevented by modifications of the flights and providing suitable baffles inside the drum (Kennedy, 1984). Some asphalt-paving technologists believe that the use of dry lime is not consistently effective, although many agencies including Georgia DOT report satisfactory results with dry lime.

- Hydrated lime slurry: This method requires additional water to be added to the aggregates which results in increased fuel costs and reduced HMA production rates.

- Dry hydrated lime to wet aggregate: In this method dry hydrated lime is added to wet aggregate, usually containing 3-5 percent water, and then mixed in a pugmill or tumble mixer to obtain a homogeneous mix.

- Hot (Quicklime) slurry: The use of quicklime (CaO) slurry has at least two advantages, (a) its cost is equal to that of hydrated lime, but when slaked the yield is 25 percent greater, and (b) the heat from slaking results in an elevated temperature which helps in the evaporation of the added moisture. However, quicklime should be handled with caution because it can cause skin burns.

The relative effectiveness of the preceding four treatments based on comparative laboratory and field studies have been generally inconclusive and, therefore, increased fuel and equipment costs and decreased HMA production rates associated with the wet process may not be justified at the present time.

2.5 Moisture Susceptibility Tests and Conditioning Systems

To combat stripping, proper mixture design is absolutely essential; however, it is possible for a properly designed mix to strip in the field if water enters into the HMA layer. Therefore, each mixture must be evaluated to determine if it is susceptible to moisture damage.

Numerous test methods have been proposed and used in the past to predict the moisture susceptibility of HMA mixes. (Al-Swailmi and Terrel, 1992; Coplantz and Newcomb, 1988; Hicks, 1991; Kandhal, 1992; Kandhal, 1994; Lottman, 1982a; Stuart, 1986; Stuart, 1990; Terrel and Al-Swailmi, 1994; Tunnicliff and Root, 1984). However, no single test has a wide acceptance, with the possible exception of the Modified Lottman

Test (AASHTO T-283, 1986), which is now a part of the SuperPave™ mixture design protocol. This is due to their overall recognized low reliability and lack of satisfactory relationship between laboratory and field conditions. Only selected test methods, which are commonly used by agencies, will be discussed briefly.

2.5.1 Qualitative or Subjective Tests

There are two main tests of this type. These tests are simple, take little time to complete, and require very little equipment. However, they do not give definitive, analytical results.

2.5.1.1 Boiling Water Test

In this test, loose HMA mix is added to boiling water. ASTM D3625 specifies a 10-minute boiling period. The percentage of the total visible area of the aggregate that retains its original coating after boiling is estimated as above or below 95 percent. This test can be used for initial screening of HMA mixtures. Some agencies use it for quality control during production to determine the presence of an anti-stripping agent. This test method does not involve any strength analysis. Also, determining the stripping of fine aggregate is very difficult. This test method generally favors liquid anti-stripping agents over lime.

2.5.1.2 Static-Immersion Test (AASHTO T-182, 1986)

A sample of HMA mix is immersed in distilled water at 77ºF (25ºC) for 16 to 18 hours. The sample is then observed through water to estimate the percentage of total visible area of the aggregate, which remains coated as above or below 95 percent. Again, this method does not involve any strength test.

2.5.2 Quantitative Strength Tests

The following tests can give quantitative results. In general however, they have not gained very wide acceptance. This is mainly due to their lack of reliability. Also, they can require long test times, complex procedures, or expensive equipment.

2.5.2.1 Lottman Test

Lottman (1982a) developed this method. Nine specimens 4 inches (102 mm) in diameter and 2 ½ inches (64 mm) high are compacted to expected field air void content. Specimens are divided into 3 groups of 3 specimens each. Group 1 is treated as control without any conditioning. Group 2 specimens are vacuum saturated (26 inches or 660 mm Hg) with water for 30 minutes. Group 3 specimens are vacuum saturated like Group 2 and then subjected to a freeze (0ºF or –18ºC for 15 hours) and a thaw (140ºF or 60ºC for 24 hours) cycle. All 9 specimens are tested for resilient modulus (Mr) and/or indirect tensile strength (ITS) at 55ºF (13ºC) or 73ºF (23ºC). A loading rate of 0.065 inch/minute (1.65 mm/minute) is used for the ITS test. Group 2 reflects field performance up to 4 years. Group 3 reflects field performance from 4 to 12 years. Retained tensile strength (TSR) is calculated for Group 2 and Group 3 specimens as follows:

TSR = ITS of Conditioning specimens / ITS of Control specimens

A minimum TSR of 0.70 is recommended by Lottman (1982a) and Maupin (1982) who reported values between 0.70 and 0.75 differentiated between stripping and non-stripping HMA mixtures. It has been argued that the Lottman procedure is too severe because the warm water soak of the vacuum saturated and frozen specimen can develop internal water pressure. However, Stuart (1986) and Parker and Gharaybeh (1987) generally found a good correlation between the laboratory and field results. Oregon has

successfully used this test with a resilient modulus ratio in lieu of tensile strength ratio (TSR).

2.5.2.2 Tunnicliff and Root Method

This method was proposed by Tunnicliff and Root (1984) under NCHRP Project 274. They proposed six specimens to be compacted to 6-8 percent air void content and divided into two groups of three specimens each. Group 1 is treated as control without any conditioning. Group 2 specimens are vacuum saturated (20 inches or 508 mm Hg for about 5 minutes) with water to attain a saturation level of 55 to 80 percent. Specimens saturated more than 80 percent are discarded. The saturated specimens are then soaked in water at 140ºF (60ºC) using a loading rate of 2 inches/minute (51 mm/minute) A minimum TSR of 0.7 to 0.8 is usually specified. The use of a freeze-thaw cycle is not mandated in ASTM D4867-88, which is based on this method. The freeze-thaw cycle is optional. The primary emphasis is on saturation of the specimen, which for a short duration of about 24 hours has been reported to be insufficient to induce moisture-related damage (Coplantz and Newcomb, 1988).

2.5.2.3 Modified Lottman Test (AASHTO T-283)

This method was initially adopted by AASHTO in 1985 (AASHTO, 1986). It combines the good features of the Lottman Test (Lottman, 1982a) and the Tunnicliff and Root Test (Tunnicliff and Root, 1984). Six specimens are compacted to 6-8 percent air void content. Group 1 of three specimens is used as a control. Group 2 specimens are vacuum saturated (55 to 80 percent saturation) with water, and then subjected to one freeze-thaw cycle as proposed by Lottman. All specimens are tested for ITS at 77ºF (25ºC) using a loading rate of 2 inches/minute (51 mm/minute), and the TSR is

determined. A minimum TSR of 0.7 is usually specified. This method is gaining acceptance by the specifying agencies.

2.5.2.4 Immersion-Compression Test (AASHTO T-165)

Six specimens 4 inches (102 mm) in diameter and 4 inches (102 mm) high are compacted with a double plunger with a pressure of 3000 psi (20.7 MPa) for 2 minutes to about 6 percent air void content. Group 1 of three specimens is treated as control. Group 2 specimens are placed in water at 120ºF (49ºC) for 4 days or at 140ºF (60ºC) for 1 one. All specimens are tested for unconfined compressive strength at 77ºF (25ºC) using a 0.2 inch/minute (5.1 mm/minute) loading rate. The retained compressive strength is determined. Many agencies specify at least 70 percent retained strength. This test has produced retained strengths near 100 percent even when stripping is evident. Stuart (1986) has attributed this to the internal pore water pressure and the insensitivity of the compression test to measure the moisture-induced damage properly. Lack of satisfactory precision has been a major problem with this test.

2.5.2.5 Other tests

The California DOT use the moisture-vapor susceptibility, swell test, and film-stripping test. Retained Marshall stability is used in Puerto Rico and some other states.

Evidently, a wide variety of test methods are being used by various agencies. However, no test has proven to be “superior” and can correctly identify a moisture-susceptible mix in all cases. This means that many HMA mixes, which might otherwise perform satisfactory in the field, are likely to be rendered unacceptable if these tests and criteria are used. Also, mixtures that may pass these tests, may not perform well in the field. The lack of robust evaluation and test systems has simply encouraged the increased use of anti-stripping agents in many states.

There are still many concerns and requirements related to the test methods, which need to be addressed:

- Proliferation of test procedures and criteria.
- Reproducibility of most test methods is not satisfactory. For example, small variations in air void content of the specimens can significantly affect the TSR results in the AASHTO T-283 test (Coplantz and Newcomb, 1988).
- Need to consider minimum wet strength (if the desired value can be established) of the conditioned specimens rather than relying solely on the TSR value. For example, some additives increase both dry and wet strengths but might have a low TSR value.
- Lack of satisfactory correlation between laboratory and field performance.

However, based on a survey of states (Kandhal, 1992) it appears that the Modified Lottman Test (AASHTO T-283) is the most widely used test method available at the present time to detect moisture damage in HMA mixes. AASHTO T-283 has been included in SuperPave™ mix design procedures. A minimum TSR of 0.70 is recommended when using this test method. This criterion should be applied to the field-produced rather than laboratory-produced mixes.

According to Choubane, Page, and Musselman (2000), the AASHTO T-283 specified range of moisture saturation may not be appropriate because TSRs of asphalt samples saturated to the lower limit of the range may be significantly different than those saturated to the upper limit. On the other hand, this procedure shows more promise for predicting stripping potential in the laboratory when the saturation level is above 90 percent and a freeze-thaw cycle is considered. A modified AASHTO T-283 procedure is proposed, including a vacuum saturation for 30 minutes with 610 mm of mercury, which represents a level of saturation between 85 to 95 percent, and a freeze-thaw cycle.

2.5.3 Mixture Performance Testing for the Evaluation of Moisture Damage

The Strategic Highway Research Program (SHRP) had two research contracts dealing with moisture susceptibility of HMA mixes. SHRP project A-003A "Performance Related Testing and Measuring of Asphalt-Aggregate Interactions and Mixtures" attempted to develop an improved test method to evaluate moisture susceptibility. SHRP project A-003B "Fundamental Properties of Asphalt-Aggregate Interactions Including Adhesion and Adsorption" studied the fundamental aspects of asphalt- aggregate bonds.

The Net Adsorption Test (NAT) was developed under the SHRP A-003B designation and completed by the National Center for Asphalt Technology (NCAT, 1996). It is a preliminary screening test for matching mineral aggregates and asphalt cement (e.g. Kandhal, 1994) and is based on the principles of adsorption and desorption. A solution of asphalt cement and toluene is introduced and circulated in a reaction column containing the aggregate sample. Once the solution temperature has been stabilized, 4 ml of solution is removed and the absorbance is determined with a spectrophotometer. Fifty grams of minus No. 4 (4.75 mm) aggregate is then added to the column, and the solution is circulated through the aggregate bed for 6.5 hours. A second 4-ml sample of the solution then is removed from the column and the absorbance is again determined. The difference in the absorbance readings is used to determine the amount of asphalt that has been removed from the solution (adsorption) because of the chemical attraction of the aggregate for the molecular components of the asphalt cement. Immediately after the second solution sample is taken, 575 mm of water is added to the column. The solution is then circulated through the system for another 2 hours. A final 4 ml of solution is taken from the column at the end of this time. The increase in the

adsorptivity is a measure of the amount of asphalt cement that is displaced by water molecules (desorption) Additional validation data are needed for the NAT.

The Environmental Conditioning System (ECS) was developed under SHRP project A-003A "Performance Related Testing and Measuring of Asphalt-Aggregate Interactions and Mixtures" (Al-Swailmi and Terrel, 1992; Terrel and Al-Swailmi, 1994), and updated by researchers at the University of Texas, El Paso (Alam, Vemuri, Tandon, Nazarian, and Picornell 1998). This system was designed specifically to evaluate the moisture susceptibility of HMA specimens by resilient modulus testing. To saturate the specimen, the Environmental Conditioning System uses a vacuum-based control panel that draws water through the specimen from a storage reservoir. Simultaneously, temperature conditioned water was cycled around the specimen to get it to a proper temperature for testing. The disadvantage with this configuration is that by flowing ambient temperature water through the specimen, adequate conductance was prevented between the permeant and the confining water. As a result, the actual temperature of the specimen was unknown during testing. The well-known sensitivity of HMA to temperature makes this approach to control questionable. Additionally, the conditioning system is inefficient relying upon a copper coil, which runs through a heated water bath. The pressurized water running through the coil relies upon conductance through the copper to condition it. This configuration required up to 16 hours before the system was stabilized at temperature precluding it from use as a production capable system. Also, the system is limited to testing at temperatures above ambient. The specificity of purpose limited the Environmental Conditioning System's design to resilient modulus testing.

Despite the significant research effort during the SHRP project, the Environmental Conditioning System has never reached acceptance by state agencies.

2.5.4 Other Developments of Interest

Based on the assumption that pore pressures were a major cause of moisture damage in mixtures, Jimenez (1974) developed a test procedure and a device to determine the stripping susceptibility of asphalt. Specimens were vacuum-saturated in a 50ºC (122ºF) water bath and then conditioned by applying a sinusoidal load from 35 to 207 kPa (5 – 30 psi) at a rate of 580 times per minute for 10 minutes. The basic premise of the loading was to induce cyclic pore pressures in the specimen that were believed to be similar to those caused by traffic loads. After conditioning, the samples were placed in a 25ºC water bath for 45 minutes before being tested for the indirect tensile strength that was compared to the indirect tensile strength of an equivalent unconditioned sample. Jimenez (1974) concluded that the new procedure was simple and repeatable but needed field-testing before it could be implemented.

Hydraulic scouring, as a result of repeated generation of pore water pressure, is considered to be the primary cause of moisture-induced damage in asphalt paving mixtures in a paper written by Mallick et al. (2003). A new process was developed for this research. Also, InstroTek, Inc. created a new piece of equipment in order to carry out this procedure (Mallick et al., 2003). Specimens were placed in a chamber that was positioned in a water bath. An immersion heater maintained the water temperature at either 40 or 60ºC depending on the specimen's group. Compressed air was forced into the chamber so that the water is forced out of and below the sample surface. Next, a vacuum was applied that pulled the water back into the chamber. Depending on the specimen's group, this procedure was cycled 2,000, 3,000, 4,000, or 6,000 times. The

tensile strength of the conditioned samples was then compared to the unconditioned samples to determine the retained strength. Mallick et al. (2003) concluded that this procedure gave comparable results with AASHTO T283 but needed further refinement.

2.6 Conclusions

Based on the literature review, the following conclusions can be reached:

- Of the five major potential mechanisms for moisture damage reported in the literature, connecting theoretical considerations to observed field behavior has proved none. Rather, these mechanisms are hypothesized based on field observation, along with limited basic laboratory characterization.

- There are currently no performance-based methods for evaluating moisture damage available that have been widely accepted by state agencies.

- The methods used to evaluate moisture susceptibility of mixtures tend to be either qualitative in nature, like the boil test, or crude quantitative techniques that may neither include the appropriate mechanism of moisture damage nor the appropriate framework for analyzing the effects of moisture damage on mixtures. These current laboratory testing procedures currently available, including the AASHTO T-283 procedure, were primarily developed to determine the degree of resistance to moisture damage by a particular combination of asphalt and aggregate, compare mixes composed of different types and quantities of aggregate, or to evaluate the effectiveness of anti-stripping agents (Al-Swailmi and Terrel, 1992; Curtis, Stroup-Gardiner, Brannan, and Jones, 1992; Lottman, 1982a; Terrel and Al-Swailmi, 1994; Tunnicliff and Root, 1984). These moisture susceptibility tests all evaluate the effects of water damage in the laboratory by measuring the relative change of a single parameter before and after conditioning (i.e., Tensile Strength Ratio, Resilient Modulus Ratio). These parameters do not distinguish between the different mechanisms present in a conditioned mixture, including the identification of the effects of pore water versus actual moisture damage.

- The current SuperPave^{TM} specification uses the AASHTO T-283 moisture susceptibility test for determining moisture sensitive mixtures. Most state agencies use the AASHTO T-283 test, although there have been questions by the community at large about the accuracy of the test. Frequent false positives and/or negatives have been reported, leading to the initiation of current studies, including a larger national study sponsored by the National Cooperative Highway Research Program (NCHRP) and entitled "NCHRP Project 9-34: Improved Conditioning Procedure for Predicting the Moisture Susceptibility of HMA Pavements."

- Depending on materials, loading, and environment, it may be that one or all of the mechanisms of water damage are present and dominant in an actual pavement. However, for a proper evaluation of any given mixture and testing procedure, it is

necessary to isolate and quantify the effects of each of the predominant mechanisms contributing to moisture damage. Water damage effects in HMA pavements may be bracketed by two extreme conditions, 1) the rapid application of cyclic pore pressures under saturated conditions that correspond to critical field conditions, and 2) the longer term continuous low level exposure to water without pore pressures. However, little research has been conducted to further clarify the most important condition – i.e. pore pressures or long term continuous low-level exposure.

In summary, there is a clear need to develop a robust performance-based framework for the evaluation of mixture moisture damage susceptibility, as well as identifying the most likely basic mechanisms of moisture damage in pavements, and finally developing an appropriate conditioning system based on this mechanism.

CHAPTER 3
MATERIALS AND METHODOLOGY

3.1 Materials

The mixing formulas for the asphalt cement used in this research were obtained from previous research conducted at the University of Florida by Dr. Bjorn Birgisson. Six limestone gradations were prepared through research performed by Nukunya (2001). Later research performed by Jaganatha Katkuri and Tipakorn Samarnrak produced granite gradations that were volumetrically equivalent to the limestone gradations. The appropriate amount of liquid asphalt was determined for each gradation as explained later in this chapter.

The limestone aggregate was obtained from the Whiterock mine in southern Florida. The granite aggregate (GA185) was attained from Georgia. Finally, AC-30 liquid asphalt was used for all research described herein.

3.1.1 Limestone

The limestone mix was made up of four components, coarse aggregate (S1A), intermediate aggregate (S1B), whiterock screenings, and mineral filler. They were blended together in different proportions to form a total of six total hot mix asphalt (HMA) mixtures of coarse and fine gradations (Nukunya, 2001; Nukunya, Roque, Tia, and Birgisson, 2001). Two previously designed SuperPave^{TM} mixtures prepared by the Florida Department of Transportation (FDOT) were used as the basis for this research. One of these was a coarse-graded mixture (C1) and one was a fine-graded mixture (F1). Two gradations were then produced by changing the coarse portions (larger than no. 8

sieve size) and two gradations were created by altering the fine portions of the gradation curve. The six limestone mixtures that were fashioned were C1, C2, C3, F1, F2, and F3/C4. The F3/C4 mixture was derived from the fine mixture (F1), but was adjusted so that it fell below the restricted zone and is thus a coarse-graded mixture. The gradations for these mixtures are shown in Table 3-1.

Table 3-1. Gradations for the Limestone Mixtures.

	Percent Passing					
Sieve Size	C1	C2	C3	F1	F2	F3/C4
19 (3/4)	100	100	100	100	100	100
12.5 (1/2)	97	91	98	96	91	95
9.5 (3/8)	90	74	89	85	78	85
4.75 (#4)	60	47	57	69	61	67
2.36 (#8)	33	30	36	53	44	37
1.18 (#16)	20	20	24	34	35	26
600 (#30)	15	14	18	23	24	20
300 (#50)	11	10	13	15	16	14
150 (#100)	7.6	6.7	9.2	9.6	9.1	8.6
75 (#200)	4.8	4.8	6.3	4.8	6.3	5.8

3.1.2 Granite

The granite mixes were also made up of a coarse aggregate (# 7 stone), intermediate aggregate (# 89 stone), screenings (W-10 granite screenings), and a mineral filler (granite dust). The granite gradations were developed to be volumetrically equivalent to the limestone gradations as mentioned above; however, the granite designs used only one material for each sieve size (i.e. all of the # 4 sieve size comes from # 89 stone). This was done to minimize error and because each of the types of granite produced large amounts of certain sieve sizes but little amounts of the others. An example of this is that 91 percent of the # 89 stone is retained on the # 4 sieve.

The conversion process started out with determining the specific gravity of each type of aggregate. This information was used to determine the volume of each sieve size retained for each type of limestone that contributed to a mix. Next, the sum of the

Table 3-2. Conversion of an F1 Limestone Mix to an F1 Granite Mix

Sieve size	S1a Whiterock Weight	WR/GA Vol.	Using Vol.	Ga # 7 Weight	S1b Whiterock Weight	WR/GA Vol.	Using Vol.	Ga # 89 Weight
12.5(1/2)	231	94.7	94.7	255	0	0	0	0
9.5(3/8)	402	164.7	192.9	519.6	69.1	28.3	0	0
4.75(#4)	220	90.2	0	0	553.8	226.8	317	852.4
2.36(#8)	33	13.5	0	0	391.7	160.4	0	0
1.18(#16)	7	3	0	0	56	22.9	0	0
600(#30)	2	0.7	0	0	9.1	3.7	0	0
300(#50)	2	0.7	0	0	3.4	1.4	0	0
150(#100)	3	1.1	0	0	13.7	5.6	0	0
75(#200)	4	1.5	0	0	13.7	5.6	0	0
<75(#200)	10	4.1	0	0	32	13.1	0	0
Sp. Gr.	2.441			2.693	2.442			2.689

Table 3-2. continued

Sieve size	Whiterock Screen Wt	WR/GA Vol	Using Vol.	W-10 Screen Wt	Whiterock filler Wt	WR/GA Vol	Using Vol.	Granite filler Wt	Total Weight
12.5(1/2)	0	0	0	0	0	0	0	0	255
9.5(3/8)	0	0	0	0	0	0	0	0	519.6
4.75(#4)	0	0	0	0	0	0	0	0	852.4
2.36(#8)	347.7	137.2	311.1	834.3	0	0	0	0	834.3
1.18(#16)	693	273.5	299.4	803	0	0	0	0	803
600(#30)	522.8	206.3	210.8	565.3	0	0	0	0	565.3
300(#50)	366.9	144.8	146.9	394.1	0	0	0	0	394.1
150(#100)	304.5	120.2	126.9	340.4	0	0	0	0	340.4
75(#200)	100.7	39.7	46.9	125.7	0	0	0	0	125.7
<75(#200)	62.3	24.6	0	0	46.1	17	58.8	159.4	159.4
									4849.1
Sp. Gr.	2.534				2.682	2.71			2.71

volume for each sieve size was found and converted into weight of granite needed. Table 3-2 shows an example of converting a 4,500-gram F1 limestone mix design to an F1 granite mix design.

3.1.3 Liquid Asphalt

The optimum amount of liquid asphalt was determined for each mix. The optimum amount of asphalt for this research was the percent of the sample, by mass, that the asphalt binder would contribute (P_b) for the sample to have 4.0% ± 0.5% air voids (V_a) when compacted to the design number of gyrations (N_{des}) – 109 gyrations for this research. This was found using calculations after the theoretical maximum specific gravity (G_{mm}) of the asphalt covered aggregate and the bulk specific gravity (G_{mb}) of the compacted sample were determined (see section 3.2.2). The mass of asphalt needed for each mixture (derived from the calculated P_b for that mixture) was added to the mix design to create a batch sheet. A different batch sheet was made for each size (four inches in diameter by six inches in height and six inches in diameter by six inches in height) of each mix.

3.2 Methodology

3.2.1 Sample Preparation

The following procedure was used to create compacted samples for this research. Raw aggregate was placed in metal pans in an oven at 260ºF (127ºC) for 8 to 12 hours to ensure that it was dry. This aggregate was then sieved and stored by sieve size. A batch of aggregate for a sample was created using the mix design of a particular batch sheet. The batch, mixing tools, and asphalt were placed in an oven at 300ºF (149ºC) for 2.5 to 3 hours. The batch was then placed in a mixing mould. The correct mass of liquid asphalt

was added according to the batch sheet. The liquid asphalt and the aggregate were thoroughly mixed in order to assure that every piece of aggregate was coated.

The mixed sample was placed in a pan and reheated in an oven at 275ºF (135ºC) for 2 hours along with the compacting tools and mould. The IPC Servopac SuperPave™ gyratory compactor was set to have an angle of inclination of 1.25º, a vertical pressure of 600 kPa (87 psi), a revolutionary rate of 30 gyrations per minute, to compact either a 4-inch diameter or 6-inch diameter sample, and to compact to a specified height. The specific height was determined per mix and was calculated to achieve a density in the sample that would generate a 7.0 ± 0.5 % of air voids. The sample was poured into the mould as a mound (so that the distribution of the sizes of the aggregate would remain as disbursed as possible) with a piece of filter paper below and above the sample. The computer program was started once a top platen was fitted in the mould (above the filter paper) and the mould was set in place in the gyratory compactor. The specimen was extruded from the mould once it was compacted. The filter paper was removed and the compacted sample was left to cool to room temperature.

3.2.2 Determining if a Sample Is Useable

This section explains how it was determined if a compacted sample met the criteria for use in this research and is consistent with AASHTO procedure T 166-93, Bulk Specific Gravity of Compacted Bituminous Mixtures Using Saturated Surface-Dry Specimens. The compacted specimen (pill) was allowed to cool for 24 hours after it had been prepared. The mass of the dry pill was measured and recorded as the dry mass (A). The pill was then submerged in a tank of water and suspended from a cable attached to the scale. The mass of the saturated sample was recorded after three minutes had passed

and the scale had stabilized. This number was recorded as the submerged mass (C), along with the temperature of the water in the tank.

The pill was then removed and a damp cloth was used to eliminate the water from the surface of the sample. The mass of the sample was again noted. This time it was recorded as the saturated surface-dry, or SSD, mass (B). Finally, the bulk specific gravity of the sample was calculated using the following formula:

$$G_{mb} = A/[B-(C*w)] \qquad \text{(Equation 3-1)}$$

where: G_{mb} = bulk specific gravity

A = dry mass (g)

B = SSD mass (g)

C = mass of sample in water (g)

w = correction factor for the water temperature (i.e., w = 1 at 25ºC)

While the G_{mb} must be calculated for each sample, the theoretical maximum specific gravity (G_{mm}) was specific and standard for each mix. The G_{mm} for each mix was determined by performing the Rice theoretical maximum specific gravity test, which was consistent with AASHTO procedure T 209-94, Theoretical Maximum Specific Gravity and Density of Bituminous Paving Mixtures.

A loose sample of asphalt-covered aggregate was created for the mix formula being tested. The sample was first measured for its dry mass (A). It was then placed in a beaker, covered in water, and placed under a vacuum to remove all the air from the aggregate. The weight of this submerged, saturated sample was then recorded as the weight of the beaker filled with the sample and water at 25ºC (E).

The sample was removed from the beaker and dried to the SSD condition. The majority of the water was drained and then the remaining water was allowed to evaporate. The moist sample was weighed every 15 minutes. The SSD condition was met when the change in weight was less than 0.5 grams during one 15-minute period and thus recorded as the mass of the SSD condition (B). The theoretical maximum specific gravity was calculated by the following formula:

$$G_{mm} = A/(B+D-E) \qquad \text{(Equation 3-2)}$$

where: G_{mm} = theoretical maximum specific gravity

A = dry mass (g)

B = SSD mass (g)

D = mass of the beaker filled with water at 25ºC (g)

E = mass of the beaker filled with the sample and water at 25ºC (g)

The percentage of air voids (V_a) in a compacted pill could then be calculated. This was found by the following formula:

$$V_a = (1- G_{mb}/G_{mm}) \times 100 \qquad \text{(Equation 3-3)}$$

The sample was considered acceptable for testing in this research project if the V_a was 7.0 ± 0.5 %.

3.2.3 Sample Testing

The samples were tested for their usability (see section 3.2.2) and then cut to a proper size. The 6-inch diameter samples were cut to be a height of 50 ± 5 mm (1.96 ± 0.2 in) and then used in a permeability test (see Chapter 5). The 4-inch diameter samples were cut to be a height of approximately 110 mm (4.3 in) and then conditioned (see Chapter 6).

After allowing them to dry for 36 hours, the conditioned samples were cut into three pucks of equivalent height with a wet saw. These pucks were rinsed to remove excess particles and left to dry. Once dry, four aluminum buttons were glued to either side of the puck in the shape of a square with the caddy-corner buttons located an inch apart. This was done in accordance with the setup of specimens that are to be tested in the indirect tensile (IDT) machine. The samples were then placed in a dehumidifier chamber for 48 hours to dry them of any remaining moisture and bring them to a constant humidity level. The specimens were then placed inside the environmental chamber of the SuperPave™ IDT machine for eight hours. This was to insure that the entire puck would acclimate to the temperature inside of the environmental chamber. The environmental chamber was set to a temperature of 10ºC (50ºF) for this research. Lastly, the samples were tested for several characteristics including their resilient modulus, fracture energy, creep compliance, and indirect tensile strength.

CHAPTER 4
PROPOSED CONDITIONING SYSTEM

The framework for the consistent evaluation of moisture damage has been established, and pore pressures have been identified as a likely major mechanism of premature moisture damage in mixtures. However, there is still a need to develop a moisture conditioning system that more closely simulates the primary mechanism of moisture damage in the field, namely cyclic pore pressures. In this chapter, a new cyclic loading and pore pressure conditioning system, based on a modified triaxial chamber, will be developed. The basic idea behind this system is to be able to both apply cyclic pore pressure and loads at the same time, if needed. If only pore pressures are desired for conditioning of mixtures, the current system could be greatly simplified into a self-contained tabletop system that would not require an external loading frame.

In the following, the basis for the development of this new system will be discussed, followed by a discussion on the design of the system, as well as basic plumbing and environmental control considerations.

4.1 Background

The cyclic loading and pore pressure conditioning system is a modified triaxial system designed specifically for the cyclic pore pressure conditioning of asphalt specimens. The concept of the cyclic loading and pore pressure conditioning system was prompted by the need to analyze better the effects of water-induced damage to an asphalt mixture. Conditioning a specimen in the triaxial environment allows for precise application of stress in three different directions, if needed. If a specimen is thought of as

a cube, these directions can be represented in the familiar x-y-z coordinate system. The laboratory created specimens are cylindrically shaped, thereby reducing the coordinate system to an axial vector (y) and a sum of radial vectors (x). These vectors, acting normal to the surface of the specimen, can be increased or decreased in a multitude of combinations allowing control of axial and confining stresses onto the specimen.

For years, the triaxial cell has been used by the geotechnical engineering community to assimilate insitu stresses on the specimen of interest and then, through deviation of the confining and axial stresses, quantify the material's reaction to an anticipated load. The advantage of soil testing in a controlled environment is of significant value and allows the engineer greater control than could be acquired in the field. At present, there are several systems in different stages of development that attempt to simulate field conditions while, at the same time, producing a testing sequence that is simpler and more accurate than systems presently used. The cyclic loading and pore pressure conditioning system is unique amongst other systems used today in that the system is designed to be versatile and comprehensive with respect to specimen testing and conditioning.

As with soil, asphalt concrete specimens have long been tested in a triaxial cell. Tests such as hydraulic conductivity (permeability), resilient modulus, complex modulus, shear strength, and creep are common in asphalt test laboratories using a triaxial device. A distinct limitation to the triaxial cells constructed today as compared with the cyclic loading and pore pressure conditioning system is the design of the force application piston and how it transfers stress onto the specimen. Traditionally, these platens are no more than a disk of rigid material that acts as a medium between the force from a shaft

and the specimen itself. The limitation occurs when stress is applied to the circumferential surface as occurs when confining stress is applied. As the confining stress increases, so too does the axial stress onto the specimen. This relationship limits the stress combinations and stress paths that can be applied onto the specimen. The initial design of the cyclic loading and pore pressure conditioning system addressed this problem by designing a top platen (piston) encased within a sleeve. This piston-sleeve design relieves the researcher of the limitation of stress paths by allowing the axial and confining stresses to be independent of one another, thereby allowing for greater control and flexibility with applied stresses. In addition, the system is designed to allow for in-place conditioning with the support of an external water temperature conditioner as well as the ability to perform both constant and falling head permeability testing without removing the specimen from the test cell. These added benefits allow for a sequence of testing and/or conditioning to be performed without the risk of damage to the specimen during transportation from one test setup to another. Also, the additional integral capabilities of the cyclic loading and pore pressure conditioning system diminish the need for auxiliary equipment required to perform testing of conditioned specimens.

4.2 Design Considerations

Prior to the commencement of the system design, a full understanding of the end purpose of the system needed to be defined. The system needed to be capable of performing tests in compression and tension, as well as applying pore pressures both independent and in conjunction with loading. As a result, the structural frame of the cell needed to be designed to allow for the corresponding forces. The tests would all be performed in effective stress state conditions, thereby creating the need to develop a saturation procedure. And lastly, the system needed to be capable of getting a specimen

to a stabilized temperature rapidly and maintain that temperature throughout the duration of the test.

Saturation of specimens, particularly those composed of soil, in triaxial cells is typically achieved by pulling permeant through the specimen's structure using vacuum techniques. For the design of the cyclic loading and pore pressure conditioning system, allowance was made so that the system would be capable of applying a vacuum as well as forcing the permeant through the specimen from the influent end.

The variation in test data, as a result of inconsistent specimen temperature during testing, is well known and of foremost concern for a test requiring a high degree of precision. Hot mix asphalt is extremely temperature susceptible (e.g. Roberts, Kandahl, Brown, Lee, and Kennedy, 1996). Repeatability of tests such as resilient modulus (M_r) determination is very unlikely if specimen groups are tested at varying temperatures. For this reason, the creation of a system that would be capable of achieving target temperature rapidly and continue to maintain that temperature throughout testing was a criterion for design.

The achievement of heating and cooling of water used in existing triaxial testing systems used at the University of Florida and in many systems are through indirect methods. Heating is achieved via conduction from thermo probes onto the base plate. The base plate would, in turn, heat the confining water. Thermo probes are commercially available and operate much like the surface heating coil on an electric stove. As electricity is passed through the probe, resistance is developed that transforms the electrical energy to heat. Typically, two probes, approximately 0.375 inches in diameter and 8 inches long, fit into the base plate of the cell via smooth borings that run parallel to

one another. The main disadvantage of this design is that the cell acts as a heat sink, requiring that it be heated prior to the confining water. The specimen is then reliant upon the conduction of heat from the confining water in order to arrive at the test temperature. The combined mass of steel and water requires a large amount of time and energy to arrive at the test temperature. Additionally, cooling of the confining water is achieved via indirect methods. Chilled water is circulated through a copper coil that travels around the exterior surface of the confining cylinder. To minimize the absorption of thermal energy from the atmosphere, the cell was wrapped with a plastic-encased sheet of fiberglass insulation. Although the insulation impedes the absorption of unwanted thermal energy, it is not completely effective and the achievement of low temperatures is not possible due to the inefficiency of the system. As with the method of heating, this configuration must condition the temperature of the cell prior to the confining water, thereby creating a lengthy conditioning period.

It was recognized early in this process that a direct method of water conditioning would need to be developed that would be capable of readying a specimen in a reasonable amount of time as to make the system useful in production testing. The rapid achievement of test temperature was largely based upon three factors:

- The selection of properly sized cooling and heating devices.
- Reduction of the length of transmission lines in order to minimize thermal losses or gains.
- The minimization of the volume of confining water space within the cell thereby minimizing the amount of energy required by the temperature conditioner to be either removed or added to the water.

The overall appearance of the cell is very typical of other existing triaxial cells. The structural core consists of two round plates separated by posts or what are referred to

in this report as struts. The structural core is encased with a cylinder and the entire package is sealed which creates an enclosed cavity capable of being pressurized. The variable of the cell's design is the proportionality of these components. The dimensions of the test specimen dictated much of the subsequent design of cell components. The diameter of specimens used with this cell was decided as 4 inches (100 millimeters). This system was developed as a prototype and it was deemed prudent to ensure it could operate properly before designing a cell capable of testing larger specimens (6 inches or 150 mm). Additionally, as the diameter of the specimen increases, the overall size of the cell increases in a near proportional manner. Therefore, in an attempt to balance overall size and cost to manufacture, the smaller specimen size was chosen.

The system was designed as a self-contained testing device. In order to achieve a saturated specimen, backpressure saturation techniques would be required. The integration of a vacuum device capable of relieving at least one atmosphere of pressure to assist with the liberation of air trapped in the specimen was required.

Although a prototype, the system was intended for use in production testing. The process for specimen installation was examined as the cell design progressed. Owing to the complexity of the installation of instrumentation used to monitor the specimen, AutoCAD generated schematics were used to ensure that these instruments could be installed in conjunction with the specimen. Traditional triaxial tests, M_r tests, and Complex Modulus tests also required that a latex membrane be placed over the specimen and overlapped over the end platens. This step is critical for ensuring the isolation of the saturated specimen from the confining water. Therefore, consideration was given to the allowances required to enable the operator to successfully position this membrane in a

limited space in order that the overall size of the cell be minimized as greatly as possible. For this, several mockups were made to determine which combination of configuration and spacing provided the optimum balance of size and function.

While trying to develop a modified Environmental Conditioning System (ECS) at the University of Texas, El Paso (Alam et al., 1998), one of the problems experienced was the lack of rigidity with the system as a whole. This lack of rigidity could contribute to erroneous data as a result of linear displacement of the specimen during dynamic testing since the system will deform slightly when induced by high-pressure loads. To avoid such a problem with this system, connectivity of components of the cell was examined prior to the construction. Where components interfaced with an o-ring incorporated to act as a seal, allowance was made to ensure that the groove in which the o-ring was seated provided proper volume to contain the compressed seal. This would allow the mating components to achieve surface-to-surface contact thereby producing a rigid connection. The center vertical core of the cell is configured to allow for all forces from the piston to be directed normal to the base plate without rotation or movement from an inclusive component. The base platen and piston employ both end bearing and thread bearing from a threaded rod and piston shaft respectively. This compliment of connectivity creates an extremely stable union of components.

Finally, a great effort was made to produce a system that not only would be simple to manufacture and operate, but would also be as cost effective as requirements would allow. Utilizing available raw metal shapes and specifying proper tolerances of machining constructed a relatively inexpensive cell. Components that required a high

degree of machining effort, such as the top and base platen, were specified only after being investigated for alternative design and necessity for the desired function of the cell.

4.3 Construction and Design

The cyclic loading and pore pressure conditioning system is composed of six sub systems:

1. Modified triaxial cell
2. High-pressure water distribution system
3. Data acquisition system (Material Testing Systems (MTS) Model 810)
4. Hydraulic load frame (MTS 22 kip)
5. Low temperature water conditioner
6. High temperature water conditioner

A schematic of the system components is shown in Figure 4-1. Although the conditioning of samples at temperatures below room temperature was not used during the

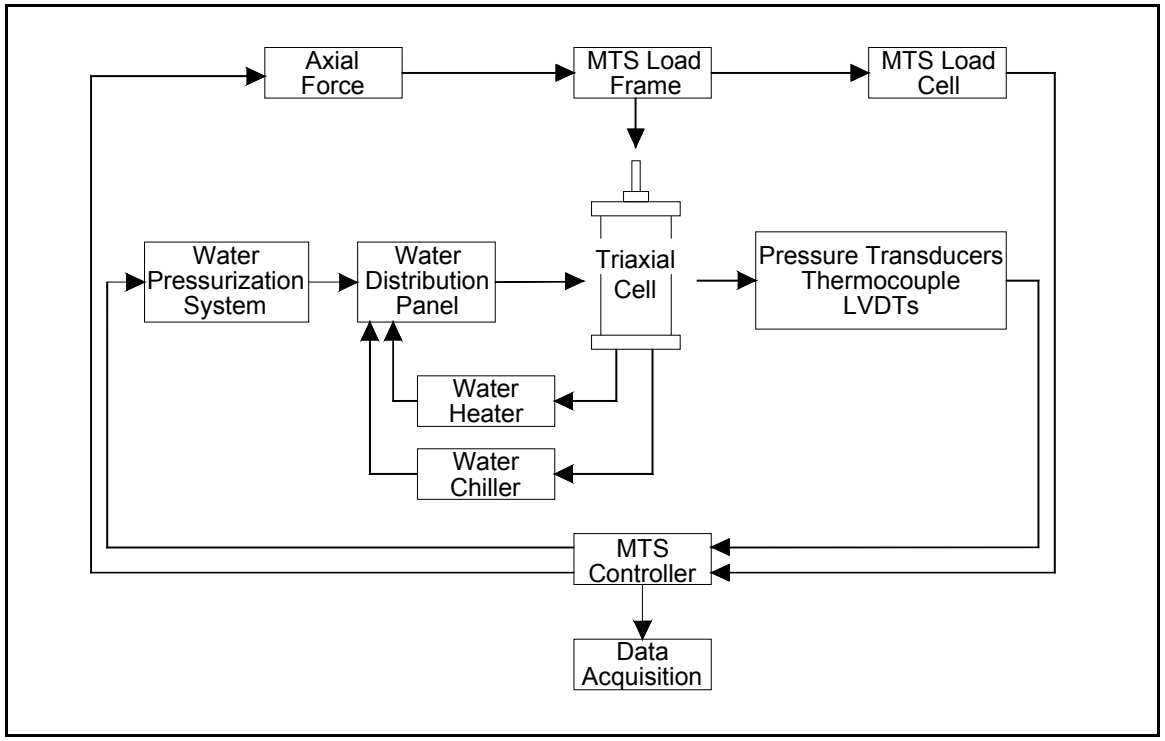

Figure 4-1. Schematic of the Cyclic Loading and Pore Pressure Conditioning System Components.

research reflected in this paper, the ability to do this was an integral part of the design of the cyclic loading and pore pressure conditioning system.

4.3.1 Cyclic Loading and Pore Pressure Conditioning System Design

The design for the modified triaxial cell was approached in the following order:

1. Determination of parameters of targeted testing that dictated design elements of the cell (e.g., size of specimens to be tested, instrumentation to be integrated with the cell, and system pressure)
2. Piston assembly design
3. Top and base plate design
4. Strut design and bearing capacity calculation
5. End platen design
6. Confining cylinder selection
7. Confining ring design
8. Seal selection and placement
9. Component tolerance specification
10. Radial LVDT holder design

4.3.1.1 Design parameters determination

The design specimen height was arrived at as a compromise between recommended aspect ratios for the two primary tests of the system, hydraulic conductivity (permeability) and resilient modulus. During the literature review of permeability testing, an aspect ratio recommendation was found to be from 0.5 to 1.0 (Carpenter and Stephenson, 1986). This translates into a specimen height of 2-4 inches (50-100 millimeters). The recommended aspect ratio of a specimen for resilient modulus testing is 1.50, which translated into a specimen 6 inches (150 millimeters) high. A

compromised design specimen height of 5.5 inches (137.5 millimeters) was decided upon in order to facilitate both of these tests into one device.

The cell was also designed for the development of a new test in which large confining pressures would be placed onto the specimen to induce a failure in tension. This meant that the cell would be expected to contain larger pressures than those in typical triaxial cells. Based upon the mechanics of the anticipated failure, the cell was designed to contain 400 psi of fluid pressure.

At this point in the design process, as with all new equipment development, reasonable engineering judgment needed to be applied for certain parameters. One of these parameters is the length of piston stroke required for the desired test. As will be discussed later, the design of the top platen assembly required that the maximum stroke length be minimized to maintain sealing integrity. Based on review of previous compression to failure testing, the maximum stroke length was concluded to be 0.75 inches.

Another issue of design was how large the cell needed to be made in order to minimize structural stresses and facilitate specimen installation. A thorough effort was made to limit the overall size of the cell without making it so compact as to interfere with specimen installation and subsequent data acquisition instrumentation such as linear variable displacement transducers (LVDTs). This effort was made out of structural concerns with regards to the sizing of the supporting struts (vertical support members) compared to the end area of the cell. As the interior diameter of the cell increased, so too did the diameter of the four supporting struts required to restrain the resulting force on the top and bottom plates of the cell. The four struts that maintain the position of the

base and top plates are analogous to the columns of a building. However, unlike columns, the struts must maintain forces in tension since the interior of the cell is pressurized. Therefore, the resulting tension forces acting on the struts will increase as the end areas of the cell (top and base plates) increase. An optimization of end area versus strut diameter was performed to produce an interior cell cavity that was adequately sized to install instrumentation, yet compact enough for reasonable structural component sizing. The cell is intended for 4-inch (100 millimeter) diameter specimens with an aspect ratio of 1.25-1.50. Side views of the cell components are shown in Figures 4-2

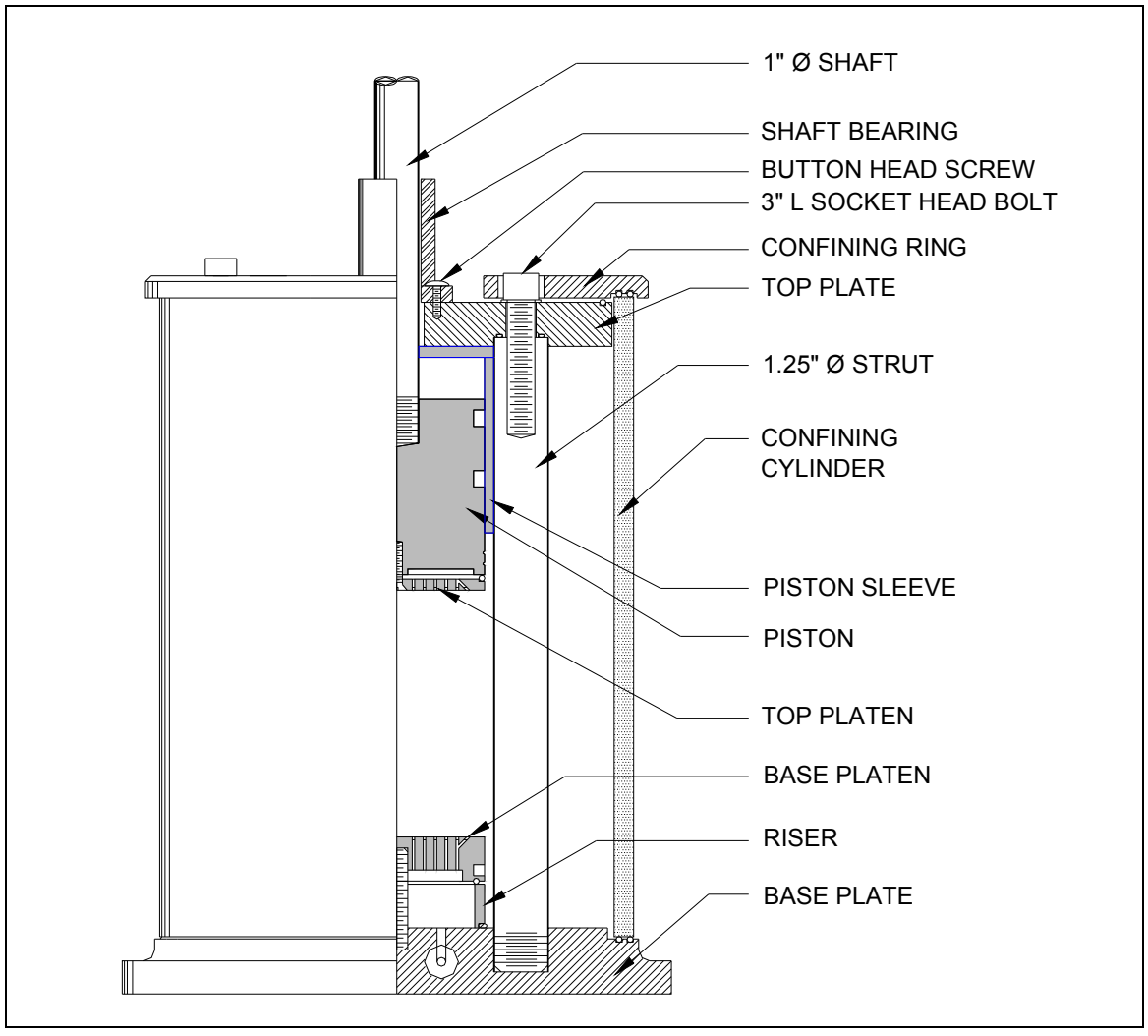

Figure 4-2. Cut-away of the Loading and Conditioning Triaxial Cell—Front View.

and 4-3. All components are fabricated of 303 stainless steel with the exception of the piston, end platens, and the confining cylinder, which were made from 6061-T6 aluminum. Stainless steel was chosen for four reasons, 1) availability, 2) high strength to unit area ratio, 3) ease of machining, and 4) corrosion resistance. Aluminum was the logical choice for components such as the confining cylinder where weight was an issue and the end platens and piston where intricate design details precluded the use of hardened steel.

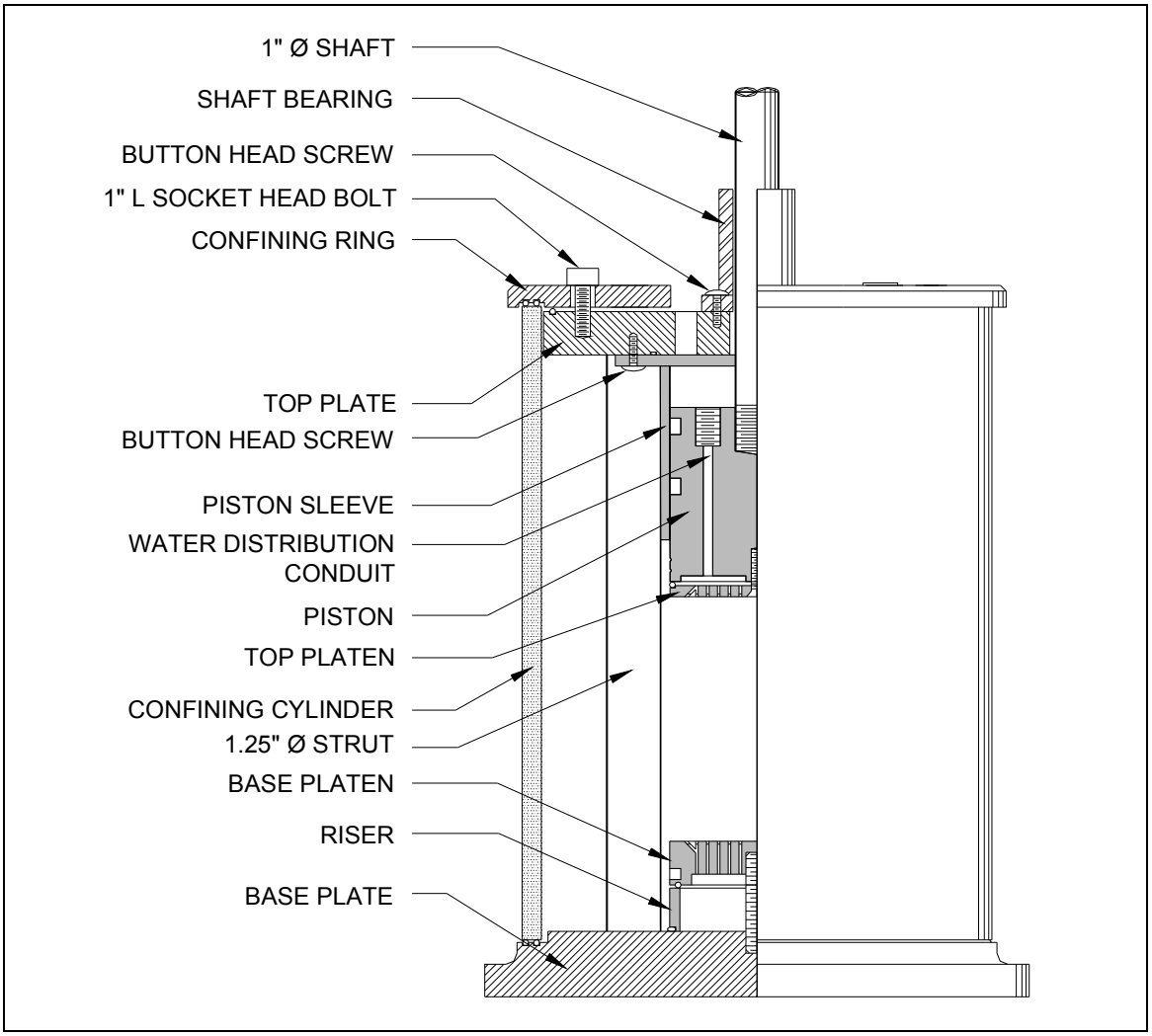

Figure 4-3. Cut-away of the Loading and Conditioning Triaxial Cell—Rotated 45º from Front View.

Throughout the design process, corrosion control of components was a factor of material selection. Owing to the aggressive environment that these components operate in, the potential for reaction between dissimilar metals was an issue for design. Aluminum and stainless steel are considered "compatible", as shown in galvanic series charts, when one material is finished with at least one coat of anodizing primer (Juvinall, 1983). Where aluminum was used, these components were anodized to retard the corrosion process. Anodizing of aluminum alloys produces a stable aluminum oxide film that provides substantial corrosion resistance (Juvinall, 1983). Additionally, separation between aluminum and stainless steel components was provided via buna-N o-rings, which further assisted with the dampening of electrical current flow through the dissimilar metal interface.

With the major design parameters defined, efforts were directed to the design of the individual components.

4.3.1.2 Piston assembly design

The piston assembly was a logical place to begin the design process in that it dictated many of the subsequent component designs. It was imperative that the sizing and function of the piston assembly be determined prior to the design and manufacture of the remaining cell components. As was previously mentioned, the most prominent distinction between the cyclic loading and pore pressure conditioning system and traditionally manufactured cells is the piston-sleeve assembly. The challenge of the design was to create an assembly that would yield low frictional contributions while simultaneously providing a leak-proof barrier between the interface of the cell and the atmosphere. The initial piston-sleeve assembly design consisted of a Frelon® bearing for a sleeve and a custom fabricated stainless steel cylinder for a piston. A Frelon® bearing

is a commonly used bearing constructed of a hollow, aluminum cylinder that is lined with a sheet of the low-friction material Frelon®. The opinion at the time was that the Frelon® bearing would act as a low friction surface for the cylinder to cycle on while, at the same time, preventing water from emigrating from the triaxial cell interior, past the Frelon® bearing, and to the exterior of the cell. The foremost advantage to this design was the immediate availability of the bearing from several suppliers with bore diameters of 4 inch and 6 inch common. After procuring a bearing for a determination of suitability, several weaknesses were discovered. First, the sheet of Frelon® that lines the bore is glued to the inside of the aluminum cylinder and results in a poor quality seam where the two ends of the sheet union. After consideration, it was decided that this seam would not be capable of restraining the increasing water pressure from within the cell during a typical testing sequence. Secondly, the roundness from true of the interior of the bearing (bore) varied in excess of 0.003 inches in diameter that would make the complimentary mating of a piston difficult. After consulting with several area machinists, it was concluded that even if a matching piston could be manufactured, the precision required between the piston and the Frelon® bearing to accomplish the aforementioned goals is too high and not practical nor cost effective for the project.

The next consideration for a piston assembly was more tolerant of geometric imperfections and proved easier and less costly to fabricate. The piston assembly is composed of two main components, a piston sleeve and a piston. The piston sleeve is affixed to the top plate of the cell and acts as a fixed member for the piston to travel within. As is illustrated in Figure 4-4, the piston sleeve was constructed using stainless steel. This material was selected for its ability to be machined to very high tolerances

and polished for low frictional contributions of seals in contact with the interior surface. Additionally, this component required welding as part of its manufacture thereby dismissing aluminum as a viable candidate. As can be seen in Figure 4-4, the piston sleeve contains a flanged ring allowing for the passage of bolts to secure it to the top plate. This flanged ring was welded to the tubular portion of the piston sleeve, which made fabrication costs lower than if the piston were to be machined from a solid piece of material. The utilization of available geometric shapes and sizes from material suppliers not only expedited the construction process, but also aided with the creation of a cost-effective cell.

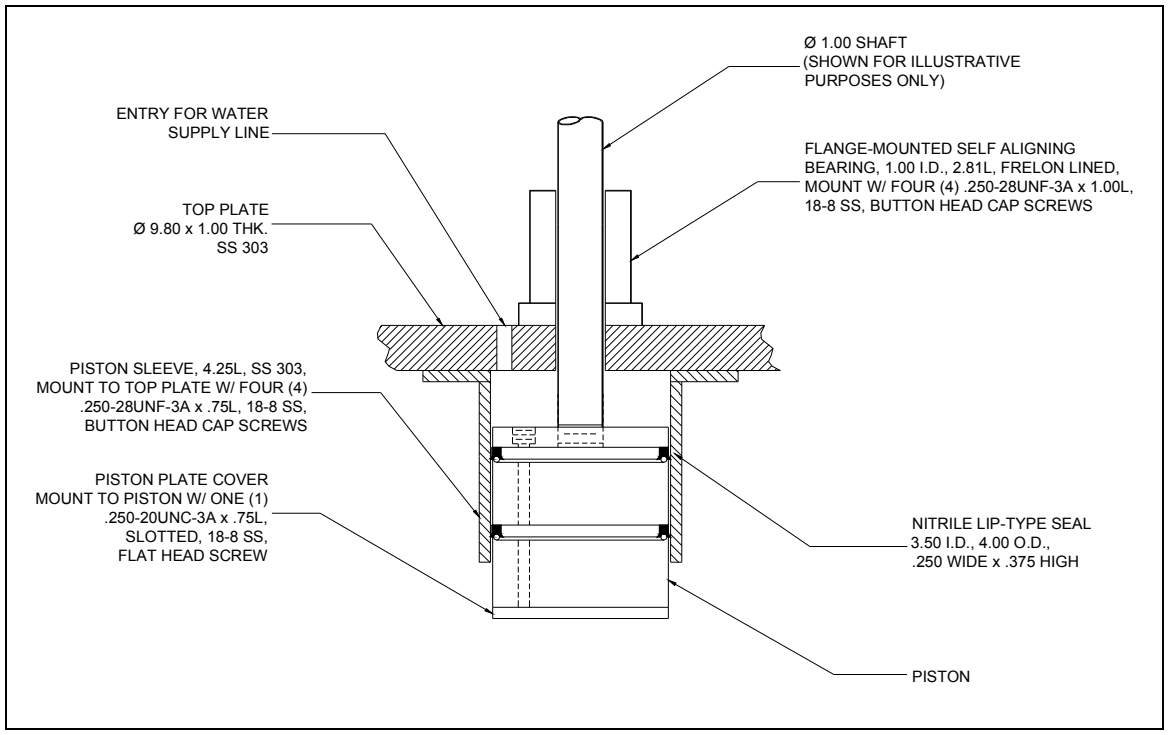

Figure 4-4. Detail of the Piston Assembly.

Conversely, the piston is machined from a billet of aluminum to provide the strength necessary for compression-based tests. The piston contains two inscribed grooves about its circumference designed to receive flexible seals. Although one seal

would have been adequate for this application, duplicity was chosen to further steady the piston inside of the sleeve and act as a backup if the primary seal were to fail. Due to the critical role these seals play in the successful operation of the cell, the grooves were designed to compliment the component specifications of the seals. These seals are made of wear-resistant nitrile lip seals and resemble a flared "U." They are installed into the grooves of the piston cupped in the downward direction, which forces any increase in water pressure to act within and outwardly through the seal. This change of pressure increases the "squeeze" of the seal onto the interior surface of the piston sleeve. These seals are appropriate for this application in that as they wear at the contact surface, the downward cup design compensates by allowing the seal to open to a greater degree, thereby assuring a tight seal against the piston sleeve. This attribute provides a much longer service life than could be expected from other seals having a more symmetrically shaped profile. Seals with a symmetrical profile such as o-rings, are less forgiving of an uneven wear pattern and are not appropriate to dynamic applications.

This configuration has performed extremely well in proof testing and throughout several production tests, having successfully prevented any bypass of water from the cell's interior. For the purpose of design, the seals are considered to be consumable components of the test system and will eventually require replacement. After many sequences of testing, the seals have performed up to the design goal and indicate no visible signs of wear.

4.3.1.3 Top and base plate design

The thickness of the base and top plate is a function of the bearing capacity required from the struts onto the plate and was calculated with a factor of safety of 2 at

the maximum safe operating pressure of 800 psi. It was anticipated that the cell would operate in the range of 0-400 psi for the types of tests the system was being designed for.

The base plate performs three basic functions. First, it acts as a staging platform for other components of the system. Secondly, it contains the watertight entrances for instrumentation cables entering the cell, and thirdly, it includes the conduits for pressurized water entry both through and around the specimen.

There are four ports (thru holes) that were specified for use with plug-in type fittings available from Geotechnical Consulting & Testing Systems (GCTS), Tempe, Arizona. These fittings consist of hollow cored, threaded male and female pieces that, when tightened together, compress a confined o-ring, thereby sealing the interface. The cables for instrumentation used for the system can be chased through these assemblies, allowing for easy installation of any combination of instruments into the cell. These cables exit the cell's interior and are neatly chased via grooves in the bottom of the plate to the data acquisition system.

The protocols for testing require that the system be capable of circulating water both through and around the specimen. The ability to transport water through the specimen is essential for achieving saturation and also is essential for permeability testing. In order to apply fluid pressure around the specimen and condition it to the testing temperature, it was required to have an entrance for fluid coming from the water distribution panel. With these requirements in mind, the base plate has two 1/8-in diameter conduits that run through the center of the base plate terminating at the specimen location and the cell cavity location.

The thickness of material chosen for the base plate was dependent upon the required bearing surface area of the threaded struts that fastened into the plate. An optimization was conducted to size the struts versus the thickness of the plate (see strut design for further discussion).

The primary function of the top plate is to act as a platform for the piston assembly. The plate is fastened to the four struts via socket head screws that pass through the plate. At this point in the design process, a block shear type of failure about the socket head screw had not been investigated. This analysis was conducted in the following component phase therefore, at this point, the thickness of the plate was assumed to be 1 inch. The piston assembly is fastened to the lower face of the top plate with four (4) stainless steel button head cap screws. A 1-inch inside diameter flange-mounted self-aligning bearing is fastened to the upper face of the plate to guide the travel of the rod attached to the piston, shown in Figure 4-4. The incorporation of a self-aligning bearing eliminates the potential for damage to the piston sleeve from a misaligned piston. Both the piston assembly and the self-aligning bearing are capable of being adjusted about the vertical axis of the cell to ensure proper alignment of the end platens on either end of the specimen.

The top plate contains two 0.50-inch diameter holes that allow the exiting of fluid from within the cell. One hole is located such that it falls over the piston. This hole allows for the placement of copper tubing for the transport of water from the top of the specimen. The second hole is positioned outside of the piston assembly profile providing an outlet for temperature-conditioned water or an inlet for pressurized air.

4.3.1.4 Strut design

By this time in the design process, the diameter of the struts was already determined during the optimization process within the base plate design stage. The connectivity of the struts to the plates was determined based upon methodology of construction. As can be derived from the connection detail shown in Figure 4-5, the success of an adequate seal along an o-ring is dependent upon the uniform compression of these seals along the length of the o-ring. To ensure uniformity, the separation between the top and bottom plates must be tolerable within a fraction of the o-ring's diameter. If, for example, the distance of separation were too far out of tolerance, one portion of the o-ring would contact before the opposing side, creating an inadequate seal. Designing a strut that would be capable of adjustment was therefore necessary to ensure uniformity of seal compression.

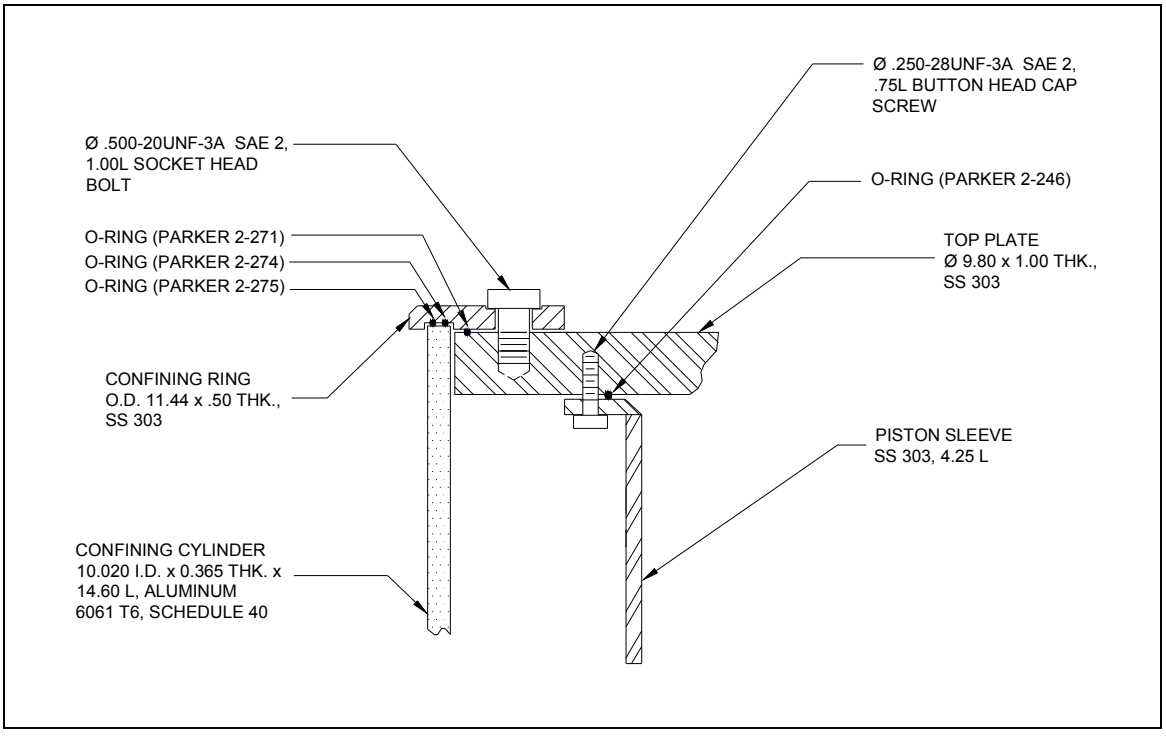

Figure 4-5. Detail of the Connection of the Confining Ring to the Top Plate.

All four struts are typical and are a combination of exterior (male) threading on the end that interfaces with the base plate, and interior (female) threading on the end interfacing with the top plate. This combination allows for the struts to be adjusted for equidistant separation prior to the top plate being installed. Subsequently, as shown in Figure 4-6, the top plate is secured using the high-strength socket head bolts.

The design of the threaded ends of the struts had to be specified. Since the struts were to be designed as tension members, the end bearing capacity of the struts were not considered and the design approach turned to the bearing ability of the threads. Bolts (as is the assimilation of the male strut end) can fail in tension in four different ways, 1) thread stripping of the bolt if it is a weaker material than the nut, 2) thread stripping of the nut if it is a weaker material than the bolt, 3) stripping of the bolt and nut if both are

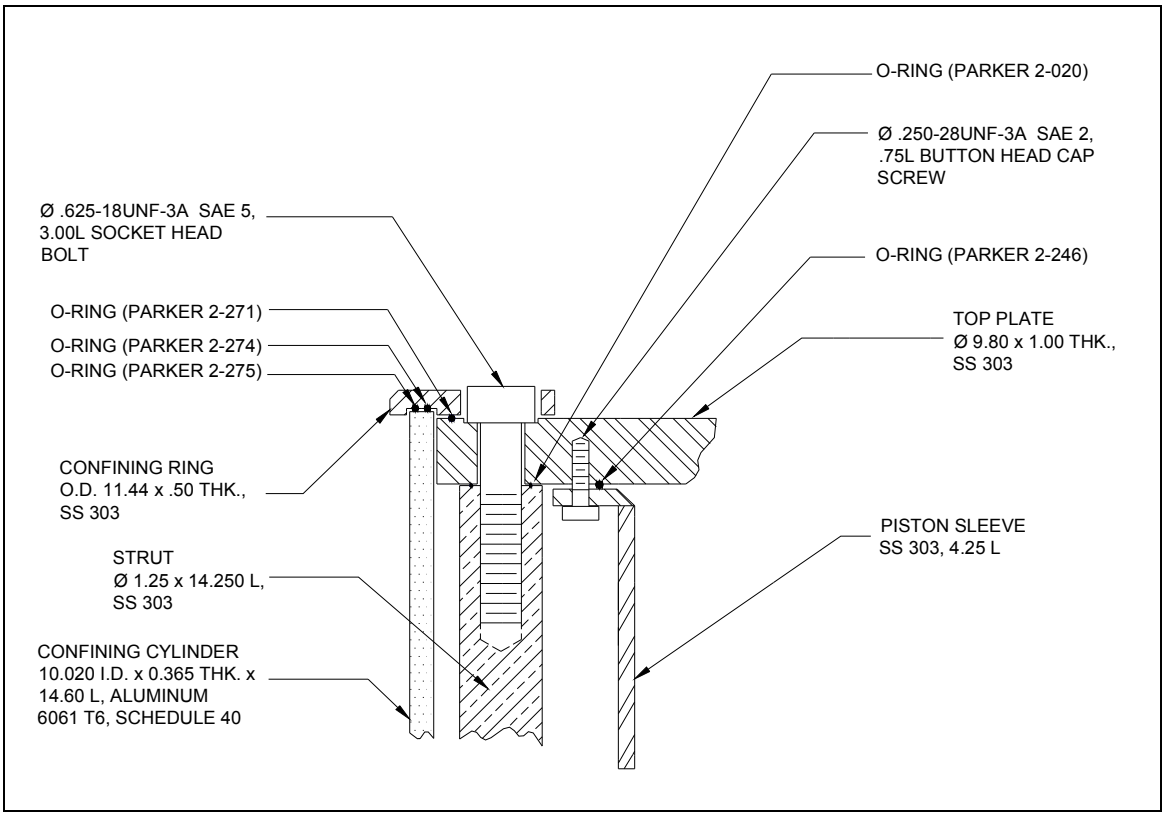

Figure 4-6. Detail of the Connection of the Strut to the Top Plate.

of similar material, and 4) shearing of the bolt if thread bearing strength surpasses the bolt's tensile strength (Juvinall, 1983). In the case of the base plate connection, where the strut (bolt) and the base plate (nut) are of the same material and limited engagement depth precludes shearing of the strut, failure mode 3 controlled the design.

Based upon the geometry of the cell, the pressures it is designed to contain, and an applied factor of safety of 2, the resulting tension force anticipated for each strut was calculated as 15.7 kips. The bolt tensile force required to yield the entire threaded cross section is defined as:

$$F = A_t S_y \approx \frac{\pi}{4}(0.9d)^2 S_y \qquad \text{(Equation 4-1)}$$

where: F = bolt tensile load required to yield the entire thread-stripping failure surface of the strut (kips)

A_t = total surface area of threads resisting tensile force (in2)

S_y = yield strength of strut (0.2% offset) (ksi)

D = major diameter of the strut (in)

The bolt tensile load required to yield the entire thread-stripping failure surface of the base plate is defined as:

$$F = \pi d(0.75t)(0.58S_y) \qquad \text{(Equation 4-2)}$$

where: F = bolt tensile load required to yield the entire thread-stripping failure surface of the base plate (kips)

d = major diameter of the strut (in)

t = depth of engagement into the base plate (in)

S_y = yield strength of strut (0.2 % offset) (ksi)

Equating the former two expressions for F yields balanced tensile and thread-stripping strengths when the depth of engagement is approximately:

$$t = 0.47d \qquad \text{(Equation 4-3)}$$

The process for calculating the design of the strut to base plate connection was as follows:

- Calculate depth of engagement using Equation 4.3
- Arbitrarily choose a thread designation and, by using the depth of engagement t solved for in step 1, determine the corresponding bolt tensile load required to yield the entire thread-stripping failure surface of the base plate, F, as defined in Equation 4.1
- Continue with iterations of differing thread designations until F, as defined in Equation 4.2 approximates the design resistance force of 15.7 kips as defined for the design

The design of the strut to top plate connection utilized the same methodology as the previous connection with the primary exception being that it has inside threads and utilizes a socket head bolt, as shown in Figure 4-6. The socket head bolts are Society of Automotive Engineers (SAE) Grade 5, with yield strength, S_y, of 92 ksi. For all sense and purpose, this level of strength far exceeds the requirement of this application. However, the cost of these bolts was reasonably low and the added level of strength is of value when considering this added strength effectively removes a failure mode from probability. The additional failure modes that needed to be checked were:

- Shearing at the reduced-area cross section
- Shearing of the bolt
- Block failure (pullout) of the top plate about the socket head and bolt interface

With the design of these connections accomplished, the structural core of the system was complete. The following components would be designed to compliment this structure.

4.3.1.5 End platen design

The approach for the design of the end platens began with a review of needs for this component from each test. Depending upon the test, these platens needed to perform different tasks. For example, tests such as resilient modulus and drained and undrained compression required that the platens resist induced compressive stresses. Additionally, any contributory end effects resulting from friction between the platens and the specimen's ends needed to be minimized as much as design would allow. Other tests such as constant and falling head hydraulic conductivity (permeability) placed a greater emphasis on the ability of the platens to conduct and distribute water with a minimal amount of interference. It is the opinion of this researcher that existing designs do not efficiently allow the transport of fluid through the specimen but rather force the fluid through specific and limited paths, thereby introducing error into the test. This becomes evident when an inventory of losses due to constrictions, expansions, and bends along the fluid's path is made. After consideration of the requirements it was concluded that different platens would be required for different tests.

Unlike more commonly used end platens, which distribute water via one hole and conducting grooves or dimples, those in the cyclic loading and pore pressure conditioning system contain many orifices across its surface. This allowed water to be transported through the test specimen uniformly and without concern for isolated piping or excessive pressure gradient development. Additionally, these platens are fabricated with concentric grooves to better distribute the water across the face of the specimen. This configuration is also advantageous in the initial specimen saturation phase since it allows for a front of fluid to pass through the specimen, which more effectively liberates entrapped air

bubbles. The presence of conducting channels across the entire profile of the platens diminishes the likelihood of entrapped air bubbles between the platens and the specimen.

The complexity of the profile coupled with the relatively small conducting orifices specified dismissed stainless steel as a material candidate. Aluminum was chosen due to its relative ease of machining and ability to harden to a level required for use by anodizing the part. Both the top and the bottom platen have identical profiles. This similarity ensures conservation of volume in and out of the specimen and decreases production costs since only one profile had to be identified for machining.

The top platen is basically a plate that caps the end of the piston. It is fastened via a screw into the piston which when tightened, compresses an o-ring placed between the two mating parts that prevents water from being conducted through the mated seam. The base platen is attached to the base plate via a threaded stud that also assists with the proper, concentric alignment of the platen about the cell. A concentric, half-round groove is machined into the mating face of the platen for installation of an o-ring serving the same purpose, as does the aforementioned o-ring. Machined into the circumference of the platen are two half-round grooves that are used to "seat" the o-rings that hold the latex membrane to it. Additionally, a 1.0 inch high hollow riser was manufactured that can be placed between the base plate and platen. The option of using a riser allows a specimen height range of 5-6 inches (127.0-152.4 millimeters).

For compression-based testing it was necessary to protect the faces of the platens from marring and increased damage. Additionally, the concentric grooving in the face of the platens introduced an unfavorable end constraint of the specimen. To lessen these end effects, several sets of low friction, high-strength Duron® platens were fabricated to

fit between the aluminum platens and the specimen. These Duron® platens are mechanically fastened to the aluminum end platens to prevent any shifting during testing. Additionally, they contain concentrically positioned holes that compliment the location of the grooves contained in the aluminum platens, thereby still allowing a method to saturate a specimen and determine its hydraulic conductivity prior to compressive testing.

4.3.1.6 Confining cylinder design

Due to the large diameter of the cell, the availability of cylindrically shaped material was limited. Early in the design process, it was understood that the larger the cell's diameter became, the less number of incremental diameters of confining cylinder would be available. With this in mind, the selection of a suitable material/diameter combination was researched. Since the cell would be operating at much higher pressures than typical triaxial cells, plastics, such as the commonly used material Lucite® with a maximum allowable wall pressure of 150 psi, would not be adequate.

The finished length of the confining cylinder, considering cumulative compression of o-rings, was calculated as 14.60 inches with a required diameter of approximately 9.5 inches or larger to accommodate the struts, specimen, and instrumentation within the cylinder. Since this component would require constant removal and reinstallation for testing, the overall weight was a concern for two reasons, 1) physical requirements for any future operators (i.e., strength) were not reasonable to assume, and 2) as the weight of the cylinder increases and becomes more unwieldy, so too does the potential for damage attributed to mishandled or colliding parts. Therefore, relatively dense materials such as stainless steel were excluded from consideration. Aluminum alloys were researched for adequacy and availability. Aluminum 6061-T6 weighs approximately 0.10 lb/in3, which is roughly one-third the weight of a stainless steel material. A 10 inch

nominal diameter, schedule 40 pipe was located which has yield strength of 40 ksi. The anticipated maximum hoop stress was calculated as (Beer and Johnston, 1992):

$$\sigma_{hoop} = (factor\ of\ safety)\left(\frac{\mathrm{Pr}}{t}\right) \qquad \text{(Equation 4-4)}$$

where: P = maximum operating pressure (psi)

r = inside radius of cylinder (in)

t = cylinder wall thickness (in)

With a factor of safety of 2, the hoop stress was calculated as 10.98 ksi, far below the allowable stress of the material. Although thinner walled material was available, it would not have been adequate since this narrower dimension would have created difficulties mating with the o-ring seals at the ends of the cylinder. It is of value to note that pipe of this dimension and material type is difficult to locate. This type and size pipe is used in specialized applications such as electric generation plants and is manufactured in lengths exceeding 10 feet. The procurement of a 15 inch long piece of these segments entailed a special cutting fee. The cylinder, while being structurally adequate, does raise a concern with similarly designed cells that may be constructed in the future. Owing to the fabrication method and subsequent storage of the material at the manufacturer, the material is slightly out of round when purchased. This distortion makes the mating of the cylinder to the o-rings contained in the lower and upper portions of the cell more difficult than if the cylinder were truly round. If additional cells are manufactured in the future, thicker walled cylinders are recommended followed by a center-less ground method of machining to create a cylinder that is truly round.

4.3.1.7 Confining ring design

The confining ring is one of the most critical of all the components. The ring compresses the seals in contact with the confining cylinder and the seal inset into the exterior face of the top plate that prevents the migration of pressurized fluid from the interior of the cell. The ring is attached to the top plate via four 1 inch long socket head bolts. These bolts resist the force applied to the ring through a gap between the confining cylinder and the top plate. The force against the ring is relatively small compared to forces exerted onto other components. For this reason, the nominal thickness of the ring is 0.50 inches. The socket head bolts employ flat washers between them and the surface of the confining ring to increase the contact area with the ring. The ring was analyzed for block shear about the bolts as well as stripping type failures of the bolt to top plate connection.

The confining ring has a recessed, concentrically located channel machined into the face that contacts the confining cylinder. This channel helps to align the top of the confining cylinder within the ring thereby "locking" the two components together. Two semi circular grooves are placed into the channel for the placement of o-rings where the confining ring interfaces with the confining cylinder. Four thru holes are positioned into the ring at locations that complement the bolt heads that connect the top plate to the struts. An additional thru hole is provided which fits over a quick disconnect fitting installed into the top plate allowing fluid to be cycled through the cell's interior.

4.3.1.8 Radial LVDT holder design

The use of LVDTs is necessary for the computation of the variation of the cross sectional area of the specimen during failure testing in compression. These LVDTs are positioned such that they are normal to the cylindrical surface of the specimen in 90º

increments. A holder was designed that allows for the installation of four LVDTs in this configuration. Machined from aluminum and anodized for corrosion resistance, the holder contains four thru holes that allow the holder to be integrated with the struts of the cell. Slightly oversized, these thru holes enable the holder to travel to any position along the length of the struts. Once positioned, the holder is affixed to the struts via eight nylon-tipped, stainless steel setscrews. The nylon tip prevents marring of the strut and is intended for applications where the setscrew is continuously reengaged. The LVDTs are placed into the holder via thru holes and restrained with stainless steel set screws. This simple configuration allows for rapid positioning of the devices at any position along the length of the specimen.

4.3.1.9 Seal selection and placement

With the exception of the U-cup seals used for the piston, all other seals were accomplished with buna-N o-rings supplied by Parker Seals, Inc. Buna-N (nitrile) is a commonly used o-ring material that is available in a wide range of diameters and cross sectional thickness. Table 4-1 lists the technical specification details related to the o-rings. This material is resistant to petroleum-based fluids and maintains its shape and pliability after a high number of compression cycles. The combination of these factors was necessary for the anticipated use of these o-rings. The design of all components relying on these seals was performed simultaneously with the o-ring selection process. This coordination ensured that specially sized o-rings would not have to be manufactured.

As shown in Figures 4-5 and 4-6, the o-rings are placed such that as the cell is assembled, the proper alignment of the o-rings with the corresponding component can be achieved easily. The cross sectional diameter of the o-rings was chosen such that an

equivalent degree of compression of all the o-rings is accomplished following the tightening of the cap head bolts about the confining ring. The consideration of group-dependent compression of the o-rings is critical to ensure that each individual seal is properly compressed to maintain the confinement pressure.

Table 4-1. Nitrile O-ring Schedule.

Component	Parker Part Number	Number Req'd	Application Description
Base Plate	10-341	1	Interface between confining cylinder and base plate
	2-008	4	Sealant for cables exiting thru base plate
Top Plate	2-272	1	Interface between top plate and confining ring
	2-160	1	Interface between top plate and Frelon bearing
Strut	2-118	4	Interface between top of strut and top plate
Confining Ring	2-275	1	Interface between confining ring and confining cylinder
Piston Plate	2-044	2	Restraining rings for membrane to piston plate
Piston Plate Cover	2-044	1	Interface between piston plate cover and piston plate
Base Platen #1	2-044	2	Restraining rings for membrane to piston platen
	2-042	1	Interface between base platen and base plate
Base Platen #2	2-044	2	Restraining rings for membrane to piston platen
	2-042	1	Interface between base platen and base plate

The grooves that accept the o-rings are predominately square in profile and of adequate cross sectional area to allow for the total inclusion of the o-ring upon compression. As was previously discussed in the design considerations section, this provision allows for proper sealing while simultaneously facilitating rigidity at the interface developed from the surface-to-surface contact. Where the aluminum base platen interfaces with the base plate, a semi-circular groove profile was specified. This shape allows for the inclusion of only half of the cross section with the remaining half being reserved for compressed deformation in the area between the two components. This configuration is intentional to prevent galvanic corrosion between these two

components. Where contact occurs between aluminum alloy and stainless steel, corrosion will be accelerated (Juvinall, 1983). Aluminum is more anodic than steel and therefore will have the greater tendency to ionize and develop a greater negative charge (electrode potential). The aluminum component acts as an anode and the steel a cathode, thereby allowing for the development of an electrical current flowing from the aluminum to the steel. This continuous discharge of aluminum ions will eventually corrode that part. Another type of corrosion, electrochemical corrosion, can occur if these parts are placed in an electrolytic solution such as fresh water or water with a high salt content. An electrolytic solution acts as an ion carrier with positively charged aluminum ions going into solution leaving an excess of negatively charged electrons on the component (electrode). This action will continue until a condition of equilibrium is reached (Halliday, Resnick, and Krane, 1992). Since these components function in an environment where water is repeatedly drained from and refilled into the cell, equilibrium would not occur and continued corrosion could be expected.

The combined use of an insulator (nitrile o-ring) and de-ionized water as a confining fluid helps to lesson the potential for corrosion of these components. Additionally, the aluminum base platen and riser was anodized to fill in the porous surface of the material, making it more resistant to the effects of corrosion and hardening it to protect the surface from abrasion. Compared to the cost of machining the intricate platen, the relatively small cost to anodize the part is prudent for maintaining its integrity.

4.3.1.10 Instrumentation ports

With these components designed, attention then turned towards the requirements for instrumentation incorporated with the cell. As a minimum, it was decided that a total of five sealed “ports” were needed to analyze the specimen during testing. Of these

ports, two are designated for axial LVDTs, two for radial LVDTs, and one for temperature monitoring by way of a thermistor probe. With the exception of the thermistor probe which is connected to an outlet conduit at the top of the cell, the remaining instruments exit the cell through the base plate and are chased neatly to the back of the cell. In order to ensure there are no leaks when the LVDT cables penetrate through the base plate, special two-piece fittings were procured. These fittings were designed such that as the two parts are screwed together an o-ring compresses against the cable that is passed through the two parts, thereby effectively sealing the penetration. Additionally, the two-part assembly contains an outer o-ring that seals against a bore made through the base plate. This configuration makes instrument installation of the cell rapid and flexible with regards to configuration.

4.3.1.11 Component tolerance specification

The specification of dimensional tolerance was required as part of the design process, as it is with any machine design. Since two different materials (aluminum alloy and stainless steel) were used in the cell, thermal expansion effects needed to be considered.

The only moveable component in the cell is the piston. As a result, this component and the tolerance of the sleeve it oscillates within, warranted special consideration. Calculation of dimensional tolerance was accomplished using tables published by the American National Standard Institute (ANSI, 1978). The piston sleeve assembly was considered as a running clearance fit, which is typical for applications requiring lubricant between the piston and sleeve (Earle, 1994). Although it was not intended for lubricant to be used, the gap created between the two components ensured that there would not be any abrasion due to contact. Any contact could cause unrecoverable damage to the

surface of the piston and diminishing the effectiveness of the u-cup lip seals. The calculated tolerances were then checked versus the anticipated expansion of the piston and sleeve to ensure that a gap would still exist at high testing temperatures. For calculation, the high test temperature was taken as 140ºF. Coefficients of thermal expansion were taken as 12 x 10-6 in/ºF for aluminum alloy and 8x10-6 in/ºF for stainless steel (Juvinall, 1983). As can be seen from these values, the higher coefficient of thermal expansion for the aluminum alloy piston validated the design considerations. If the gap between the piston and the sleeve were too small, the piston could become engaged with the sleeve at high operating temperatures. Since the piston was to be anodized, the diameter and tolerance were defined as post-coating.

All thru-hole locations were specified using rectangular coordinates. Over-sizing of holes, in locations where bolts would be used, was specified with common drill diameters. This relieved the fabricator from the needless effort of obtaining an over-prescribed tolerance. This over-sizing made all the mechanical connection points flexible with regards to orientation of the mating parts. This flexibility allowed for mild adjustments, which created optimal sealing conditions for the structural components. The length of the confining cylinder was defined to the hundredth of an inch. Although a more stringent overall length could have been specified, doing so would have placed an undue burden on the fabricator and resulted in higher than necessary cost. The ability for the struts to be lowered or raised meant that the clear distance of the top and bottom plate controlled with the struts could correct any error in the overall length of the confining cylinder.

Square-profiled grooves for o-rings were specified to a tolerance as recommended by the manufacturer. These tolerances represent the manufactured tolerance of the o-rings, which, due to their elastic property, can adjust to minor dimensional intolerance.

4.3.2 Fluid Distribution System

The fluid distribution system is critical for effective stress state tests and cyclic pore pressure conditioning without any other application of stresses. The system is composed of four basic components, 1) a hydraulically driven volume changer, 2) a 50 mL capacity graduated burette/annulus, 3) a manually controlled fluid routing board, and 4) a vacuum/pressurized air control panel. A schematic of this system is shown in Figure 4-7.

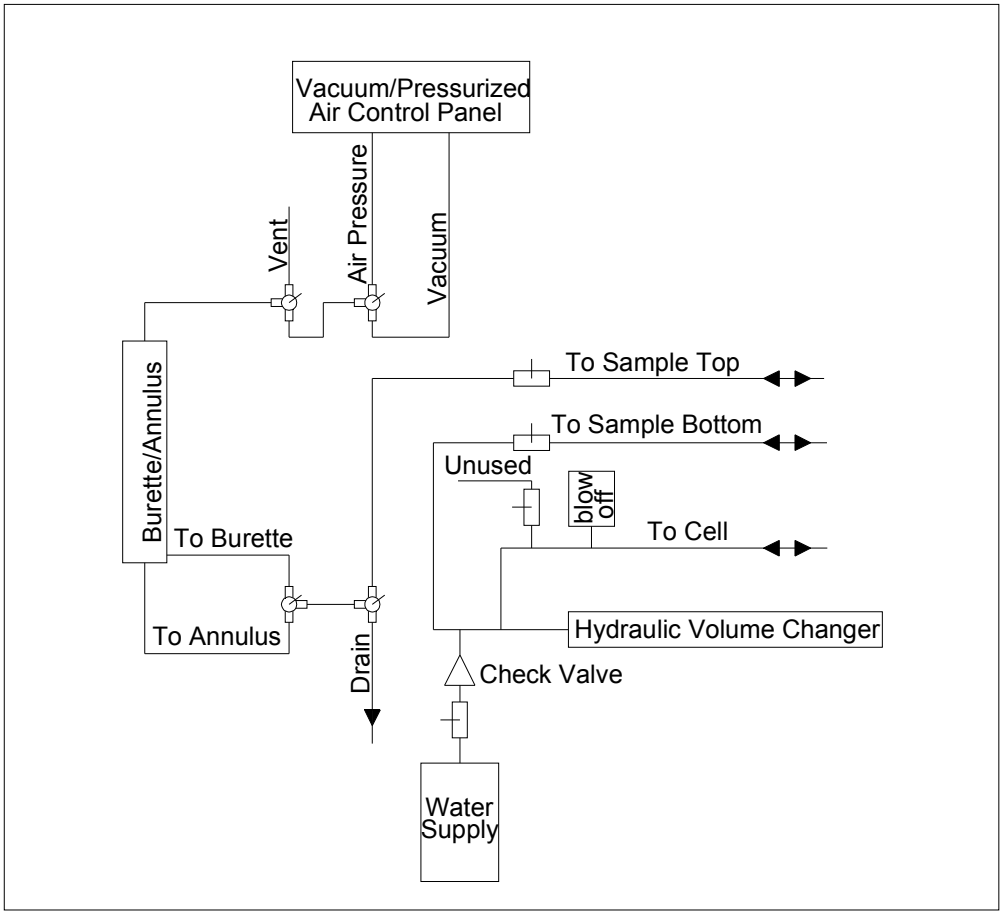

Figure 4-7. Schematic of the Fluid Distribution System.

The water delivery and pressurization system is separate and free standing from the cell. All fittings and conduits are high-pressure capacity with the minimum pressure fitting having a capacity of 1200 psi. This surplus of capacity over and beyond the maximum test pressure is owed to the availability of fittings from common suppliers. The valves are gate valves manufactured from carbon steel.

In determining the layout of the distribution lines, an effort was made to limit the length of each respective line. In long conduits, a phenomenon referred to as a dynamic front can occur where pressure exerted at one end of the conduit is delayed from developing at the opposite end of the line. This is attributed to sidewall friction, which retards the pressure transmittance. The valves were positioned such that they limit the length of conduit between the area of interest and the pressure transducer monitoring that line.

The system is pressure-driven via a servo-controlled, hydraulically actuated volume changer. This volume changer acts similarly to a syringe in that it draws water from a bore-type reservoir and then plunges this water into the system. Through a network of unidirectional valves, the volume changer is capable of refilling with de-aired water from an inline storage reservoir without allowing a decrease in pressure in the network beyond it. From the volume changer, pressurized water can be distributed through one or any combination of three conduits, bottom of specimen, top of specimen, or cell interior (confining space around the specimen). Each of these three lines is monitored with a pressure transducer that communicates to the volume changer through a system controller, thereby allowing for the control of exerted pressures within and around the specimen. This closed loop control allows for precise measurement and rapid monitoring

of pressure. Additionally, the volume changer is monitored by an LVDT, which reports the displacement of the piston within it. As with the pressure transducers, this LVDT acts in a closed loop with the system controller allowing for rapid monitoring and command of positioning. By calibrating the volume of water discharged from the volume changer per linear displacement, the quantity of fluid forced through the specimen can be determined. This is a critical design element in that this quantity allows for the verification of saturation of the specimen.

In order to protect the cell against damage due to an accidental over-pressure, a blow-off valve was installed in the distribution system that is gauged to open if line pressure exceeds 400 psi. This valve is located in the distribution line that supplies water around the specimen. This position was logical since the test with the greatest anticipated pressure is the indirect tension (extension) test wherein the pressure around the specimen is increased until failure occurs. Since the volume changer is rated at 1200 psi, far exceeding the capability of the cell, it was believed prudent to allow for the safe release of unwanted pressure if a system malfunction occurred. Measures such as this are essential in designing a safe system considering that the relative incompressibility of water can yield compounding values of pressure with very little displacement of the volume changer.

The basis for designing this system is for the testing of specimens in effective stress conditions. Therefore, it is necessary to ensure that the specimen is saturated and that the fluid used for saturation is free from dissolved air. The water used for all testing is first de-aired using a 2-liter capacity vortex de-airer. This fluid is then stored in a large volume until testing. For the initial filling of the cell to begin a testing sequence, the

large volume is drawn on directly via a filling line that utilizes elevation head to expedite filling. For the distribution of fluid through the specimen, the water is first conveyed to a smaller storage tank where, through a network of check valves, the fluid can be introduced into the volume changer or burette.

Backpressure saturation is possible from a water volume storage tank and vacuum line integrated into the water distribution system. This allows for a specimen to be installed into the cell and saturated and conditioned in-place prior to testing.

For flow measurements through the specimen, the system is outfitted with a calibrated 50 mL burette that is designed specifically for use when performing permeability testing.

4.3.3 Water Temperature Conditioning Systems

For temperature control, the water delivery system can be connected to either a heater or chiller unit. The heater and chiller are each capable of pumping water through the water delivery system and into and out of the cell cavity prior to returning in a closed-loop path. Temperature conditioning in this manner utilizes the principle of conduction as the mode of energy transference.

The combination of the heating and chiller units allows the test specimen to be controlled within the range of 2-75ºC. Unlike other systems which use indirect conditioning methods (i.e., a closed conduit running through a temperature bath), this configuration has proven very responsive and capable of conditioning a specimen from room temperature to the aforementioned range limits in less than 90 minutes. A discussion on conditioning confirmation with this system is presented later.

4.4 Targeted Testing

The compilation of systems was designed to provide a more efficient manner in which to perform a multitude of tests in one workstation. The cyclic loading and pore pressure conditioning system is designed to test asphalt specimens in both effective and total stress conditions, as well as moisture condition specimens with or without any other stresses present. Protocols were developed which allowed the system to perform:

- In-place saturation and conditioning
- Constant head permeability determination
- Falling head permeability determination
- Compression testing
- Resilient modulus testing
- Complex modulus testing

Future development will allow the system to perform other tests such as creep testing and tension testing. The successful development of these protocols will allow the user to perform a multitude of tests without relocating or damaging the specimen. The improvements incorporated into this new system also makes the excitation of pore water pressure more easily controlled, thereby allowing for a better assessment of specimen response to these pressures.

Cyclic Loading and Pore Pressure Conditioning System Specifications

Overall Dimensions…… 18.95 inches High x 12.50 inches Diameter

Maximum Operating Pressure…..…… 400 psi

Maximum Design Pressure…….…… 800 psi

Maximum Piston Travel Length…….……..…… 0.75 inches

Specimen Diameter…….. 4 inches (100 millimeters)

Specimen Aspect Ratio…….…… 1.25 – 1.50

Accessory Ports…….…… 4 Thru Base Plate, 1 Thru Top Plate

LVDT Orientation Capability……..…… 2 Axial, 4 Radial

Volume of Water to Fill Cell……. 3.6 gal (825in3)

Structural Frame Material…….…..….. Stainless Steel 303

Confining Cylinder Material……... Aluminum 6061-T6

Piston & End Platen Material…….. Aluminum 6061-T6

Soft Seal Material……..…… Buna-N o-rings

Piston Seal Material……...… 2-Nitrile U-cup Lip Seals

Water Conditioning Range…….. 2-75ºC

4.5 Temperature Control System

Fluid was used for temperature control. This required the specimen to be sealed with a 3.048 x 10^{-4} m (0.012-in.) thick latex membrane during testing. For temperatures above 2ºC, circulating water was used for temperature control. The water delivery system can be connected to either a heater or chiller unit. The heater and chiller are each capable of pumping water through the water delivery system and into and out of the cell cavity prior to returning in a closed-loop path. Conditioning in this manner utilizes the principle of conduction as the mode of energy transference. Figure 4-8 depicts a schematic of the heating/cooling system used.

The combination of the heating and chiller units allows the test specimen to be controlled within the range of 2ºC to 75ºC. Unlike other systems, which use indirect conditioning methods (i.e., a closed conduit running through a temperature bath), this configuration has proven very responsive and capable of conditioning a specimen from room temperature to the aforementioned range limits in less than 90 minutes.

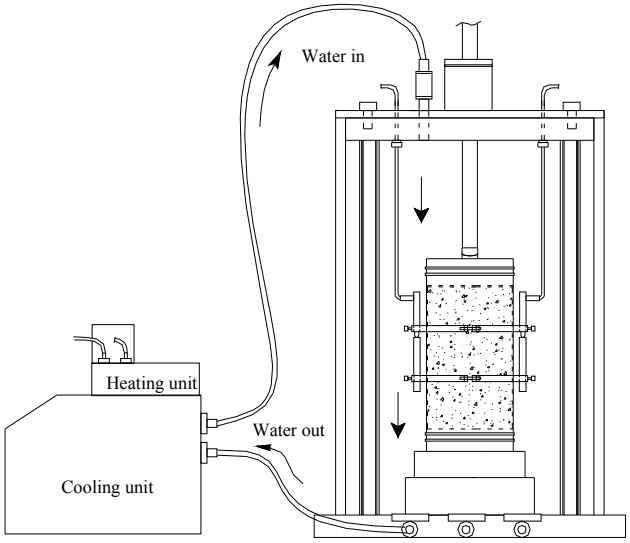

Figure 4-8. Diagram of the Water Circulation System that Controls the Sample Temperature.

At the time the specimen is first placed into the system, it is stabilized at room temperature. The specimen is surrounded about its circumferential perimeter by confining water. This water acts as a medium for temperature conditioning of the specimen. As the temperature-conditioned water surrounding the membrane-encased specimen is cycled through the system, thermal energy is either drawn from the specimen, as occurs during cooling, or added to it, as occurs during heating. During the cooling process, heat is conducted from the specimen to the "colder" confining water; the opposite is true for the heating process. As this process continues, concentric layers of the cylindrically shaped specimen reach thermal equilibrium starting from the outer layer and migrating towards the central core (Çengal, 1997).

The transfer of energy from more energetic particles to less energetic adjacent particles through interactions is the thermodynamic process of conduction. The equation for the rate of heat conduction is defined as:

$$Q_{cond} = kA \frac{\Delta T}{\Delta x} \qquad \text{(Equation 4-5)}$$

where Q_{cond} = rate of heat conduction, (W)

k = thermal conductivity of the layer, (W/(m·K))

A = area normal to the direction of heat transfer, (m2)

ΔT = temperature difference across the layer, (K)

Δx = thickness of layer, (m)

The "layer" referenced in the variable definition, Δx, is the latex membrane that encapsulates the specimen. Thermal conductivity of the latex membrane is approximately 0.13 W/m · K with a thickness, Δx, of 0.3048 mm (0.012 in.). A circumferential surface area of approximately 0.045 m^2 simplifies Equation 4-5 to:

$$Q_{cond} = 19.19 \cdot \Delta T \text{ (W)} \qquad \text{(Equation 4-6)}$$

As can be seen from Equation 4-6, the larger the difference in temperature across the layer, the greater the rate of heat conduction. Additionally, it can be inferred that, as the temperature on either side of the layer approaches equilibrium, the rate of heat conduction decreases. Therefore, to achieve a specimen target temperature rapidly, the temperature difference between the specimen and the circulating water must be as large as possible to maximize the rate of heat conduction without surpassing the target temperature.

4.5.1 Specimen Set-up for Temperature Calibration

The final portion of the specimen to reach temperature equilibrium is the central core. Therefore, it is this region of the specimen that controls the length of conditioning time prior to the establishment of thermal equilibrium. Since the testing protocol for specimen temperature conditioning relies upon conductance for specimen heating or

cooling, it was necessary to plot the change in temperature of the confining water and the core of the specimen versus time.

Although both the heater and chiller units used with the system digitally report the water temperature within their fluid reservoirs, thermal losses or gains that occur along the fluid distribution panel can vary from the reported temperature by several degrees. A series of trials were conducted for both cooling and heating to determine the most time conservative sequence to rapidly achieve the target temperature. Since the rate of heat conduction is directly proportional to the temperature difference across the layer (latex membrane), initially set temperatures were significantly lower (in the case of cooling) or higher (in the case of heating) than the target temperature to expedite thermal equilibrium. The large combined mass of the triaxial cell, water, and components of the distribution panel required a large rate of energy exchange be implemented in order to achieve the target temperature.

Two type-K thermocouple probes connected to digital gages were used to report the temperature of the confining water and the core of the specimen throughout a series of heating and cooling sequences. The thermocouples used were bare-tip and were connected to digital gages that had a recording tolerance of ±0.1ºC. Prior to implementation, the thermocouples were calibrated using a certified laboratory grade mercury thermometer. From these calibrations, offsets were determined across the anticipated range of temperatures. These offsets were applied to the raw recorded data to derive a time versus temperature relationship.

The calibration of the specimen in conditions as close as is possible to those anticipated during testing is extremely important to fully account for variables of energy

transference. These variables are present due to thermal sources and sinks (metal cell components), as well as insulators (latex membrane). Thermocouple 1, used to monitor the confining water temperature, was installed through one of the accessory ports located at the base of the triaxial cell. In order to avoid false readings that may have occurred by contact between the probe and metal components of the cell, the end of the probe was suspended within the volume of the cell with cotton thread. Thermocouple 2, which was required to be inside of the specimen, was more difficult to install. To simulate testing conditions, the specimen was required to be wrapped in the latex membrane thereby preventing routing of the thermocouple into the cell like that of the formerly discussed probe. Routing of the thermocouple wire through the cell's piston was eventually decided as the only viable option to achieve placement of the probe even though it required dismantling of active components of the system. The specimen used for calibration was prepared by first cutting the ends to facilitate contact between the specimen and the end platens. To allow for the installation of the probe into the specimen, a 0.25-inch diameter hole was drilled into the specimen, parallel with the longitudinal axis, starting centered on the end of the specimen and terminating at a depth equal to ½ the length of the specimen. The thermocouple was then inserted through the cell's piston and into the void in the specimen. In order to affix the thermocouple in its position and prevent energy transfer from the air-filled void to the end of the piston, the end of the specimen was sealed with silicone. The specimen was then set aside for 24 hours to allow the silicone to cure. Following the 24-hour cure time, the specimen was positioned between the end platens, wrapped with latex membrane, and secured to the end platens with o-rings.

As previously discussed, the installation of the thermocouple into the specimen required partial dismantling of the piston assembly. The removal of components used to conduct water through the specimen prevented a saturation sequence as is typical with test specimens. Therefore, it was decided to calibrate the heating and cooling times of the specimen in a dry condition. Water is a more efficient conductor of thermal energy than is air, 0.613 W/(m · K) and 0.026 W/(m · K), respectively, therefore testing with a dry specimen yields conservative calibration times for thermal equilibrium.

4.5.2 Method of Cooling and Heating Calibration

At the commencement of the cooling conditioning process, both the specimen and the conditioning water were approximately 25ºC which was the typical ambient temperature of the room in which testing occurred. A multitude of chiller set temperature combinations were run to determine the most expedient sequence for equilibrium with a target end temperature of 10ºC ± 0.1ºC for the specimen. Owing to the efficiency of the chiller unit, care was taken not to allow the chiller to run lower than the target temperature for too long. Once the specimen temperature is achieved in the cooling process, any increase in temperature can only occur due to thermal conduction from the surrounding warmer environment.

The heating conditioning sequence began with the specimen at approximately the target temperature of the cooling process (10ºC). This was done in order to allow for future nondestructive testing of specimens at low and high temperatures progressively. As with the temperature combination iterations with the cooling process, those for the heating process followed the same logic. The target end temperature was set at 40ºC ± 0.1ºC for the specimen.

Initially, 60 minutes of conditioning time was the target for achievement of thermal equilibrium within the specimen. This target conditioning time was used as a basis for sizing of the heater and chiller used with the system. After several calibration sequences, it was validated that this limited conditioning time was sufficient to achieve the target temperature but that an additional 30 minutes would allow for further stabilization. Although the specimen may be at the target temperature, the entire mass of the system may not. Therefore, the additional energy exchange can help to bring more of the system to the target temperature, which acts as a thermal blanket around the specimen.

4.5.3 Cooling Calibration Results

For the target temperature of 10ºC, the chiller was initially set at 7ºC. Initial conditions for the specimen and circulating water were 27.1ºC and 25.0ºC, respectively. The chiller set temperature was held for 40 minutes at which time the set temperature was increased to 8ºC and maintained for an additional 50 minutes. The specimen reached the target temperature of 10ºC after a total of 61 minutes of conditioning time. Further conditioning was conducted for 29 minutes at which time the specimen stabilized to 10.0ºC. The chiller was then turned off thereby terminating the flow of conditioned water through the system. The specimen core temperature was monitored for an additional 30 minutes wherein the end temperature of the specimen was 10.1ºC. This range of temperature (10ºC ± 0.1ºC) was considered acceptable for the anticipated testing. Water circulation was maintained throughout testing.

As is shown in Figure 4-9, the chilled circulating water achieved the set temperature very rapidly. Prior to stabilizing at the initial set temperature of 7ºC, the water temperature is shown to drop to a temperature lower than the set temperature. This is attributed to the response sensitivity of the chiller itself. In order to rapidly lower the

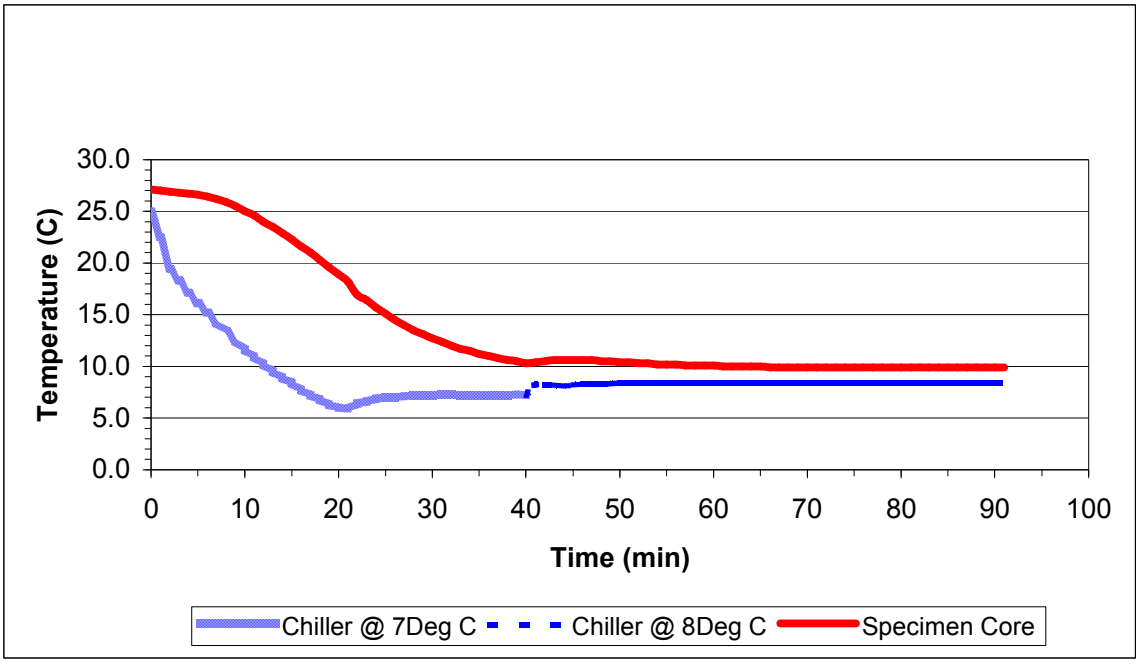

Figure 4-9. Graph of the Time vs. Temperature in a Typical GA-C1 Specimen—Chilling from Room Temperature to 10ºC.

temperature of the circulating water, the chiller maximizes the amount of energy that it can draw from the fluid. As the circulating water approaches the set temperature, the chiller decreases the rate of energy transference, thereby decreasing the change in temperature per time. As was observed in all cooling sequences conducted, a DT of 18ºC (initial temperature of 25ºC to a set temperature of 7ºC) was large enough that the efficiency of the chiller exceeded its ability to decrease the rate of heat conduction. As a result, the chiller "overshot" its target temperature. Additionally, it is shown that for the maintenance of the target temperature inside of the specimen, the chiller must be set to a lower temperature. For a specimen target temperature of 10ºC, the chiller is required to be set to 8ºC. This loss of 2ºC from the time the fluid left the chiller to reaching the interior of the cell is attributed to the conditioning water gaining energy from the ambient temperature as the fluid is conducted through the distribution lines and the cell itself.

The prescribed protocol for cooling the specimen to 10ºC is summarized as:

- Set chiller to 7ºC and run for 40 minutes;
- Change chiller set temperature to 8ºC and run for 50 minutes; and
- Perform testing.

4.5.4 Heating Calibration Results

Initial conditions for the specimen and circulating water at the commencement of the heating process was 10.2ºC and 26.5ºC, respectively. For the target temperature of 40ºC, the heater was initially set at 45ºC. The heater set temperature was held for 55 minutes at which time the set temperature was decreased to 40ºC and maintained for an additional 35 minutes. At the end of the total 90 minutes of conditioning, the specimen core temperature had reached 40.0ºC. The heater was then turned off thereby terminating the flow of conditioned water through the system. The specimen core temperature was monitored for an additional 30 minutes wherein the end temperature of the specimen was 39.9ºC. This range of temperature (40ºC ± 0.1ºC) was considered acceptable for the anticipated testing. During anticipated testing, the heated water circulation is maintained throughout testing.

As is shown in Figure 4-10, the circulating water achieved the set temperature very rapidly at which it was allowed to stabilize while the specimen core temperature increased. Also notable is the near parallelism of the rate of temperature increase in specimen and heater from 0 to 35 minutes of test time. This parallelism is consistent with the equation for the rate of heat conduction.

Using this parallelism it was determined that because the sample and the water used during the conditioning in this research started at a temperature of about 22.0ºC (71.6ºF), instead of the sample having a starting temperature of 10.9ºC as shown in the graph, less

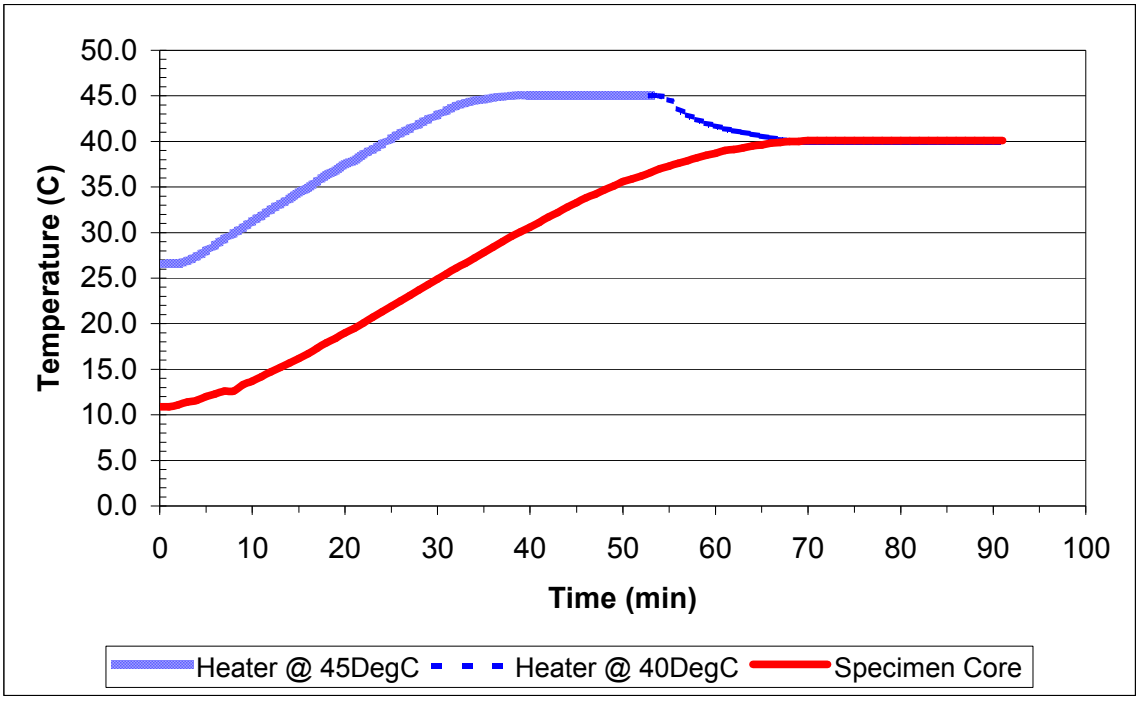

Figure 4-10. Graph of the Time vs. Temperature in a Typical WR-C1 Specimen—Heating from 10ºC to 40ºC.

time would be required to raise the temperature to the 40.0ºC. Therefore, the Haake P5 was allowed to run at 45.0ºC for 30 minutes and then at 40.0ºC for an additional 15 minutes. At this point the heating blanket would have already been put in place and would continue maintaining the appropriate temperature in the cell throughout the rest of the conditioning process.

The prescribed protocol for heating the specimen to 40ºC is summarized as:

- Set heater to 45ºC and run for 30 minutes;
- Change heater set temperature to 40ºC and run for 15 minutes; and
- Perform conditioning sequence.

The protocols for cooling and heating were initially developed using both the GA-C1 and WR-C1 mixes with percent voids of 7.0% ± 0.5%. It is recommended that this protocol be used with the mixes used in this research and other coarse mixes with approximately similar air void percentage. For other mixes, a baseline should be

developed using the same methodology as presented herein to ensure the amount of time and temperature to stabilize the core of the specimen.

CHAPTER 5
ASPHALT MIXTURE CHARACTERISTICS

This chapter introduces two quantitative characteristics of asphalt mixtures. First, results of the Florida Method of Test for the Measurement of Water Permeability of Compacted Asphalt Paving Mixtures are shown. Secondly, a performance-based fracture criterion for flexible pavements, dubbed the "Energy Ratio," will be discussed.

5.1 Permeability

The Florida Method of Test for the Measurement of Water Permeability of Compacted Asphalt Paving Mixtures has the designation of FM 5-565. This test uses a falling head permeability setup to determine the water conductivity of an asphalt sample. The measurements from this test are used to calculate the one-dimensional, laminar flow of water through a specimen based on Darcy's law. Please note that this research was conducted in 2002. At the time, there was a possibility of a change in the methodology. The end of the outflow pipe was left at an elevation well below that of the bottom of the sample during this research.

This test was performed to help find a correlation between the permeability of a mix and the mixes' susceptibility to moisture damage. The permeability of a mix has been linked to the void connectivity throughout a sample. The expanse of the connections between voids determines the amount of surface area and the depth to which water can affect compacted asphalt. Six granite mixtures that had been developed, as discussed in section 3.1.2, were subjected to this permeability testing procedure. Table 5-1 shows the results of this testing.

Table 5-1. Results of the Florida Method Permeability Test.

Sample	average % AV	average permeability K (x10^-5 cm/s)	Sample	average % AV	average permeability K (x10^-5 cm/s)
F1	6.9	25	C1	7.1	48
F2	6.8	9	C2	6.7	43
F3/C4	6.8	34	C3	6.8	62

5.2 Hot-Mix Asphalt Fracture Mechanics

Birgisson, Roque, and Page (2003) showed that moisture damage strongly affects the fracture resistance of mixtures. This means that HMA fracture mechanics can also be used to quantify the effects of moisture damage on mixtures.

The central feature of the hot mix asphalt fracture mechanics framework developed by the University of Florida (Zhang, Roque, Birgisson, and Sangpetngam, 2001) is the threshold concept. Cracks in hot-mix asphalt have been observed to grow in a discontinuous (stepwise) manner (Jacobs, Hopman, and Molenar, 1996; Kim , Lee, and Little, 1997; Roque, Zhang, and Sankar, 1999; Zhang, Roque, Birgisson, and Sangpetngam, 2001). Traditional linear elastic fracture mechanics assume that a continuous crack growth curve can be fitted to the crack growth data, which is inconsistent with the observations of a discontinuous crack growth. Zhang, Roque, Birgisson, and Sangpetngam (2001) discovered that a damage threshold exists, which defines the development of stepwise macro-cracks at any point in the mixture. Damage below the threshold is considered micro-damage (i.e., damage not associated with crack initiation or crack growth) and appears to be fully healable after a resting period, while macro-damage (i.e., damage associated with crack initiation or growth) occurs when the threshold is exceeded, and does not appear to be healable.

Zhang, Roque, and Birgisson (2001) and Zhang, Roque, Birgisson, and Sangpetngam (2001) showed that the dissipated creep strain energy (DCSE) limit and the fracture energy limit (FE) of asphalt mixtures suitably define the lower and upper thresholds, respectively. These energy limits can be easily determined from the stress-strain response of a tensile strength test and resilient modulus test using the SuperPave™ Indirect Tensile Test following the procedures developed by Roque and Buttlar (Buttlar and Roque, 1994; Roque and Buttlar, 1992).

The rate of damage growth under the energy threshold is governed by the creep properties of the mixture. The creep compliance of mixtures can be represented using the following power function:

$$D(t) = D_0 + D_1 t^m \qquad \text{(Equation 5-1)}$$

In this case, D(t) is creep compliance and D_0, D_1, and m are parameters obtained from creep tests. Hence, it is assumed that the rate of micro-damage is controlled by the m-value and D_1.

Based on the concepts and HMA fracture model, the following key parameters appear to govern the cracking performance of asphalt mixtures:

- DCSE limit: dissipated creep strain energy to failure,
- m-value: parameter governing the creep strain rate, and
- D_1 parameter: parameter governing the creep strain rate.

In addition, the tensile stress in the pavement controls where and how fast a crack initiates and grows for a given pavement configuration. Figure 5-1 shows a conceptual illustration of the HMA fracture mechanics framework, the energy thresholds (FE and DCSE), and the effects of rate of creep and m-value on rate of damage. The higher the

m-value, the faster the rate of accumulation of DCSE per cycle becomes, and thus the faster the DCSE limit is reached.

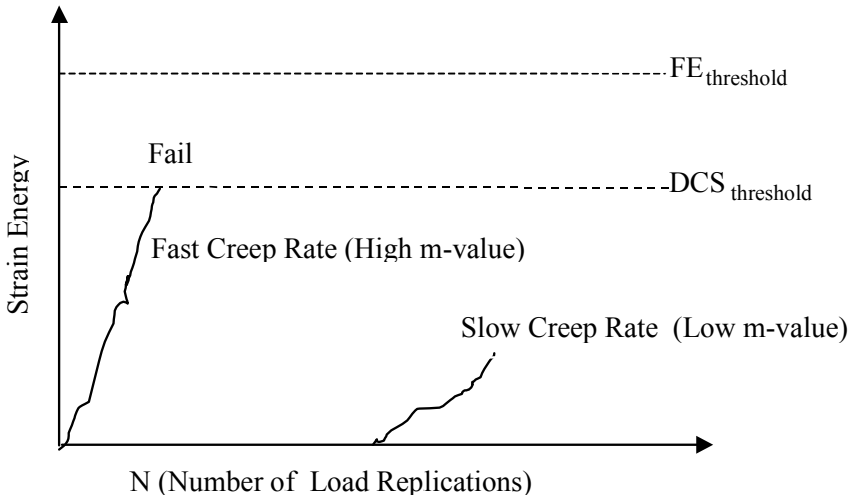

Figure 5-1. Graph Showing Energy Thresholds and the Effects of Rate of Creep and m-value on Rate of Damage.

Based on detailed forensic investigations of 36 field pavement sections of known cracking performance in Florida, an HMA fracture mechanics-based performance specification criterion, termed the "Energy Ratio" (ER), was developed by Jajliardo (2003). This parameter is a measure of the fracture resistance of mixtures, and is expressed by:

$$ER = \frac{DCSE_f}{DCSE_{min}} = \frac{a \times DCSE_f}{m^{2.98} \times D_1} \qquad \text{(Equation 5-2)}$$

where: $DCSE_f$ = Dissipated Creep Strain Energy (in kJ/m^3),

$DCSE_{min}$ = Minimum Dissipated Creep Strain Energy for adequate cracking performance (in kJ/m^3),

D_1 and m are creep parameters in 1/psi, and

$$a = 0.0299\sigma^{-3.1}(6.36 - S_t) + 2.46 \times 10^{-8}$$

where: σ = tensile stress of asphalt layer (in psi), and

S_t = tensile strength (in MPa).

Based on the observed pavement performance from these 36 field sections, Jajliardo (2003) was able to determine a minimum DCSE for adequate cracking performance for the mixtures used. Jajliardo (2003) also recommended a minimum required ER (ER_{min}) for various traffic levels. For 3 million ESALs, the recommended ER_{min} is 1.1, for 10 million ESALs, ER_{min} is 1.3, and for 30 million ESALs, ER_{min} is 1.7. Hence, ER forms the basis for a performance-based fracture criterion for flexible pavements.

CHAPTER 6
SPECIMEN CONDITIONING

6.1 Procedure Overview

The conditioning of the asphalt specimens takes place by exerting cyclic pore pressure on all water accessible voids of the sample. This is accomplished by saturating the sample and then placing it into an airtight, water-filled chamber. Water is forced into the chamber to build up pressure. This pressure is transferred to every surface that the water is in contact with. When this pressure is cycled into the chamber, it can accelerate moisture damage in a sample. Additionally, while this conditioning procedure produces a pore pressure effect, the aggregate structure is not placed under any stress. This is unlike the Lottman tests (see sections 2.5.2.1 and 2.5.2.3) where a saturated sample is subjected to a freeze-thaw cycle in which the expansion of the frozen water will place stress upon the aggregate skeleton.

Stripping of the asphalt from the aggregate is a consequence that occurs because of water being pumped in and out of the voids. As in the boiling water test (section 2.5.1.1), this research attempted to accelerate this effect by increasing the temperature of the water in the conditioning chamber during one of the four conditioning settings. However, unlike the boiling water test, this conditioning system provides the effects of increased pore pressure.

In this research, the pore water pressure is the only load placed upon the sample, making the effective stresses within the sample zero. Therefore, the aggregate structure

is under no stress. It is possible, however, for the asphalt film to experience damage (as discussed in Chapter 2).

The structural layers of SuperPave™ asphalts are considered to have completely interconnected voids. This is not the case in actuality as some small pockets of air may become trapped throughout a sample. The asphalt film enclosing an air void will flex with increased pressure due to the compressibility of the air. The asphalt film may be too weak to withstand this pressure. The parts of the asphalt film that are not immediately affected by this pressure may weaken during the conditioning process because of spontaneous emulsification (see section 2.3.3) or other factors to the point that it is susceptible to the pressure. While a static positive pressure may cause these effects, it is this researchers opinion that the long-term repetitive cycling of pore pressure can cause fatigue failure in the asphalt film as well. Once the film fails, water can be forced into new channels, fissures in the aggregate, or even between the aggregate and the asphalt. Additionally, the pressurized water may then be attempting to open new voids. While a static negative pressure may stress the asphalt film just as well, this negative pressure might close these channels and fissures, possibly decelerating the moisture damage effects. A simplified diagram of the sample being loaded with increased pore pressure is shown in Figure 6-1. This diagram shows an enlargement of channels through a sample and the pressure exerted on them by increased pore pressure.

6.2 Sample Conditioning

This section describes the process used to create the conditioned set of samples. A sample that had been determined to meet the Va standard (see section 3.2.2) was placed on a mesh, metal riser in a saturation chamber. The chamber was filled with enough water to cover the sample by approximately one inch. The riser allowed the water to

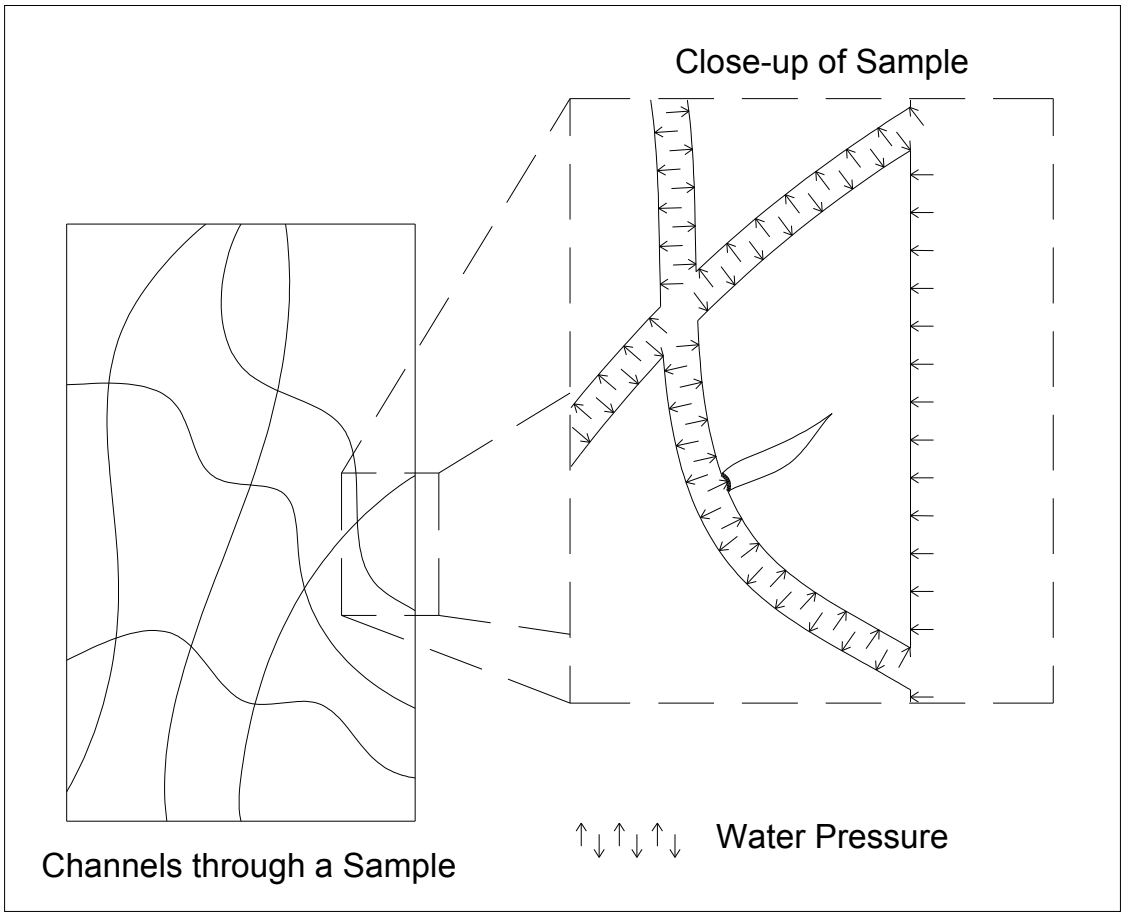

Figure 6-1. Diagram of the Pressures Exerted on the Channels Through a Sample with Increased Pore Pressure.

reach all surfaces of the pill. The lid was placed on the chamber and the vacuum pump that was attached to it was turned on. The control knob was adjusted so that the pressure in the chamber dropped to negative 25 ± 2 inHg (12.28 ± 0.98 psi).

The sample was allowed to sit in this vacuum for 15 minutes. The sample was slightly agitated to remove some of the air bubbles clinging to the surface of the specimen before releasing the vacuum. The pill was allowed to sit submerged for 20 minutes at normal pressure. This allowed the water to infiltrate the deeper voids in the specimen that was previously filled with air. The sample was considered saturated after this process was completed a second time (with more agitation before releasing the

pressure). No specific saturation levels were targeted, since each mix has a unique void structure that may enhance or reduce the saturation capacity of the mixture. It was felt by the researchers that forcing a target saturation level might cloud the effective differences between mixtures in resisting moisture ingress and therefore may possibly cause inadvertent moisture damage.

The cyclic loading and pore pressure conditioning system (see section 4.3.1) was cleaned of debris from the previous experiments and the o-rings were fitted in place with vacuum grease to improve the ability of the chamber to become airtight. The sample was placed on the pedestal inside the chamber. The chamber wall and lid were fitted exactly to insure their seal.

A test pressure was applied to the chamber to determine if the seals would hold during the conditioning cycle. A pressure of five psi greater than the maximum pressure that would be used during the conditioning was placed directly into the chamber. The valves into the chamber were then closed. The chamber was considered airtight if the pressure gauge did not read a drop of more than 0.5 psi after 30 seconds. This was a necessary step, even though it could potentially induce some damage to the sample. This task was performed on every conditioned sample to maintain repeatability and could save several hours of setup time and the partial conditioning of a sample if a leak was discovered early. The test pressure was released and the chamber was filled with room temperature water.

When conditioning samples at 40ºC, the process described below was used to heat the water in the cell. The water was circulated through the Thermo Haake DC10 P5/U at 45ºC for 30 minutes and then at 40ºC for an additional 15 minutes to insure even heating

throughout the sample (see section 4.5.4). A heating pad was connected to its power source and temperature gauge while the water was circulating. The heating pad was wrapped around the chamber wall. An insulation blanket was then placed around this and the two were secured using bungee cords. The heating pad was switched on once the water temperature inside the cell reached 39.0ºC. This was to insure that the heating pad did not try to increase the water temperature too fast and overshoot the correct temperature by a large margin.

The following procedure was followed for all samples being conditioned. The tubes of the hydraulic setup were purged of air as much as possible by pushing water through them using the volume changer. The chamber was connected to the hydraulic volume changer setup via these tubes (see section 4.3 for the plumbing setup). Water was then pushed into the bottom of the chamber with the upper part of the chamber connected to the annulus tubes with their vent open. This allowed most of the air in the chamber to be forced out. It was evident that the cyclic loading and pore pressure conditioning chamber was filled with water when as much water filled the annulus as was pushed into the chamber by the volume changer.

Approximately three-quarters of the excess water in the annulus were drained. Next, the vent to the annulus was closed and the valve connecting the tube from the vacuum portion of the vacuum/pressurized air control panel (vacuum tube) to the annulus was opened. The pressure was decreased by approximately 10.2 inHg (5.0 psi) over 2 minutes in order to remove any air that was still in the system or had gotten into the sample during the transfer from the vacuum chamber to the conditioning chamber. This decrease in pressure was held for approximately 15 minutes or until the majority of the

air bubbles coming into the annulus subsided. The valve to the vacuum tube was closed and the vent was slowly opened. This allowed water to recede back into the chamber to replace the air that had just been removed. The setup was allowed to sit for another 15 minutes before this final air removal process was completed a second time. At this point in the conditioning procedure, a saturated sample had been enclosed in an airtight conditioning chamber completely filled with water (either at room temperature or 40ºC) at normal pressure. The valves to the top and bottom of the conditioning chamber had been closed and the valve connecting the hydraulic volume changer to the water source was opened.

Finally, the computer program controlling the conditioning procedure was turned on. The program started by drawing water from the source into the volume changer. The water source valve was then closed and the valve to the bottom of the conditioning chamber was opened. The program was instructed to continue and did so by signaling the hydraulic volume changer to push water into the chamber until the pressure transducer, which was connected to the top of the chamber, read a change of 5.0 psi (10.2 inHg). Next, the bottom chamber valve was closed and the water source valve reopened. The hydraulic volume changer recharged by drawing its piston back and sucking in the water from the source hose. The water source valve was again closed and the bottom chamber valve reopened. The hydraulic volume changer then continued to the main stage of the conditioning where it would push water into the chamber until the pressure reached the required maximum limit of 15, 25, or 30 psi (30.5, 50.9, or 61.1 inHg) for a change of 10, 20, or 25 psi (20.3, 40.7, or 50.9 inHg), respectively. The piston would then recede, drawing out the excess water until the pressure in the chamber was a positive 5-psi again.

This cycle was repeated once every three seconds (0.33 Hz), following a sine waveform, for a total of 5,800 cycles. Once these cycles were completed, the pressure was released by drawing back the piston. Lastly, the heating blanket was removed (if used) and the chamber was emptied. The temperature of the water was recorded if the procedure was completed at room temperature. The sample was now considered conditioned.

CHAPTER 7
RESULTS AND CONCLUSIONS

7.1 Overview

In this Chapter, the moisture conditioning system described in Chapter 4 is evaluated for use in asphalt mixtures. Using five mixtures with aggregates of known moisture damage susceptibility, the primary objective of this research was to evaluate the use of a new cyclic pore pressure-based moisture conditioning system, using a fracture mechanics-based criterion, the ER, for inducing and quantifying the effects of moisture damage in mixtures. The conditioned mixtures were tested with the SuperPave™ IDT test for fracture properties and the results were compared to unconditioned mixtures.

The results presented show that cyclic pore pressure conditioning of mixtures results in accelerated moisture damage and stripping of the granite mixtures. In comparison, the limestone mixtures are shown to be resistant to pore pressure induced moisture damage. The Energy Ratio (ER), discussed previously in Chapter 5, is shown to be a useful parameter for detecting a range of moisture damage in mixtures.

Based on the results presented, cyclic pore pressure conditioning of mixtures, followed by SuperPave™ IDT testing of fracture parameters with the ER may form the basis of promising combined performance-based specification and testing criteria for evaluating the effects of moisture damage in mixtures as well as the overall resistance to fracture.

This chapter deals with the use of the new cyclic loading and pore pressure conditioning system discussed in Chapter 4 along with a SuperPave™ IDT-based fracture

performance-based criterion, the ER, for the conditioning and subsequent evaluation of moisture damage on mixtures containing aggregates of known stripping performance. Below, a description is provided of the materials and methodologies used, followed by the cyclic pore pressure protocol used. The ER for conditioned and unconditioned mixtures is compared. In addition to the Energy Ratio, the key SuperPave™ IDT fracture parameters that were monitored include creep properties, resilient modulus, tensile strength, fracture energy limit, and dissipated creep strain energy limit.

Three granite mixtures were developed, using the method described in section 3.1.2, and used. These consisted of crushed granite from Georgia that has shown potential for stripping. The two limestone mixtures were known to be highly resistant to stripping. The purpose of selecting granite and limestone mixtures of varying gradation was to ensure that the mixtures tested were of different aggregate type, permeability, and other volumetric properties. The resulting gradations are shown in Table 7-1. The mixtures ranged from what could be described as fine, uniformly-graded and fine, dense-graded to coarse, uniformly-graded and coarse, gap-graded. Table 7-2 shows the

Table 7-1. List of Gradations for the Granite and Limestone Mixtures.

	Percent Material Passing each Sieve Size				
Sieve Size (mm)	GA-C1	GA-F1	GA-F3	WR-C1	WR-F1
19.0	100.0	100.0	100.0	100.0	100.0
12.5	97.4	94.7	94.6	97.0	96.0
9.5	89.0	84.0	85.1	90.0	85.0
4.75	55.5	66.4	65.1	60.0	69.0
2.36	29.6	49.2	34.8	33.0	53.0
1.18	19.2	32.7	26.0	20.0	34.0
0.60	13.3	21.0	18.1	15.0	23.0
0.30	9.3	12.9	12.5	11.0	15.0
0.15	5.4	5.9	7.7	7.6	9.6
0.075	3.5	3.3	5.8	4.8	4.8

volumetric properties for the mixtures used. For each pore pressure and temperature combination, three samples of each mix were prepared. In addition, three unconditioned specimens for each mixture were prepared.

Table 7-2. List of the Volumetric Properties of the Granite and Limestone Mixtures.

Properties	Mixture				
	GA-C1	GA-F1	GA-F3	WR-C1	WR-F1
Asphalt Content (%)	6.63	5.68	5.14	6.50	6.30
Specific Gravity of Asphalt	1.035	1.035	1.035	1.035	1.035
Bulk Specific Gravity	2.345	2.374	2.404	2.235	2.244
Theoretical Max. Specific Gravity	2.442	2.473	2.505	2.328	2.338
Air Voids (%)	4.0	4.0	4.0	4.0	4.03
Voids in Mineral Aggregate (%)	18.5	16.6	15.1	15.4	15.6
Voids filled with Asphalt (%)	78.5	75.9	73.3	74.16	74.17
Effective Specific Gravity of Aggregate	2.710	2.706	2.720	2.549	2.554
Absorbed Asphalt (%)	0.3	0.3	0.5	1.3	1.1
Effective Asphalt (%)	6.3	5.4	4.7	5.3	5.3
Dust to Asphalt Ratio	0.6	0.6	1.2	0.7	0.8
Surface Area (m^2/kg)	3.3	4.1	4.9	4.9	6.1
Theoretical Film Thickness, microns	19.9	13.4	9.9	11.2	9.0

The SuperPave™ IDT test was used to perform Resilient Modulus (MR), Creep Compliance, and Strength tests (Buttlar and Roque, 1994; Roque, et al., 1997; Sedwick, 1998) from which the following properties were determined, tensile strength, resilient modulus, fracture energy limit (FE), dissipated creep strain energy limit (DCSE), and creep properties. Using these mixture properties and the fracture mechanics-based Energy Ratio fracture performance criterion developed at the University of Florida, the effects of moisture damage on the fracture resistance of the mixtures were calculated.

7.2 Evaluation of Cyclic Pore Pressure Induced Moisture Damage Using the Energy Ratio

In the following, the effects of moisture damage on the fracture resistance of mixtures are evaluated. Table 7-3 shows a summary of the SuperPave™ IDT fracture properties for the mixtures tested. The ER for conditioned mixtures is lower for all granite mixtures, as expected. Figures 7-1A, 7-2A, 7-3A, and 7-4A show a comparison between the changes in ER for conditioned and unconditioned mixtures, testing pressures and temperatures. Similarly, Figures 7-1B, 7-2B, 7-3B, and 7-4B show the ratio of the conditioned versus unconditioned ER for all mixtures, pressure, and temperature conditions tested. The granite mixtures (GA-1, GA-F1, and GA-F3) all showed a decrease in ER with cyclic pore pressure conditioning, whereas the limestone mixtures (WR-C1 and WR-F1) showed only a slight drop in ER. Visual observations confirmed that all the granite mixtures showed stripping, whereas the limestone mixtures showed little or no evidence of stripping. The GA-C1 mixture was expected to show a greater change in ER than observed for all pressures at the testing temperature of 25ºC. However, cyclic pore pressure conditioning at an elevated temperature of 40ºC resulted in the expected drop in the ER for the GA-C1 mixture. Hence, based on these limited results, it appears that in addition to the application of pressure, elevated conditioning temperatures may be required to produce a consistent response in conditioned mixtures, as determined by the energy ratio parameter, ER.

7.3 Summary

The primary objective of this study was to accurately determine the effects of cycling pore pressures in SuperPave™ samples. This paper evaluated four different cyclic pressure/temperature conditions. An introduction to this project was presented in

Table 7-3. Summary of Mixture Properties for Conditioned and Unconditioned Samples

Material	Resilient Modulus, M_R (GPa)	Creep Compliance at 1000 seconds (1/GPa)	Tensile Strength, S_t (MPa)	Fracture Energy (kJ/m^3)	Failure Strain (10^{-6})	m-value	D_1 (1/psi)	DCSE (kJ/m^3)	Energy Ratio, ER	ER_{cond}/ER_{uncond}
Unconditioned										
GA-C1	6.32	15.60	2.10	12.50	7343.9	0.65	1.12E-06	12.15	2.75	--
GA-F1	8.75	7.88	2.59	11.20	5434.8	0.57	1.10E-06	10.82	3.49	--
GA-F3	10.21	4.89	3.00	8.20	3581.4	0.54	8.19E-07	7.76	3.69	--
WR-C1	8.53	2.54	2.14	2.50	1939.0	0.53	9.51E-07	2.23	1.09	--
WR-F1	8.56	5.00	2.17	3.00	1923.2	0.51	1.01E-06	2.72	1.40	--
Conditioned at 5-15 psi and 25°C										
GA-C1	7.70	12.74	2.03	8.40	5144.8	0.71	6.49E-07	8.13	2.46	0.89
GA-F1	8.54	9.48	1.71	2.45	1950.0	0.67	6.26E-07	2.28	0.89	0.25
GA-F3	9.46	7.60	1.78	2.65	2117.8	0.67	4.85E-07	2.48	1.22	0.33
WR-F1	8.68	12.00	2.09	5.10	3230.0	0.65	9.19E-07	4.85	1.35	0.97
Conditioned at 5-25 psi and 25°C										
GA-C1	6.75	12.19	2.02	8.00	5083.4	0.71	6.13E-07	7.70	2.49	0.90
GA-F1	8.24	9.94	1.67	2.55	2051.2	0.61	1.03E-06	2.38	0.77	0.22
GA-F3	9.69	6.69	1.91	2.65	1891.7	0.63	5.87E-07	2.46	1.20	0.33
WR-F1	8.68	12.00	2.09	5.10	3230.0	0.65	9.19E-07	4.85	1.35	0.97
Conditioned at 5-30 psi and 25°C										
GA-C1	6.76	21.67	2.17	8.20	7115.6	0.86	3.81E-07	7.85	2.23	0.81
GA-F1	7.94	11.92	1.77	3.60	2677.4	0.72	5.57E-07	3.40	1.19	0.34
GA-F3	10.03	5.98	3.60	3.60	2345.9	0.51	1.24E-06	2.95	0.98	0.27
WR-F1	8.68	12.00	2.09	5.10	3230.0	0.65	9.19E-07	4.85	1.35	0.97
Conditioned at 5-15 psi and 40°C										
GA-C1	7.68	11.51	1.59	3.60	2853.8	0.63	1.10E-06	3.44	0.94	0.34
GA-F1	7.30	8.44	1.59	2.90	2458.3	0.53	2.33E-06	2.73	0.59	0.17
GA-F3	9.89	5.88	1.69	1.90	1561.3	0.54	9.38E-07	1.76	0.86	0.23
WR-C1	8.53	5.59	2.45	2.25	2017.0	0.44	1.45E-06	1.90	1.01	0.93
WR-F1	8.68	12.00	2.09	5.10	3230.0	0.65	9.19E-07	4.85	1.37	0.98

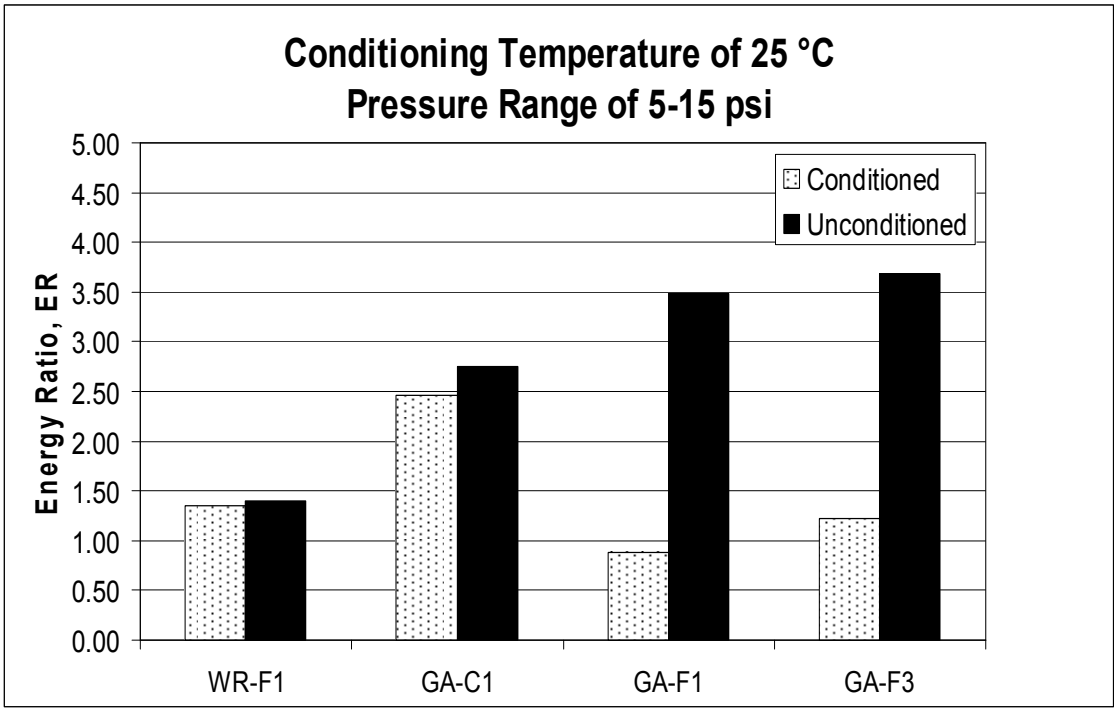

A

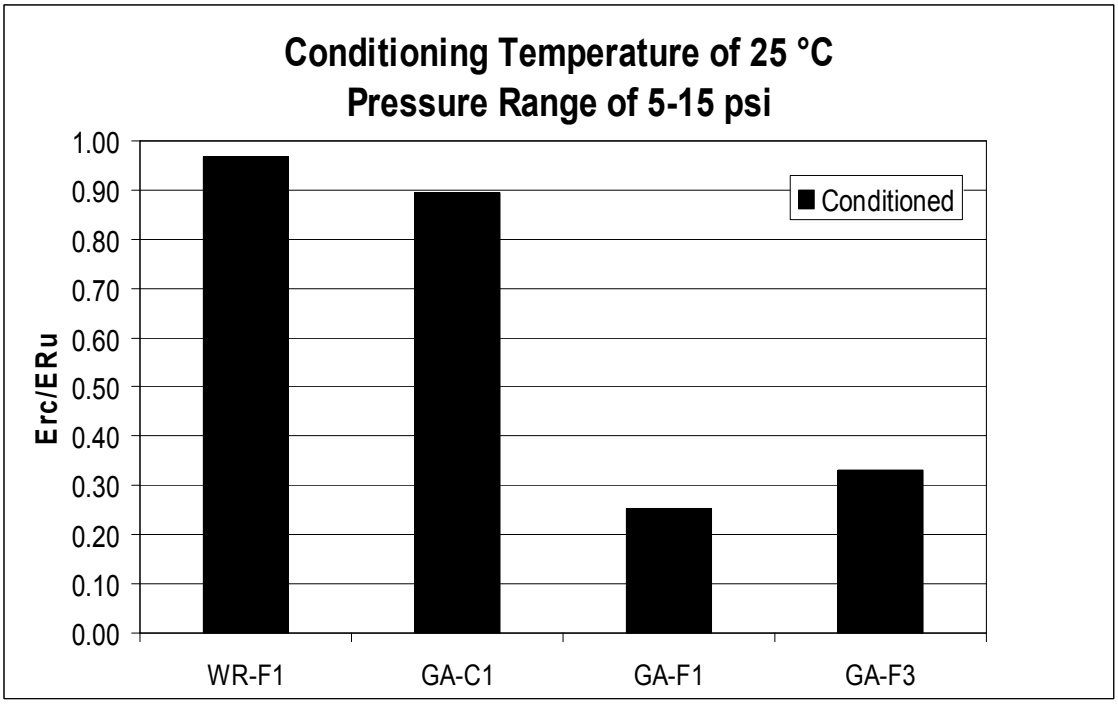

B

Figure 7-1. Two Graphs Depicting Energy Ratio Values for Mixtures Conditioned at Cyclic Pore Pressures of 5-15 psi and a Temperature of 25ºC. A) Is a Comparison of Energy Ratio Values Between the Conditioned Mixtures and the Unconditioned Mixtures and B) Shows the Percentage of Energy Ratio Retained After the Mixture Was Conditioned.

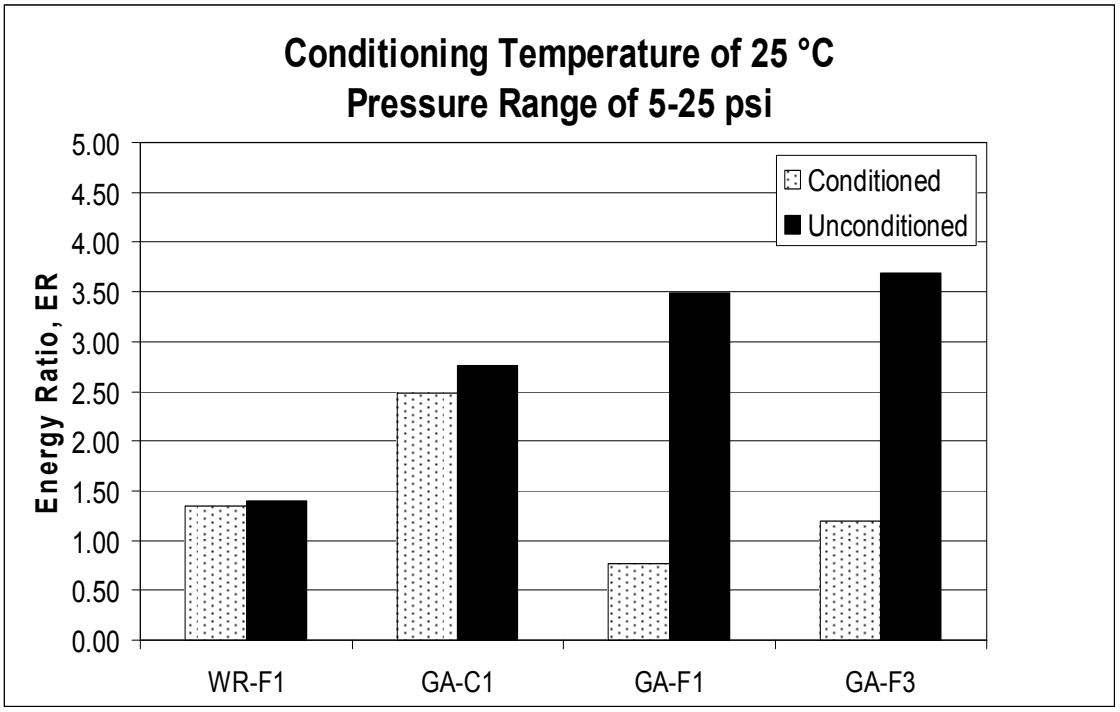

A

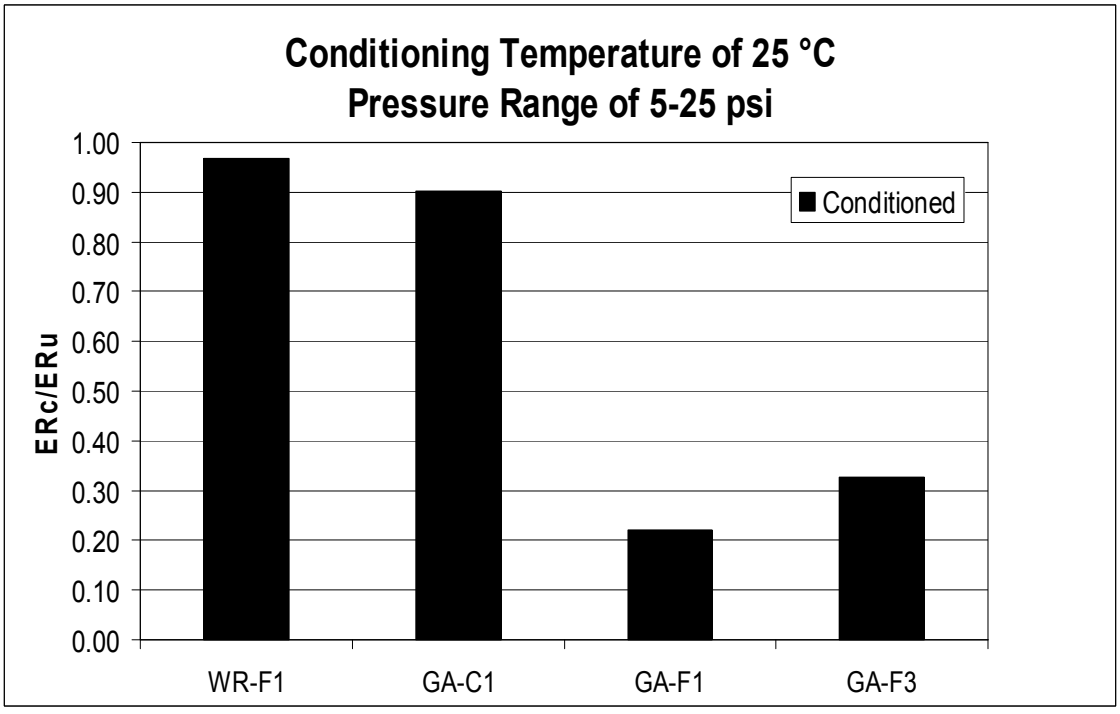

B

Figure 7-2. Two Graphs Depicting Energy Ratio Values for Mixtures Conditioned at Cyclic Pore Pressures of 5-25 psi and a Temperature of 25ºC. A) Is a Comparison of Energy Ratio Values Between the Conditioned Mixtures and the Unconditioned Mixtures and B) Shows the Percentage of Energy Ratio Retained After the Mixture Was Conditioned.

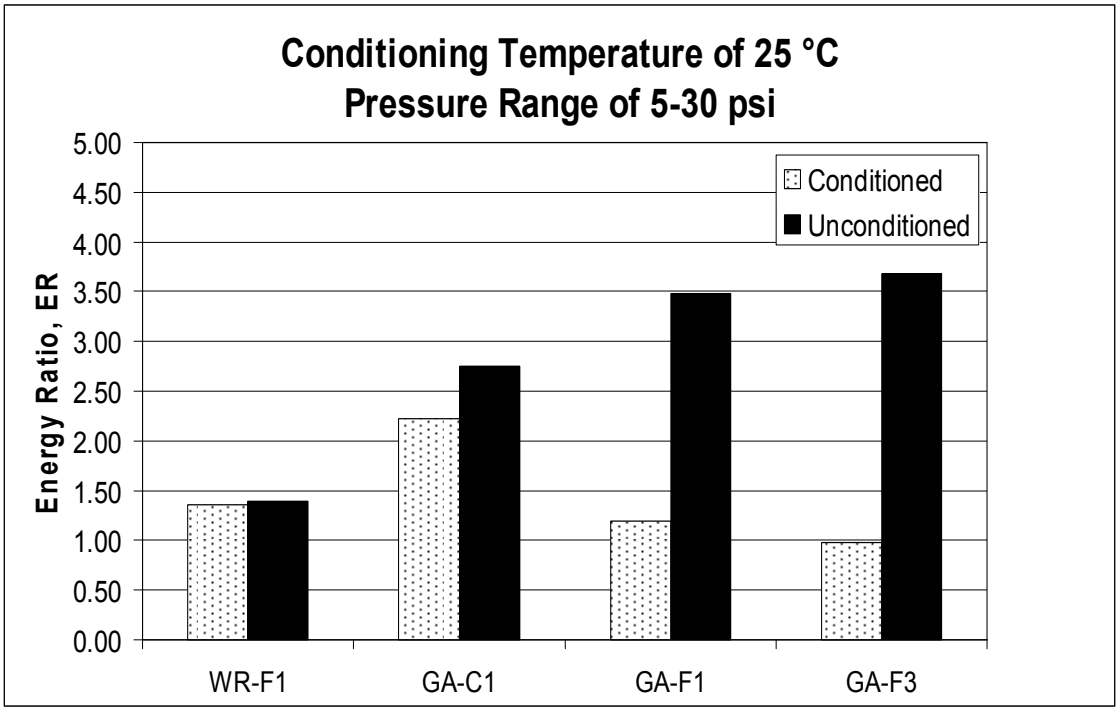

A

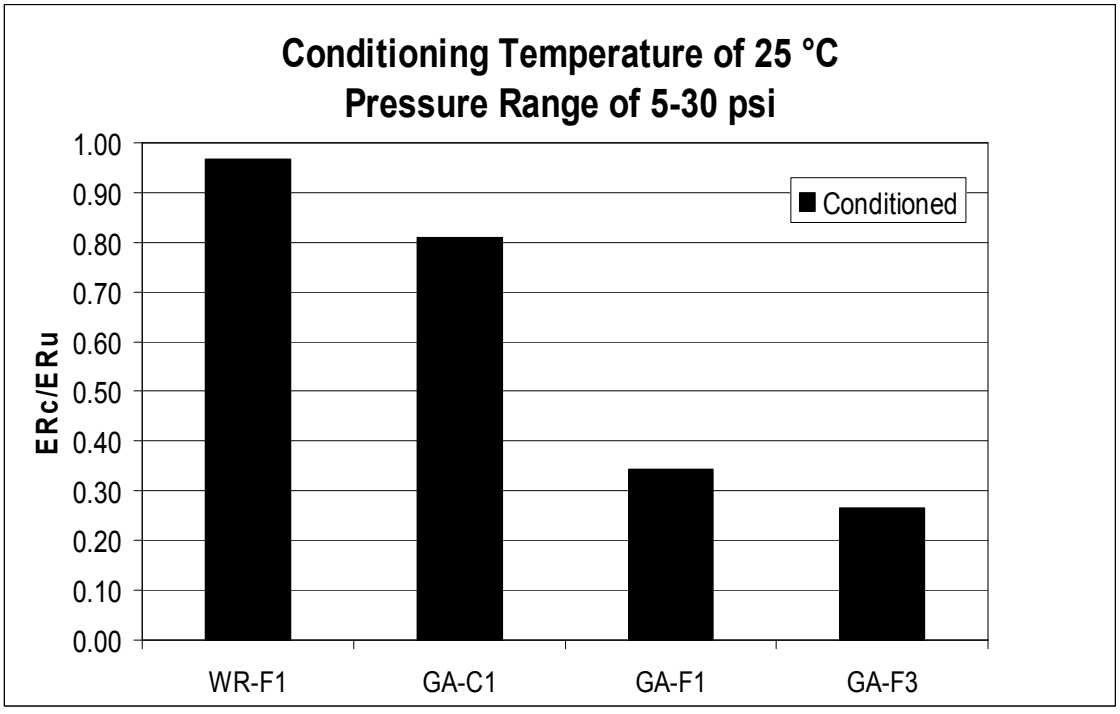

B

Figure 7-3. Two Graphs Depicting Energy Ratio Values for Mixtures Conditioned at Cyclic Pore Pressures of 5-30 psi and a Temperature of 25ºC. A) Is a Comparison of Energy Ratio Values Between the Conditioned Mixtures and the Unconditioned Mixtures and B) Shows the Percentage of Energy Ratio Retained After the Mixture Was Conditioned.

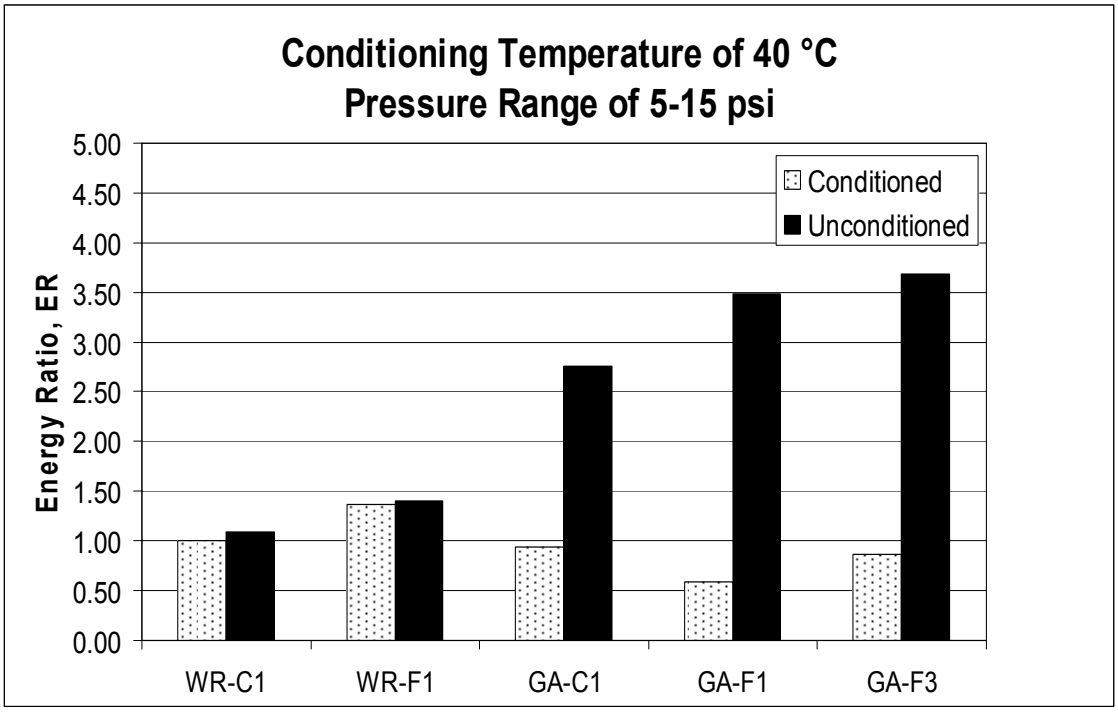

A

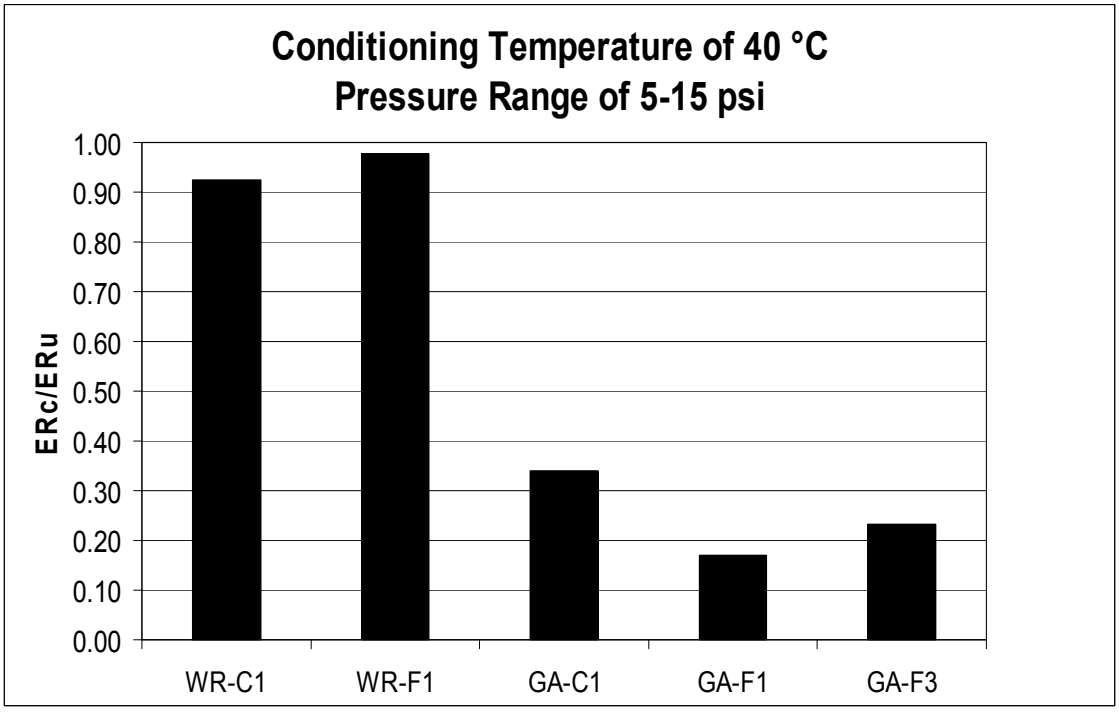

B

Figure 7-4. Two Graphs Depicting Energy Ratio Values for Mixtures Conditioned at Cyclic Pore Pressures of 5-15 psi and a Temperature of 40ºC. A) Is a Comparison of Energy Ratio Values Between the Conditioned Mixtures and the Unconditioned Mixtures and B) Shows the Percentage of Energy Ratio Retained After the Mixture Was Conditioned.

Chapter 1. An introduction to different mechanisms of moisture damage and previous research was presented in Chapter 2. The materials and methodologies used are located in Chapter 3. Chapter 4 describes the equipment used during this project. Chapter 5 contains the permeability results as well as the hot-mix asphalt fracture mechanics discussion. In Chapter 6, the specimen conditioning procedure was discussed. Finally, this chapter states the results of the project and recommendations for future research.

7.4 Conclusions

The results from this chapter show that cyclic pore pressure conditioning at an elevated temperature of 40ºC results in moisture damage patterns that are consistent with expected behavior. Limestone mixtures with proven field performance track records showed little or no moisture damage. The Georgia granite mixtures, which are known to exhibit moisture damage without the presence of anti-stripping agents, showed moisture damage.

The Energy Ratio (ER) can be used to evaluate the effects of moisture damage, independent of the conditioning procedure. Using a consistent framework for evaluating the detrimental effects of moisture damage, the effects of various conditioning procedures can also be evaluated more thoroughly. Similarly, conditioning mixtures by cycling pore pressures can be done with or without the use of ER testing for evaluation.

These results show that the use of cyclic pore pressure conditioning of mixtures accelerates the moisture damage induced in laboratory mixtures. Further research is needed to determine the amount of conditioning needed to induce damage in a "laboratory" sample that would consistently predict the performance of a "field" sample.

7.5 Recommendations

The new cyclic loading and pore pressure conditioning system that was described in this paper incorporated many useful characteristics (i.e., the fluid routing board and the temperature control system for the sample). However, this system was designed to carry out many possible tests and could be greatly simplified if it was only to be used for cyclic pore pressure conditioning. A simplified version meant only for this task would not require the external loading frame. A simple, sealable container able to withstand moderately high positive and negative pressures, similar to an asphalt pressure aging vessel, with one conduit through the base and one through the lid to allow for water passage would be sufficient. These conduits could be attached to a fluid distribution system similar to the one described in Chapter 4 with a pressure transducer in line with the top attachment to measure the pressure within the container.

It could be possible to shorten the conditioning time dramatically using a simplified container such as this as well as a slightly altered fluid distribution system (i.e., larger plumbing and a more specialized volume changer). This would allow a reduction in setup time, as it would be possible to saturate the sample in the container and not have to transfer it. The system may have the ability to maintain a higher frequency during conditioning while maintaining a stable cyclic sine waveform by using these modifications. Different conditioning parameters might be used as well. It would be possible to use negative pore pressures during the conditioning process in a simplified container with these kinds of parameters.

It is possible that simplified conditioning procedures requiring even less equipment may work as well. A static pressure conditioning system is worth investigation. If holding a saturated sample in either a positive or a negative pore pressure environment

will induce a measurable amount of damage consistently, then the conditioning system can be reduced to an air tight container, some tubing, and an air pump. Further research with setups like these would be required to determine if an acceptable amount of conditioning could be mass-produced consistently.

LIST OF REFERENCES

Adamson, A.W. *Physical Chemistry of Surfaces*, Third Edition. New York: John Wiley & Sons, 1976.

Alam, M.M., N. Vemuri, V. Tandon, S. Nazarian, and M. Picornell. *A Test Method for Identifying Moisture Susceptible Asphalt Concrete Mixes*. University of Texas at El Paso, 1998.

Al-Swailmi, S. and R.L. Terrel. Evaluation of Water Damage of Asphalt Concrete Mixtures Using the Environmental Conditioning System (ECS). *Proceedings of the Association of Asphalt Paving Technologists,* Vol. 61, pp. 405-445. St Paul, Minnesota, 1992.

American Association of State Highway and Transportation Officials (AASHTO). *AASHTO T283-86: Resistance of Compacted Bituminous Mixture to Moisture Induced Damage.* AASHTO, Part II—Methods of Sampling and Testing. Washington, D.C., August 1986.

American National Standard Institute (ANSI). *ANSI B4.2: Preferred Hole Basis Clearance Fits*. Washington, D.C., 1978.

Beer, F.P. and E.R. Johnston, Jr. *Mechanics of Materials*, Second Edition. New York: McGraw-Hill, Inc. 1992.

Birgisson, B., R. Roque, and G. Page. Evaluation of Water Damage Using Hot Mix Asphalt Fracture Mechanics. *Journal of the Association of Asphalt Paving Technologists,* Vol. 73, pp. 424-462, 2003.

Buttlar, W.G. and R. Roque. *Development and Evaluation of the Strategic Highway Research Program Measurement and Analysis System for Indirect Tensile Testing at Low Temperatures*. Transportation Research Record 1454, Transportation Research Board, National Research Council. Washington, D.C., pp. 163-171, 1994.

Carpenter, G.W. and R. Stephenson. Permeability Testing in the Triaxial Cell. *Geotechnical Testing Journal* Vol. 9, No. 1, pp. 3-9, 1986.

Çengal, Y.A. *Thermodynamics and Heat Transfer*. Boston: Irwin/McGraw-Hill, 1997.

Choubane, B., G.C. Page, and J.A. Musselman. *Effects of Different Water Saturation Levels on the Resistance of Compacted HMA Samples to Moisture Induced Damage.* Paper presented at the 80th Annual Transportation Research Board Meeting. Washington D.C., 2000.

Coplantz, J.S. and D.E. Newcomb. *Water Sensibility Test Methods for Asphalt Concrete Mixtures—A Laboratory Comparison*. Transportation Research Record 1171, Transportation Research Board, National Research Council. Washington, D.C., 1988.

Curtis, C.W., K. Einsley, and J. Epps. *Fundamental Properties of Asphalt-Aggregate Interactions Including Adhesion and Absorption*. Strategic Highway Research Program - SHRP-A-341, National Research Council. Washington, D.C., 1993a.

Curtis, C.W., K. Einsley, and J. Epps. *Fundamental Properties of Asphalt-Aggregate Interactions Including Adhesion and Absorption*. Strategic Highway Research Program Final Report SHRP A-003B, National Research Council. Washington, D.C., 1993b.

Curtis, C.W., M. Stroup-Gardiner, C.J. Brannan, and D.R. Jones. *Adsorption of Asphalt on Aggregate to Evaluate Water Sensitivity.* Transportation Research Record 1362, Transportation Research Board, National Research Council, Washington, D.C., 1992.

Earle, J.H. *Engineering Design Graphics*, Eighth Edition. New York: Addison-Wesley Publishing Company, 1994.

Fromm, H.J. The Mechanisms of Asphalt Stripping from Aggregate Surfaces. *Proceedings of the Association of Asphalt Paving Technologists,* Vol. 43, pp. 191-223. St Paul, Minnesota, 1974.

Halliday, D., R. Resnick, and K. Krane. *Physics*, Fourth Edition. New York: John Wiley & Sons, Inc., 1992.

Hicks, R.G. *Moisture Damage in Asphalt Concrete*. National Cooperative Highway Research Program (NCHRP) Synthesis of Highway Practice 175, Transportation Research Board, National Research Council. Washington, D.C., October 1991.

Jacobs, M.M.J., P.C. Hopman, and A.A.A. Molenaar. Application of Fracture Mechanics Principles to Analyze Cracking in Asphalt Concrete. *Journal of the Association of Asphalt Paving Technologists,* Vol. 65, pp. 1-39, 1996.

Jajliardo, A. *Development of Specification Criteria to Mitigate Top-Down Cracking.* Master's thesis, University of Florida, Gainesville, 2003.

Jimenz, R. A. *Testing for Debonding of Asphalts from Aggregates.* Transportation Research Record 515, Transportation Research Board, National Research Council. Washington, D.C., pp 1-17, 1974.

Juvinall, R.C. *Fundamentals of Machine Component Design*. New York: John Wiley & Sons, Inc., 1983.

Kandhal, P.S. *Moisture Susceptibility of HMA Mixes: Identification of Problem and Recommended Solutions*. National Asphalt Pavement Association (NAPA) Quality Improvement Publication 119, December 1992.

Kandhal, P.S. *Field and Laboratory Investigation of Stripping in Asphalt Pavement: State of the Art Report*. Transportation Research Record 1454, Transportation Research Board, National Research Council. Washington, D.C., pp 114-124, 1994.

Kandhal, P.S., C.W. Lubold, and F.L. Roberts. Water Damage to Asphalt Overlays: Case Histories. *Proceedings of the Association of Asphalt Paving Technologists,* Vol. 58, pp. 40-67. St Paul, Minnesota, 1989.

Kandhal, P.S. and I.S. Rickards. Premature Failure of Asphalt Overlays from Stripping: Case Histories. *Proceedings of the Association of Asphalt Paving Technologists,* Vol. 72, pp 102-123. St Paul, Minnesota, 2001.

Kennedy, T.W. *Use of Hydrated Lime in Asphalt Paving Mixtures*. National Lime Association, Bulletin 325, 1984.

Kiggundu, B.M. and F.R. Roberts. *Stripping in HMA Mixtures: State-of-the-Art and Critical Review of Test Methods*. National Center for Asphalt Technology (NCAT) Report 88-2, 1988.

Kim, Y.R., H-J. Lee, and D.N. Little. Fatigue Characterization of Asphalt Concrete Using Viscoelasticity and Continuum Damage Theory. *Journal of the Association of Asphalt Paving Technologists,* Vol. 66, pp. 520-569, 1997.

Lottman, R.P. *Laboratory Test Method for Predicting Moisture-Induced Damage to Asphalt Concrete*. Transportation Research Record 843, Transportation Research Board, National Research Council. Washington, D.C., 1982a.

Lottman, R.P. *Predicting Moisture-Induced Damage to Asphaltic Concrete—Field Evaluation*. National Cooperative Highway Research Program (NCHRP) Report 246, Transportation Research Board, National Research Council. Washington, D.C., 1982b.

Mallick, R. B., J. S. Gould, S. Bhattacharjee, A. Regimand, L. H. James, and E. R. Brown. *Development of a Rational Procedure for Evaluation of Moisture Susceptibility of Asphalt Paving Mixes*. Paper presented at the Transportation Research Board Meeting. Washington, D.C., 2003.

Masad, E., B. Birgisson, A. Al-Omari, and A. Cooley (in press). Analysis of Permeability and Fluid Flow in Asphalt Mixes. *American Society of Civil Engineers (ASCE) Journal of Materials in Civil Engineering*, 2005.

Maupin, Jr., G.W. The Use of Anti-stripping Additives in Virginia. *Proceedings of the Association of Asphalt Paving Technologists,* Vol. 51, pp. 342-362. St Paul, Minnesota, 1982.

National Center for Asphalt Technology (NCAT). *Hot Mix Asphalt Materials, Mixture Design and Construction*. Auburn University, Alabama, 1996.

Nukunya, B. *Evaluation of Aggregate Type and Gradation and Other Volumetric Properties as Criteria for the Design and Acceptance of Durable SuperPave™ Mixtures*. Doctoral dissertation, University of Florida, Gainesville, 2001.

Nukunya, B., R. Roque, M. Tia, and B. Birgisson. Evaluation of VMA and Other Volumetric Properties as Criteria for the Design and Acceptance of SuperPave™ Mixtures. *Journal of the Association of Asphalt Paving Technologists,* Vol. 70, pp. 38-66, 2001.

Parker, Jr., F. and F.A. Gharaybeh. *Evaluation of Indirect Tensile Tests for Assessing Stripping of Alabama Asphalt Concrete Mixtures*. Transportation Research Record 115, Transportation Research Board, National Research Council. Washington, D.C., 1987.

Rice, J.M. Relationship of Aggregate Characteristics to the Effect of Water on Bituminous Paving Mixtures. *Symposium on the Effect of Water on Bituminous Paving Mixtures: American Society for Testing and Materials (ASTM) Special Technical Publication 240*, pp. 17-34, 1958.

Roberts, F.L., P.S. Kandhal, E.R. Brown, D. Lee, and T.W. Kennedy. *Hot Mix Asphalt Materials, Mixture Design, and Construction*, Second Edition. National Asphalt Pavement Association (NAPA) Research and Education Foundation, Lanham, 1996.

Roque, R. and W.G. Buttlar. The Development of a Measurement and Analysis System to Accurately Determine Asphalt Concrete Properties Using the Indirect Tensile Mode. *Journal of the Association of Asphalt Paving Technologists,* Vol. 61, pp. 304-332, 1992.

Roque, R., W.G. Buttlar, B.E. Ruth, M. Tia, S.W. Dickison, and B. Reid. *Evaluation of SHRP Indirect Tension Tester to Mitigate Cracking in Asphalt Pavements and Overlays*. Final Report of the Florida Department of Transportation, University of Florida, Gainesville, August 1997.

Roque, R., Z. Zhang, and B. Sankar. Determination of Crack Growth Rate Parameters of Asphalt Mixtures Using the SuperPave™ Indirect Tension Test (IDT). *Journal of the Association of Asphalt Paving Technologists*, Vol. 68, pp. 404-433,1999.

Scott, J.A.N. Adhesion and Disbonding Mechanisms of Asphalt Used in Highway Construction and Maintenance. *Proceedings of the Association of Asphalt Paving Technologists,* Vol. 47, pp. 19-48. Minneapolis, Minnesota 1978.

Sedwick, S.C. *Effect of Asphalt Mixture Properties and Characteristics on Surface Initiated Longitudinal Wheel Path Cracking*. Master's thesis, University of Florida, Gainesville, 1998.

Stuart, K.D. *Evaluation of Procedures Used to Predict Moisture Damage in Asphalt Mixtures*. Federal Highway Administration (FHWA) Report FHWA/RD-86/091. McLean, Virginia, 1986.

Stuart, K.D. *Moisture Damage in Asphalt Mixtures: A-State-of-the-Art Report*. Federal Highway Administration (FHWA) Report FHWA-RD-90-019. McLean, Virginia, August 1990.

Taylor, M.A. and N.P. Khosla. *Stripping of Asphalt Pavements: A-State-of-the-Art Report*. Transportation Research Record 911, Transportation Research Board, National Research Council. Washington, D.C., 1983.

Terrel, R.L. and S. Al-Swailmi. *Water Sensitivity of Asphalt Aggregate Mixes: Test Selection*. Strategic Highway Research Program (SHRP) Report SHRP-A-403, National Research Council, Washington, D.C., 1994.

Thelen, E. *Surface Energy and Adhesion Properties in Asphalt-Aggregate Systems*. Highway Research Board, Bulletin 192. Washington D.C., 1958.

Tunnicliff, D.G. and R.E. Root. Anti-stripping Additives in Asphalt Concrete: State-of-the-Art Report. *Proceedings of the Association of Asphalt Paving Technologists,* Vol. 51, pp. 265-293. St Paul, Minnesota, 1982.

Tunnicliff, D.G. and R.E. Root. *Use of Anti-stripping Additives in Asphaltic Concrete Mixtures*. National Cooperative Highway Research Program (NCHRP) Report 274, Transportation Research Board, National Research Council. Washington, D.C., 1984.

Zhang, Z., R. Roque, and B. Birgisson. *Evaluation of Laboratory Measured Crack Growth Rate for Asphalt Mixtures*. Transportation Research Record No. 1767, Transportation Research Board, National Research Council, Washington, D.C., pp. 67-75, 2001.

Zhang, Z., R. Roque, B. Birgisson, and B. Sangpetngam. Identification and Verification of a Suitable Crack Growth Law. *Proceedings of the Association of Asphalt Paving Technologists,* Vol. 70, pp. 206-241. St Paul, Minnesota, 2001.

BIOGRAPHICAL SKETCH

Tait K. Karlson was born on April 4, 1978, in Trenton, New Jersey. One month later his family moved to central Florida where he grew up. Upon completing high school, he enrolled in the University of Florida where he received his Bachelor of Science in Civil Engineering in 2001. He continued his education by enrolling in the civil and coastal engineering graduate program at the University of Florida under the direction of Dr. Bjorn Birgisson. During his graduate career he studied asphalt materials and transportation engineering.